Summer 1981

Analysis of Structural Dynamic Characteristics of an Explosion Driven Hydrodynamic Conical Shock Tube

Walter R. Sanders
University of Central Florida

ANALYSIS OF STRUCTURAL DYNAMIC CHARACTERISTICS OF AN EXPLOSION DRIVEN HYDRODYNAMIC CONICAL SHOCK TUBE

BY

WALTER RICHARD SANDERS
B.S.E., University of Central Florida, 1976

RESEARCH REPORT

Submitted in partial fulfillment of the requirements
for the degree of Master of Science in Engineering
in the Graduate Studies Program of the College of Engineering
at the University of Central Florida, Orlando, Florida

Summer Quarter
1981

ABSTRACT

Previous tests of an explosion driven hydrodynamic shock tube revealed peak pressure data significantly lower than values predicted from the semiempirical scaling laws. It was hypothesized that part of the deviation was due to error in determining shock wave parameters and part might be due to measurement error caused by mechanical vibration of the tube.

This investigation was conducted in two parts. In the first part, shock wave parameters were determined using a digital computer and curve fitting techniques to analyze digitized shock wave data. The second part involved determining the frequency components of the shock wave data noise content and comparing this to the dynamic characteristics of the tube which were investigated through an impulse testing technique. From these efforts higher values for the peak pressure were verified but no evidence was found that vibration of the tube caused signficant degradation of shock wave test data.

ACKNOWLEDGEMENTS

I would like to express my thanks to several members of the University of Central Florida faculty for their help in this research effort. Dr. C.E. Nuckolls provided the technical information on which much of the research was based. Madjid Belkerdid obtained and assembled the electronic test equipment and aided in conducting tests and writing computer programs. Dr. R.L. Phillips assisted with advice and discussion of test results.

I would especially like to thank my wife, Gina, for her support and help in typing and organizing this paper.

TABLE OF CONTENTS

LIST OF TABLES

LIST OF ILLUSTRATIONS

I. INTRODUCTION

An explosive driven hydrodynamic conical shock tube was developed to test the integrity of a device in an explosive underwater environment. Previous calibration tests of the shock tube were conducted to determine performance parameters. These parameters had been determined through graphical analysis and primarily qualitative methods. The parameters obtained deviated significantly from those theoretically predicted. Furthermore, the magnitude of the deviations increased as the explosive charge weight increased. Thus, it appeared that use of the tube for tests at the required level might cause permanent structural damage.

It was hypothesized that part of the difference between measured and predicted results might originate from two sources. One believed source of error was the inaccuracy of the method used to determine tube performance parameters. Another, was shock wave measurement error due to vibration of the shock tube structure. Therefore, it was deemed desirable to perform a quantitative analysis of shock wave data and investigate shock tube dynamic characteristics.

This investigation was conducted using a digital

computer, a signal processing software package and a number of specialized computer programs to analyze digitized shock tube data. The two main purposes of this analysis were to verify previously obtained shock tube performance parameters and to determine if the noise in shock wave data is caused by vibration of the tube structure.

The performance parameter identification effort was conducted first. This portion of the analysis involved fitting a theoretical curve to the test data. Also, accomplished was an effort to isolate the noise (difference between the theoretical best fit curve and the test data) and determine its frequency content. To accomplish the curve fitting, a computer program was written using a least squares technique. Program results include graphical representations and calculated parameters. The frequency content of the noise was determined using another computer program and the Fast Fourier Transform (FFT) capability of the software.

The dynamic characteristics of the tube were investigated using an impulse testing technique. This technique consisted of exciting the shock tube with a measured and recorded impulse while simultaneously recording the response. By varying the position of the excitation and or response a series of impulse and/

response time functions were obtained. Using several computer programs and the software FFT capabilities a series of frequency response functions were obtained. From these, the vibration characteristics of the shock tube were investigated.

This paper is divided into several chapters to illustrate the various portions of the research effort. The first chapter consists of background information. Included in this chapter are a description of the shock tube and test equipment, a description of the required test level and a summary of the performance parameters previously derived. The next chapter describes the curve fitting and shock wave data noise investigation. The next chapter describes the investigation of shock tube dynamic characteristics through impulse testing. The final chapter includes conclusions and recommendations.

II. BACKGROUND

This chapter includes a description of shock tube design, test requirements, calibration test instrumentation and a brief discussion of the parameter derived during calibration testing. The discussion of tube design is a description of the physical features of the tube and other hardware used during calibration tests. The portion pertaining to test requirements consists of a description of the environmental conditions to be simulated and shock wave parameters necessary to yield those conditions. The description of calibration test instrumentation included detail information on two pieces of test equipment and a summary of the function of each device in the test configuration. The discussion of shock tube parameter includes a summary of the performance parameters derived during calibration tests and a description of the methods used to obtain them.

Shock Tube Description

The shock tube and breach end plate were fabricated from mild steel in the configuration shown in Figure 1. The body of the tube was made in two sections to facilitate placement and cleaning. The concical hole in the center of the tube was created using electro discharge

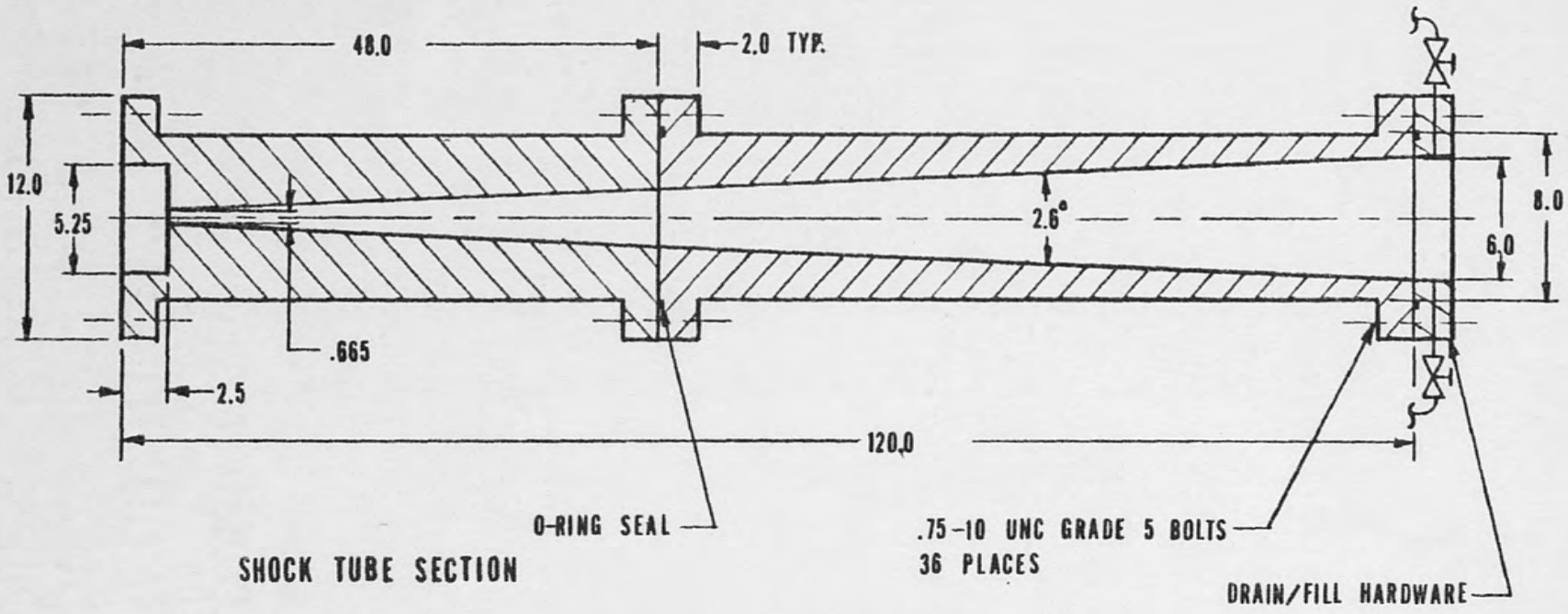

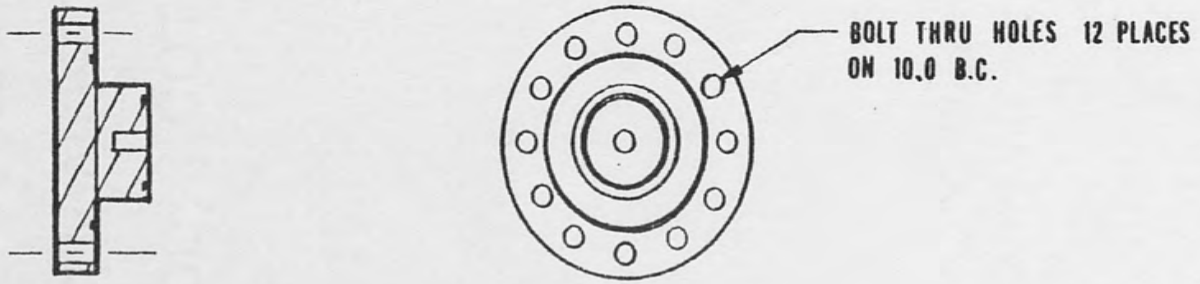

Figure 1. Shock Tube Configuration

machining. The tube joints are bolted using a symmetrical pattern of twelve, 3/4 inches, grade 5 bolts and sealed with o-ring glands. The breach plate houses the explosive charge. The muzzle end plate normally would house the device under test. However, for calibration tests a dummy plate (not shown) was used to support a conduit mounted pressure transducer. Additional hardware (not shown) was used to fill the tube and support it. Figure 2 is a photograph of the shock tube configuration from the breach end (1).

Test Requirements

The purpose of the shock tube is to test a specific device in an underwater explosive environment. The test requirement is to simulate the pressure shock wave profile caused by detonation of a 125 pound spherical charge of TNT at a range of eleven feet. Both the peak pressure and the wave, time profile are to be simulated. The pressure versus time profile has been shown to be of the form (2)

$$P(t) = P_m \exp(-t/\theta) \qquad \text{II-1}$$

where:

P_m is the peak pressure in psi

θ is the time constant

t is the time from the beginning of the wave.

This corresponds to instantaneous rise in pressure

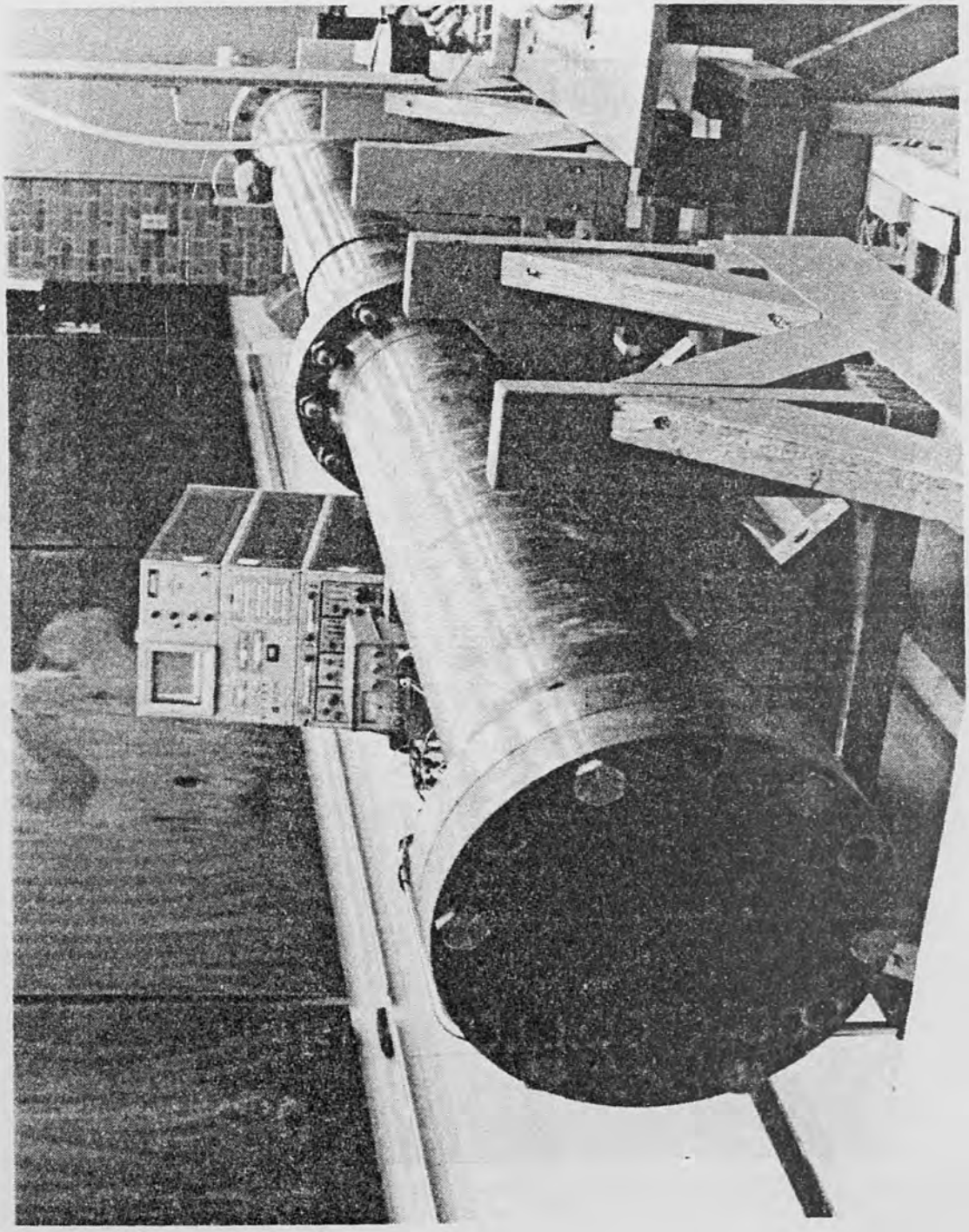

Figure 2. Shock Tube

followed by an exponential decay. From the scaling laws the relations for peak pressure (P_m) and time constant (θ) have been determined to be:

$$P_m = k_1 \ (W^{1/3}/R)^{\alpha} \qquad \text{II-2}$$

$$\theta = k_2 \ (W^{1/3}) \ (W^{1/3}/R)^{\beta} \qquad \text{II-3}$$

where:

W is the weight of charge in pounds

R is the range from the charge center in feet

k_1, α, k_2, and β are constants empirically derived for the particular explosive material.

For TNT:

$k_1 = 2.16 \times 10^4$

$\alpha = 1.13$

$k_2 = 58$

$\beta = -0.22$.

Therefore, solving equation II-2 and II-3 using 125 pounds of TNT at eleven feet

$P_m = 8.86$ ksi

$\theta = 345 \ \mu$ sec .

Thus, a pressure shock wave of

$$P(t) = 8.86 \exp (-t/345 \times 10^{-6} \text{ sec}) \quad (\text{ksi})$$

is required to satisfy the test requirements.

Calibration Test Instrumentation

Instrumentation required during calibration tests included a dynamic pressure transducer and supporting conduit (stinger), a digital processing oscilloscope,

a trigger accelerometer, signal conditioning and trigger electronics and explosive firing circuitry. The configuration is shown schematically in Figure 3. The pressure transducer assembly consisted of a .25 inch diameter tourmaline disk transducer mounted on a .75 inch diameter aluminum conduit. The sensitivity and natural frequency of the transducer were determined to be 2703 psi/volt and 170 k Hz, respectively. Figure 4 is a photograph of the pressure transducer, with cable, mounted on a one foot long stinger. The digital processing oscilloscope (DPO) was a Tektronic 7704-A. This scope has the capability of storing a 512 sample, digitized waveform in each of four separate memory locations. Each of the other devices shown in Figure 3 were obtained with the operating parameter required to perform its particular task.

During the process of recording shock wave data the instruments and devices shown in Figure 3 performed the functions indicated below:

1. Firing circuit - detonates the explosive

2. Trigger accelerometer - converts excitation from the passing shock wave to a weak trigger signal.

3. Trigger amplifier - smoothes and amplifies the signal from the accelerometer such that, adequate trigger is provided for the DPO.

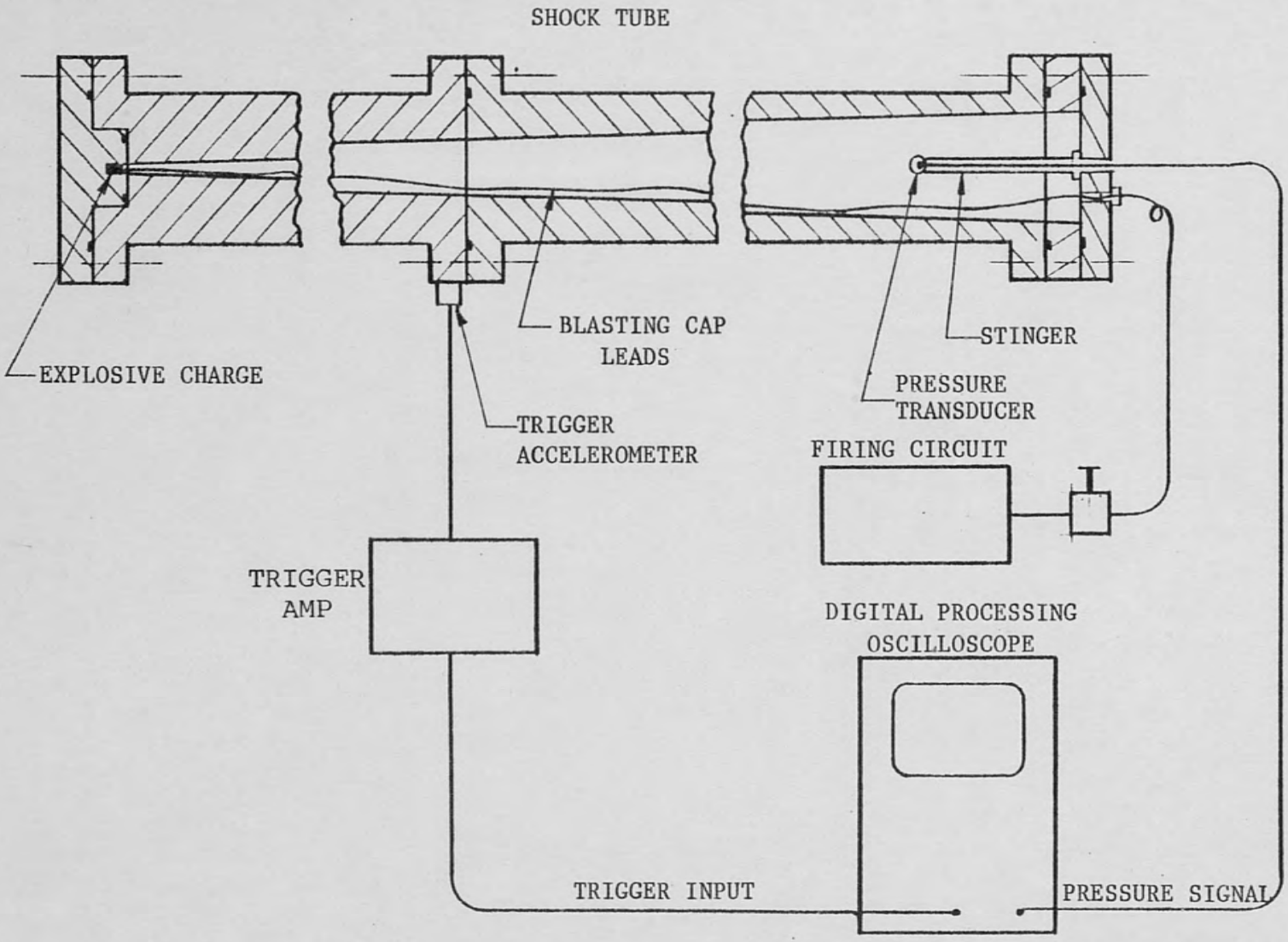

Figure 3. Shock Tube Calibration Test Configuration

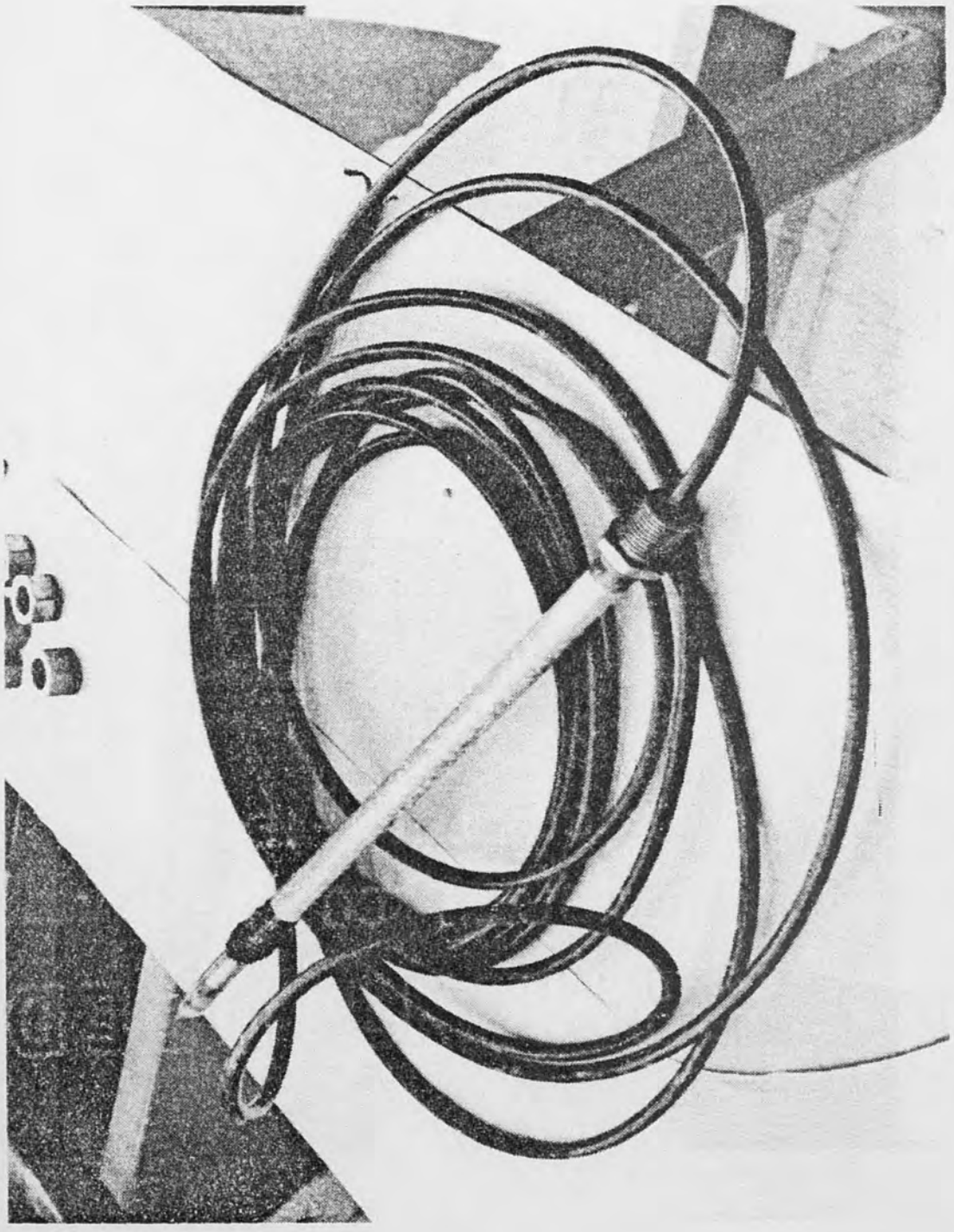

Figure 4. Stinger Mounted Pressure Transducer

4. Pressure transducer - senses the shock wave pressure and creates a proportional voltage signal.

5. DPO - receives a trigger from the trigger amp and records the shock wave pressure data as a function of the sweep time.

Calibration Test Parameters

Shock tube performance was predicted and calibration parameters were determined during previously conducted design and testing. A summary of the predicted and measured performance is included below.

Using scaling laws and shock tube configuration Connell (1) predicted an actual charge weight of 7.3 grams TNT would be required to achieve the specified test requirements. The corresponding amplifications factor (AF), based on tube geometry, is 7770, where the amplification factor is defined as:

$$AF = W_{ACTUAL} / W_{APPARENT} \qquad \text{II-4}$$

where:

W_{ACTUAL} is the weight of charge used in the shock tube

$W_{APPARENT}$ is the weight of charge being simulated

Most of the data used during calibration was obtained using a significantly lower charge weight than (W_{ACTUAL}). Therefore, different values of pressure wave parameter were derived. The charge weight used in all tests, except one, was that of a number 8 blasting cap (W = 0.001616 pounds of TNT). The parameters estimated

by Connell (1) for this weight at a range of 9 feet (1 foot from the muzzle end plate) are:

$$P_m = 3.2 \text{ ksi}$$

$$\theta = 150 \ \mu \text{ sec} .$$

From the estimated peak pressure a new value for k_1 in equation II-3 was calculated to be $k_1 = 4.72 \times 10^5$. The true amplification factor was then calculated as follows:

$$AF_{TRUE} = W_F/W_T \Big|_{P_m, R}$$

$$P_{mF} = P_{mT} = k_{1T} (W_T^{1/3} /R)^{\alpha} = k_{1F}(W_F^{1/3}/R)^{\alpha}$$

$$AF_{TRUE} = (k_{1T}/k_{1F})^{3/\alpha} \qquad \text{II-5}$$

to have the value 3600 compared with a predicted value of 7700. From the calculated AF_{TRUE} and the weight of the cap, the apparent weight of explosive was calculated to be 5.8 pounds. Also, the efficiency was calculated to be

$$\eta = AF_{TRUE} /AF_{THEORY} \qquad \text{II-6}$$

$$\eta = .46 \text{ or } 46\%$$

Using the calculated apparent weight and equation II-3 the theoretical time constant θ was calculated to be 148 μ sec at a range of 9 feet. This compared very well with the value estimated from shock wave data of 150 μ sec.

One data point was obtained using a greater charge

weight than the blasting cap. In this case a charge weight of 3.37 grams of detaprime plus a number 8 blasting cap was used. The shock wave history was recorded and analyzed. The peak pressure estimate obtained was 12% lower than the value predicted from the scaling laws based on the blasting cap data and the calculated AF of 3600. From this trend it appeared that the charge weight needed to reach the required test level might cause damage to the shock tube structure.

Efforts to verify the performance parameters determined during calibration testing are discussed in the next chapter.

III. SHOCK WAVE DATA ANALYSIS

This chapter contains a summary of the methods used and results obtained during computer aided analysis of shock wave data. Included in this chapter is a description of the shock wave data and of the circumstances under which it was recorded. Another section of the chapter describes the methods used to obtain time domain curve fits to the shock wave data and to determine the frequency of shock wave data noise. The final section discusses the results obtained from the analysis. Included in this section is a discussion of the curve fitting results and the shock wave parameter derived from them. Also, included is a summary of the results obtained from the investigation of the frequency content of the shock wave data noise.

Description of Shock Wave Data

Shock wave pressure data, used in this analysis, were obtained from firing the shock tube and stored in digital form in a permanent memory device. The form of the data was a 512 sample array with a time increment (SA) and both vertical and horizontal units. Data of this form were referred to as waveforms (3). The data were recorded in a memory location of the DPO, as

previously discussed and indicated in Figure 3. From the DPO the shock wave pressure waveforms were transfered directly to a data file on a floppy disk in the PDP 11/34 digital computer. At this point the waveforms were in volts versus time which are the units recorded on the DPO. Later in the curve fitting process the sensitivity of the pressure transducer was taken into account.

Two shock wave pressure waveforms were obtained for this analysis. One was stored in data file "SHOCK.DAT" on the floppy disk. This waveform is shown in Figure 5. The following conditions were present when this data was recorded. The pressure transducer position was approximately 9 feet from the charge. The initial water pressure was line pressure of about 50 psi. The explosive used was a Dupont number 8 blasting cap. The DPO time scale was 50 μ sec per division. The second waveform, shown in Figure 6, was stored in file "SHOCK1.DAT". The conditions present were similar to the previous ones. The transducer was again at 9 feet from the charge, the initial pressure was the same and the explosive was a number 8 cap. Also, the DPO scale was the same. However, for this shot a linoleum gasket was placed in the bolted flange between the 4 and 6 foot tube sections.

This portion of the investigation was based

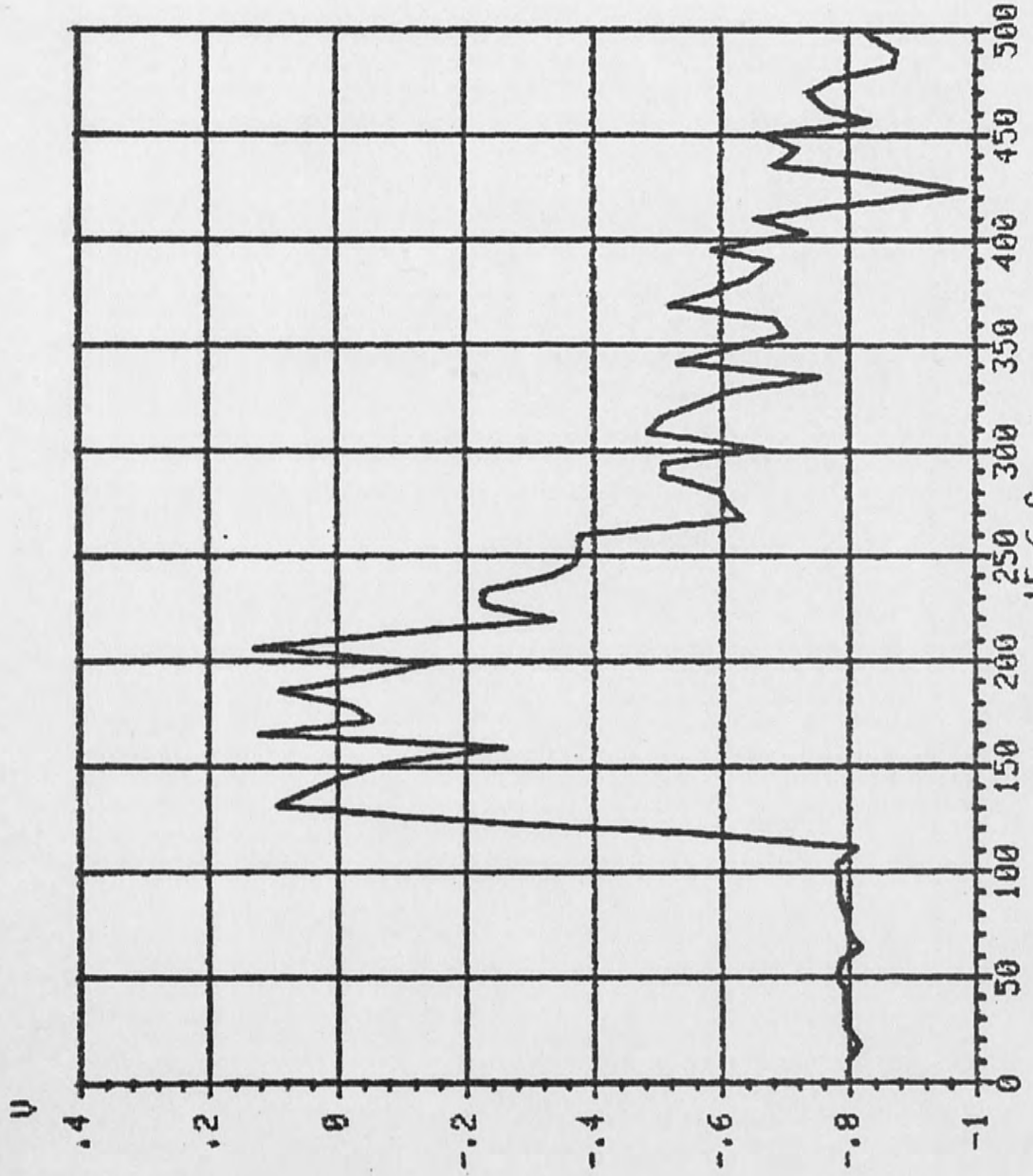

Figure 5. Shock Wave Data From "SHOCK.DAT"

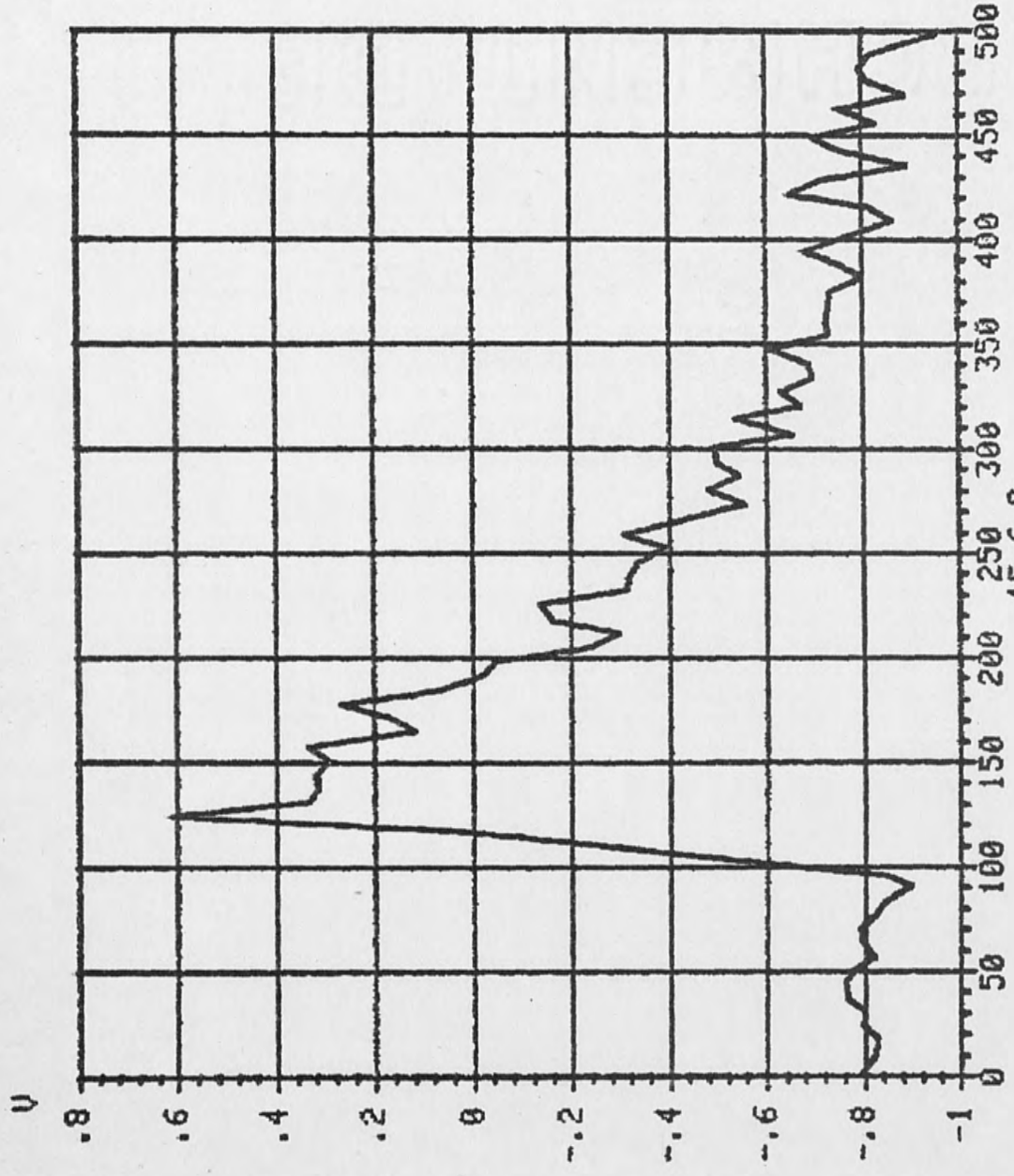

Figure 6. Shock Wave Data From "SHOCK1.DAT"

entirely on these two waveforms. This may appear to be a serious weakness. However, these shock wave pressure curves have been shown to be repeatable by Connell (1).

Method of Analysis

This section includes a summary of the methods used to perform time domain curve fitting on the shock wave data and to investigate the frequency content of shock wave data noise. This and all other computer aided data analysis was accomplished through the uses of a PDP 11/34 digital computer and Tektronix Signal Processing Software in Basic (TEK SPS BASIC or SPS BASIC) (3).

As previously mentioned, the method used to conduct this portion of the investigation involved fitting a curve of an assumed form to the shock wave pressure data. The curve fitting was accomplished via computer using a computer program "NFIT.BAS". A description and printout of program "NFIT.BAS" are included in Appendix A.

The assumed curve is of the form discussed in the Background chapter equation II-1.

$$P(t) = P_m \exp(-t/\theta)$$

where:

P_m is the peak pressure

t is time measured from arrival of shock wave

θ is the decay time constant .

However, this equation contains a discontinuity at t=0

which is not demonstrated in the data. Therefore, a linear curve was assumed for the portion of the curve between zero, at the arrival of the wave, and the peak pressure. Thus the equation of the assumed curve fit to the shock wave data is:

$$P(t) = mt + b \quad \text{for} \quad 0 \leq t \leq t_p$$

and

$$P(t) = P_m \exp(-(t-tp)/\theta) \quad \text{for} \quad t \geq t_p .$$

where:

t_p is the time of the arrival of the wave to the peak pressure

m is the slope of the linear rise time curve

b is the intercept of the rise time curve.

Both portions of the assumed curve were fit to the shock wave data. The exponential portion of the curve was fit using a least squares technique. The linear curve was established between the point where the wave appeared to start, to the point where the peak in the initial rise appeared to be, or from the start of the wave with an assumed slope.

The range of the data fit to the exponential curve and the two points or point and slope which establish the linear curve were chosen by the user. Therefore, some variations in the curves obtained was possible. However, the quality of the fit was judged on the basis

of three criteria. The first was by observation. The curve fitting program, "NFIT.BAS", creates a plot of the data and fitted curve concurrently for easy inspection. Thus, the quality of the fit was determined visually. The second criteria for judging quality of fit was the correlation coefficient which the program calculates following the exponential fit. The correlation coefficient (ρ) is defined as (4):

$$\rho^2 = \sigma_2^2 - \sigma^2 / \sigma_2^2$$

where:

σ is the variation in the dependent variable for known independent variables

σ_2 is the variation in the dependent variables for unknown independent variables

Thus, ρ tells what proportion of the variation of the dependent variables can be attributed to the linear relationship. A perfect correlation yields a ρ value of 1 or -1, depending on slope, and no correlation yields a ρ of 0. The third criteria involved in judging the curve fitting results was the belief that the fit curves for both data waveforms should have approximately the same rise time slope, peak pressure and time constant. The argument supporting this belief is that since both shock wave pressure waveforms were obtained using the same charge weight and at the same distance from the charge they should both be measurements of the same shock wave.

The difference in the two waveforms should be the noise due to differences in the transmissibility of the tube or other effects.

Based on these three criteria, the final curve fits were obtained using an iterative process. During this process attempts were made to achieve the best visual fit, obtain correlation coefficients near ±1 and obtain fitted curves for both waveforms with approximately the same peak pressure, time constant and rise time curve slope. This was accomplished by running the fitting program on each data waveform a number of times and each time selecting a different portion of the data curves to be fit.

The final curve fits were used to determine shock tube performance parameters in a similar manner to that discussed in the background chapter. The curve fitting results and the performance parameters obtained will be discussed in the next section.

The method used to determine the frequency content of the shock wave data noise involved the use of the computer and a computer program, "ADFFT1.BAS". A description and printout of "ADFFT1.BAS" are included in Appendix A.

Program "ADFFT1.BAS" was used to process the shock wave data and fitted waveforms in a number of steps.

The first step was to read the shock wave data waveform and the fitted curve waveform obtained in program, "NFIT.BAS". The next step was to obtain the noise portion of the shock wave data by subtracting the data waveform from the fitted curve waveform. Then the FFT of the noise waveform was obtained. This transformation yields the real and imaginary parts and the magnitude of the noise frequency content. These frequency domain waveforms are the results of the program and are plotted for visual inspection. Other plots made during execution of the program include real and imaginary parts and magnitudes of the data and fitted curve waveforms transforms.

The results obtained from this investigation are included, along with a discussion, in the next and final section of this chapter.

Shock Wave Data Analysis Results

This section contains a discussion of the results obtained from the analysis of shock wave data. Included are a summary of the final curve fitting results and the calculation of shock tube performance parameters. Also, included are the results of the investigation of shock wave data noise frequency content.

Results of curve fitting of shock wave data from file "SHOCK1.DAT" are shown in Figures 7 and 8. It

```
   ***EXPON. CURVE FIT***

ENTER STARTING TIME FOR EXPON. DECAY CURVE FIT.
?128E-6
ENTER INITIAL TIME FOR EXPON. CURVE FIT
?128E-6
ENTER FINAL TIME FOR EXPON. CURVE FIT
?360E-6

   LINEAR EQN.    Y =( 8.33749) + X (-11259.6)

   LINEAR FIT CORRELATION COEFF. = -.972189

   EXPON. EQN.-   Y = ( 4177.61) EXP(-11259.6X)

   ***LINEAR RISE TIME CURVE FIT***

ENTER STARTING TIME FOR RISE TIME CURVE FIT
?99E-6
ENTER (0) FOR POINT TO POINT OR (1) FOR POINT SLOPE FIT
?0

ENTER FINAL TIME FOR RISE TIME CURVE FIT
?124E-6

  LINEAR EQN.  Y = ( 201.001) + X ( 1.38753E+08)

  MAX PRESSURE =  4177.61
  AT TIME =  1.27930E-04
```

Figure 7. Curve Fitting Data For "SHOCK1.DAT"

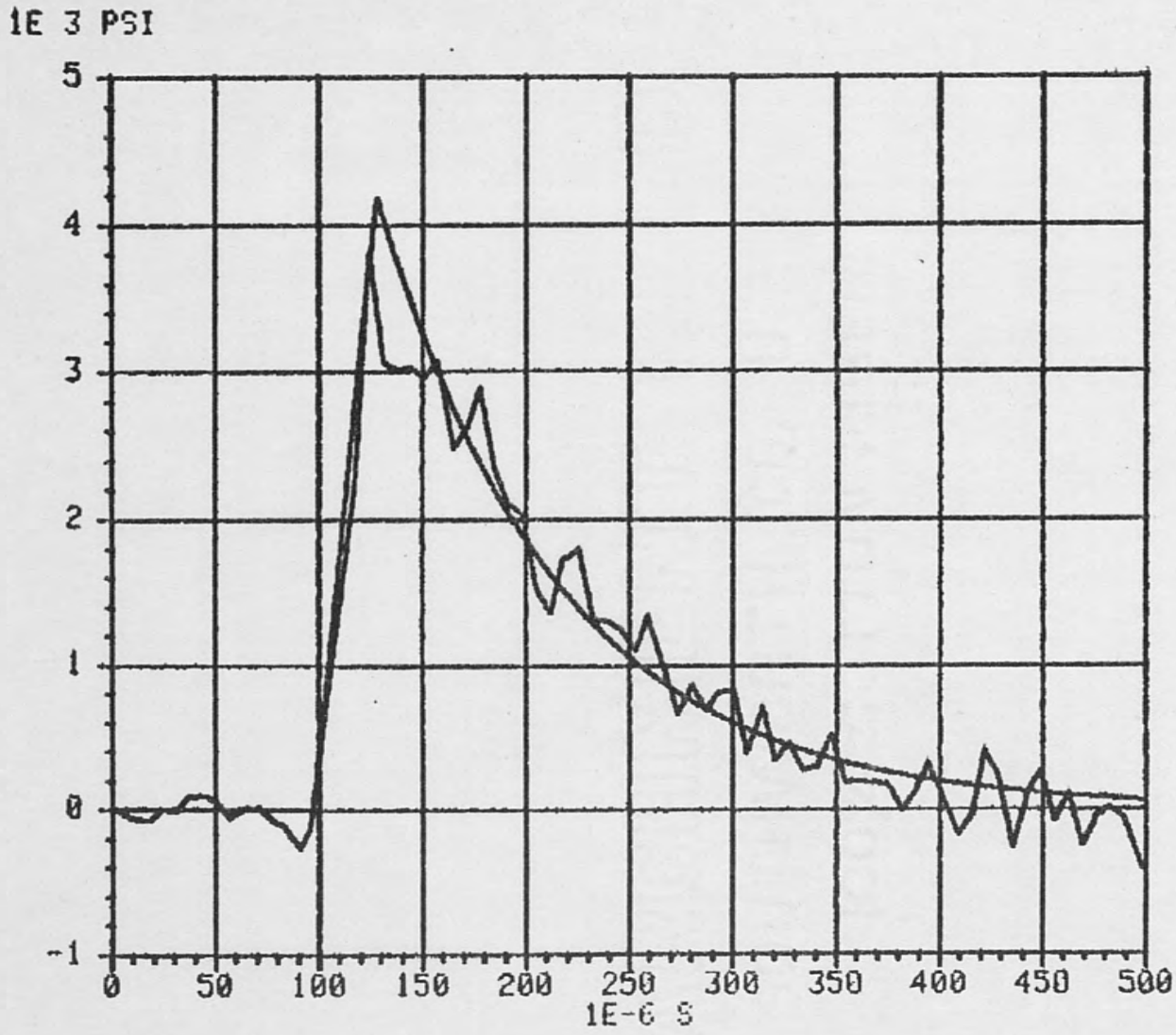

Figure 8. Curve Fitting Plot For "SHOCK1.DAT"

should be noted at this point that the pressure transducer sensitivity assumed to obtain these results was 2.7×10^3 psi/volt, as established by Connell (1). Figure 7 is a printout produced by program, "NFIT.BAS". This printout contains the linear equation fit to the log of the shock wave decay, the correlation coefficient for this linear fit, the corresponding equation of the exponential curve, the linear equation of the rise time curve, and the peak pressure and its time of occurrence. Figure 8 is a plot of the shock wave data and the fitted curve.

The results of curve fitting of shock wave data from file "SHOCK.DAT" are shown in Figures 9 and 10. These figures contain information similar in description to that in Figures 7 and 8.

These results require some further discussion at this time. First, a peak pressure of 4177 psi and 3919 psi were indicated in Figures 7 and 9, respectively. The average of these values, approximately 4049 psi, about 800 psi or 25% greater than the value determined by Connell (1) at the same distance and charge weight. Also, the decay time constant θ was indicated to be 88.8 μ sec in Figure 7 and 85.2 μ sec in Figure 9. This is significantly less than the 150 μ sec determined by Connell (1). However, the computer predicted time

```
   ***EXPON. CURVE FIT***

ENTER STARTING TIME FOR EXPON. DECAY CURVE FIT.
?141E-6
ENTER INITIAL TIME FOR EXPON. CURVE FIT
?180E-6
ENTER FINAL TIME FOR EXPON. CURVE FIT
?335E-6

   LINEAR EQN.     Y =( 8.27382) + X (-11733.9)

   LINEAR FIT CORRELATION COEFF. = -.889785

   EXPON. EQN.-    Y = ( 3919.9) EXP(-11733.9X)

   ***LINEAR RISE TIME CURVE FIT***

ENTER STARTING TIME FOR RISE TIME CURVE FIT
?113E-6
ENTER (0) FOR POINT TO POINT OR (1) FOR POINT SLOPE FIT
?1

ENTER SLOPE OF LINEAR CURVE
?1.38753E8

  LINEAR EQN.  Y = ( 62.7484) + X ( 1.38753E+08)

  MAX PRESSURE =  3919.9
  AT TIME =  1.39648E-04
```

Figure 9. Curve Fitting Data From "SHOCK.DAT"

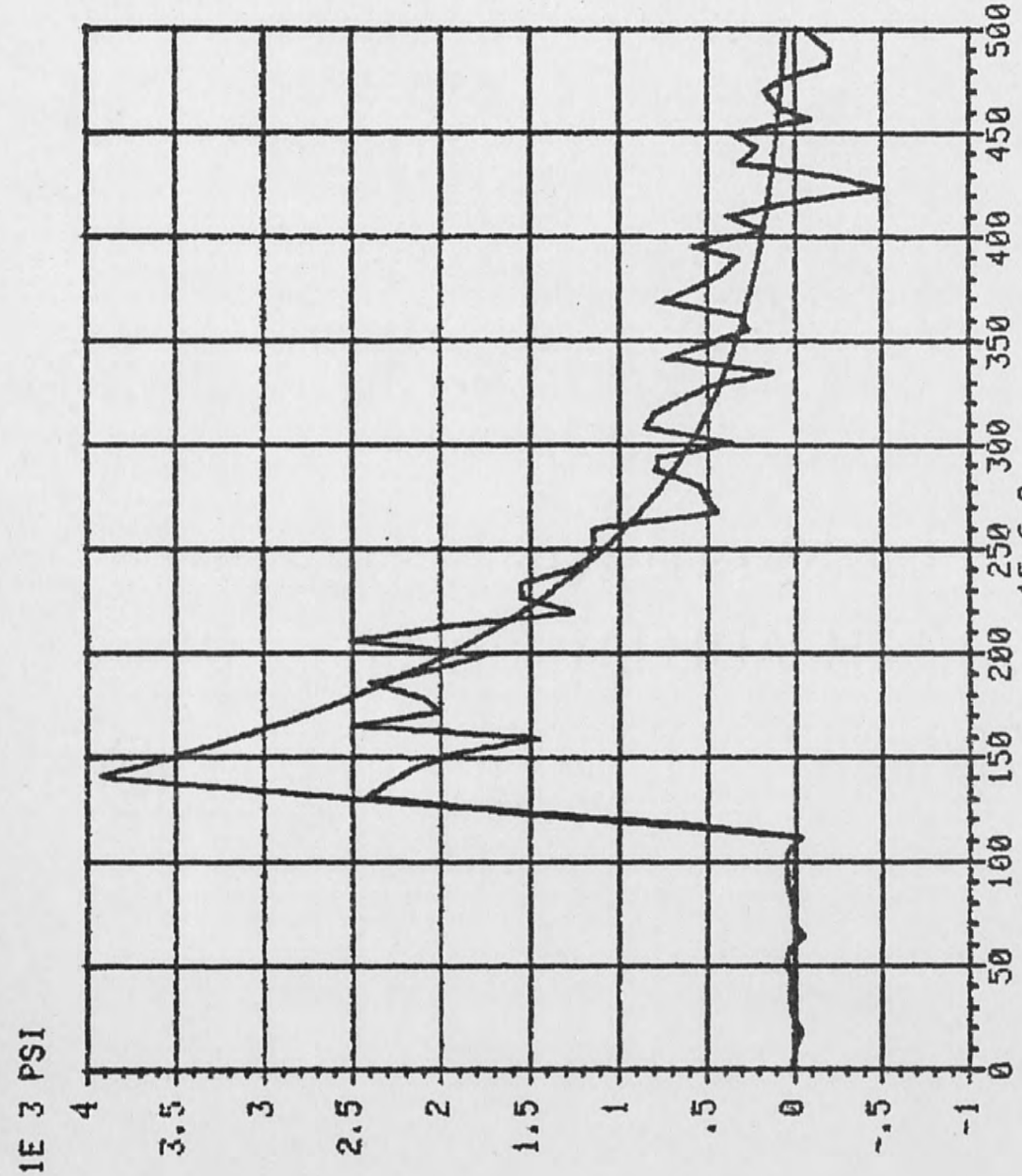

Figure 10. Curve Fitting Plot For "SHOCK.DAT"

constant is based only on the exponential portion of the curve. The shock wave actually begins approximately 28 μ sec before. Therefore, the predicted value of θ should perhaps be adjusted to approximately 101 μ sec. This would take into account the average of the two predicted values plus the addition of one half of the rise time.

From the average of the two peak pressures ($\overline{P}_m$ = 4048 psi) and the methods discussed in chapter II, the performance parameter of the shock tube were calculated. First, equation II-2 was solved for a new value of k_1,

$$k_1 = P_m \, (W^{1/3} / R)^{-\alpha}$$

where:

P_m is the peak pressure determined from curve fitting (4048 psi)

W is the actual weight of charge (0.001616 pounds)

R is the range from the explosion to the pressure transducer (9 feet)

α is the exponent determined for TNT detonation (1.13).

The new value of k_1, thus determined, was 5.458×10^5. Next, using equation IV-5, the true amplification factor can be found to be:

$$AF_{TRUE} = (5.458/.216)^{3/1.13}$$

$$AF_{TRUE} = 5292.1$$

and the efficiency is calculated from equation II-6 to

be

$$\eta = 5127/7700$$

$$\eta = .687 \text{ or } 68.7\%$$

Next, the decay time constant θ derived from the curve fitting should be compared to the theorectically determined value. Using the amplification factor of 5292.1, an apparent charge weight can be calculated to be 8.28 pounds. From this value and equation II-3, a theoretical value of θ can be determined as follows:

$$\theta = (58)(8.28)^{1/3}((8.28)^{1/3}/9.0)^{-0.22}$$

$$\theta = 163 \ \mu \text{ sec}$$

Thus, the adjusted prediction of $\theta = 101 \ \mu$ sec approximately 38% less than that calculated from the scaling laws.

At this point no statements will be made about the implication of the performance parameters determined above. Discussion of these results as well as the result of the remaining portions of this analysis are included in chapter V of this report.

The results obtained from the shock wave data noise frequency analysis are shown in Figures 11 and 12. Figure 11 is a plot of the magnitude of the transformed shock wave noise waveform for data from file "SHOCK1.DAT". Figure 12 is a plot of similar data obtained for shock wave data in file "SHOCK.DAT". From

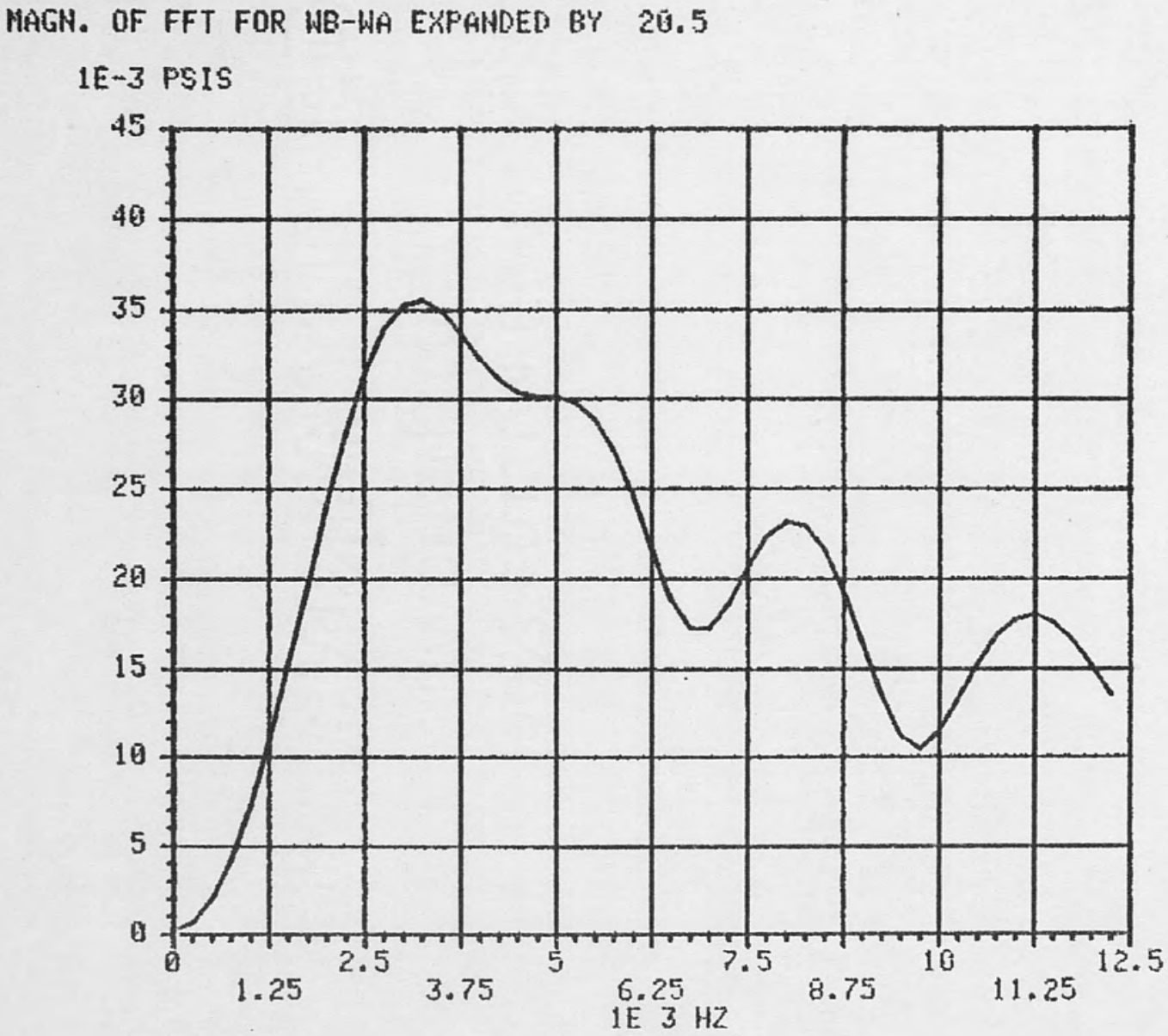

Figure 11. Data Noise Frequency Content From "SHOCK1.DAT"

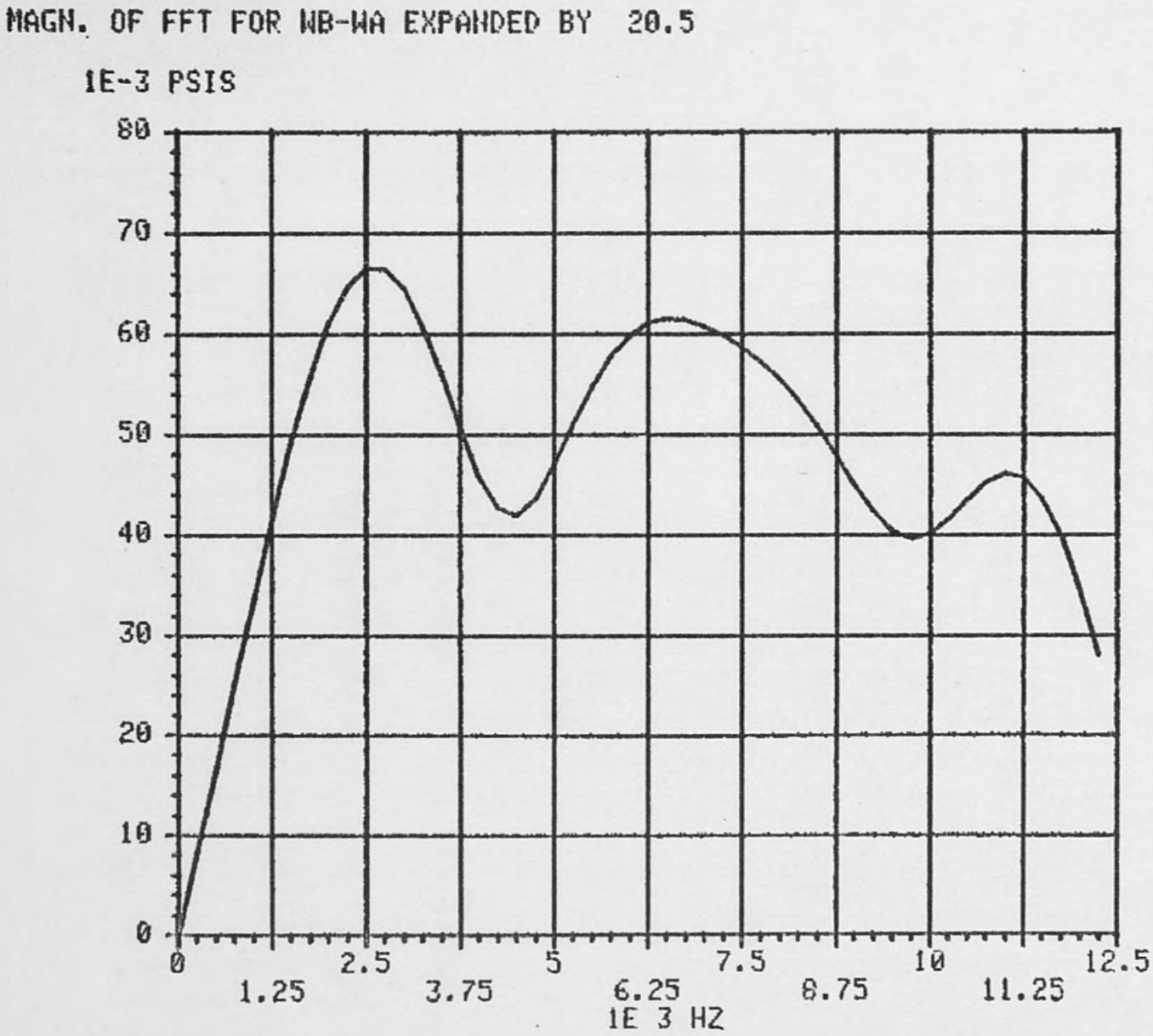

Figure 12. Data Noise Frequency Content From "SHOCK.DAT"

Figure 11, it appears that the major peak in the frequency spectrum occurs at around 3000 Hz. The next peak appears to be around 5000 Hz. From Figure 12 the first and second peaks in the spectrum appear to be around 2500 and 6250 Hz respectively. Also, the first peak in Figure 12 is approximately twice the magnitude of the one in Figure 11. Any further conclusions drawn from these results will be included in chapter IV.

IV. ANALYSIS OF SHOCK TUBE DYNAMIC CHARACTERISTICS

This chapter contains a summary of the methods used and the results obtained during the analysis of the dynamic characteristics of the shock tube. The first section discusses the theoretical basis for the impulse test technique used. The next portion includes a discussion of the methods, equipment, procedures and computer programs used to perform the analysis. The final part of this section is a summary of the results obtained.

Impulse Testing Theory

This section contains a summary of the theory of impulse testing. It is not intended to be an exhaustive theoretical derivation but rather a light treatment of the subject to yield insight into the methods used in this analysis. A more rigorous explanation of this technique can be found in reference (5), from which most of this material was extracted.

The theory behind the impulse method or so called transfer function method is based on solution of the structural dynamic model. Assuming, the structure under test can be modeled as a n degree of freedom system. This system can be characterized by a set of n simultaneous, second order, non-homogeneous, ordinary differential

equations, which in matrix form are

$$[M]\{\ddot{x}\} + [C]\{\dot{x}\} + [K]\{x\} = \{f\} \qquad \text{IV-1}$$

where:

$\{x\} \equiv$ n dimensional displacement vector

$\{\dot{x}\} \equiv$ n dimensional velocity vector

$\{\ddot{x}\} \equiv$ n dimensional acceleration vector

$\{f\} \equiv$ n dimensional forcing function vector

$[M] \equiv$ n × n real valued symmetric mass matrix

$[C] \equiv$ n × n real valued symmetric damping matrix

$[K] \equiv$ n × n real valued symmetric stiffness matrix.

For simplicity, a single degree of freedom system will be considered first assuming the results obtained can be extended to the multi-degree of freedom case. For a linear single degree of freedom system with damping and external forces the differential equation is:

$$m\ddot{x}(t) + c\dot{x}(t) + kx(t) = f(t) \qquad \text{IV-2}$$

where:

$x, \dot{x}$ and $\ddot{x} \equiv$ displacement, velocity and acceleration

$m \equiv$ mass of inertial element

$k \equiv$ stiffness of elastic element

$c \equiv$ damping of dissipative element

$f \equiv$ external force

Taking the Laplace transform of both sides of equation IV-2 yields

$$(ms^2 + cs + k)\, X(s) = F(s), \qquad \text{IV-3}$$

assuming initial conditions are zero,

where:

$X(s) \equiv$ Laplace transform of displacement

$F(s) \equiv$ Laplace transform of forces.

For the homogeneous case ($f(t) = 0$);

$$(ms^2 + cs + k)\, X(s) = 0,$$

which yields the so called system characteristics equation

$$ms^2 + cs + k = 0. \qquad \text{IV-4}$$

The roots of this equation are:

$$s_{1,2} = -c/(2m) \pm \sqrt{(c/(2m))^2 - k/m}\ . \qquad \text{IV-5}$$

Returning to the nonhomogeneous case in equation IV-3, define

$$B(s) = ms^2 + cs + k,$$

such that

$$B(s)\, X(s) = F(s).$$

Thus, for a known forcing function $F(s)$ and its response $X(s)$, $B(s)$ could be calculated from:

$$B(s) = F(s)/X(s).$$

Next define the system transfer function as

$$H(s) = 1/B(s)$$

$$= X(s)/F(s)$$

$$= 1/m/(s^2 + cs/m + k/m)$$

To simplify the derivation define the critical damping

(c_c) as the value which reduces the radical portion of equation IV-5 to zero.

$$c_c = 2\sqrt{km}$$
$$= 2\ m\ \omega_n$$

where:

$\omega_n = \sqrt{k/m} \equiv$ undamped natural frequency.

Also, define the damping ratio (ζ) as

$$\zeta = c/c_c$$
$$= c/(2m\ \omega_n).$$

The roots of the characteristic equation can now be written as,

$$s_{1,2} = -\zeta\ \omega_n \pm \omega_n \sqrt{\zeta^2 - 1}\ .$$

Considering only the case for which $\zeta < 1$ (underdamped), the above equation becomes

$$s_{1,2} = -\sigma \pm j\omega_d$$

where:

$\sigma = \zeta\ \omega_n \equiv$ damping factor

$\omega_d = \omega_n\sqrt{\zeta^2 - 1} \equiv$ damped natural frequency .

The system transfer function now becomes

$$H(s) = 1/m\ /((s-p)(s-p^*)), \qquad \text{IV-6}$$

where:

$p = s_1 = -\sigma + j\omega_d \equiv$ pole of transfer function

$p^* = s_2 = -\sigma - j\omega_d$, the complex conjugate of p.

From a partial fraction expansion

$$H(s) = C_1/(s - p) + C_2/(s - p^*). \qquad \text{IV-7}$$

The constants C_1 and C_2 are in general complex and are called the residues of the transfer function. These residues are directly related to the amplitude of the impulse response function. They can be evaluated as:

$$C_1 = 1/m\ /(j2\omega_d)$$

and

$$C_2 = C_1^* = 1/m\ /(-j2\omega_d).$$

Factoring out 1/2j yields a more convenient form of equation IV-7,

$$H(s) = R/(2j(s - p)) - R^*/(2j(s - p^*)) \qquad \text{IV-8}$$

where:

$$R = 1/m/\omega_d$$

$$R^* = 1/m/\omega_d\ .$$

In general R will occur in conjugate pairs but for this case it is real valued with $R = R^*$.

Next the impulsive response of system can be determined from equation IV-8 and recalling that the transform of a unit impulse is:

$$F(s) = 1,$$

then

$$H(s) = X(s) = R/(2j(s - p)) - R^*/(2j(s - p^*)).$$

Then from the inverse transform it can be shown

that

$$h(t) = R\, e^{-\sigma t} \sin(\omega_d t).$$

Therefore, the quantity R, which is related to the residue, is the amplitude of the impulsive response. Also, the damping factor σ and the damped natural frequency are the decay time constant and the frequency of oscillation, respectively.

The frequency response function, which is the result of an actual impulse test measurements, is the transfer function evaluated along the $j\omega$ axis. Thus:

$$H(\omega) = r/(2j(j\omega - p) - R^*/(2j(j\omega - p^*)),$$

and

$$H(\omega) = \tfrac{1}{2} \left[R/((\omega_d - \omega) + j\sigma) - R^*/((-\omega_d - \omega) + j\sigma)\right] \qquad \text{IV-9}$$

This function is also the ratio of the Fourier transforms of x(t) to f(t),

$$H(\omega) = X(\omega)/F(\omega) .$$

It should be noted from equation IV-9 that the value of the frequency response function at a particular frequency is a function of residue, damping and damped natural frequency.

To get a feel for this frequency response function return to the nonhomogenious equation IV-3 (6)

$$(ms^2 + cs + k)\, X(s) = F(s)$$

and

$$H(s) = 1/(ms^2 + cs + k).$$

Then dividing by k and substituting ω_n and ζ,

$$H(s) = 1/k/((m/k)s^2 + (c/k)s + 1),$$

and

$$H(s) = 1/k/((1/\omega_n^2)s^2 + (2\zeta/\omega_n)s + 1).$$

The frequency response function can then be written as:

$$H(\omega) = 1/k/(1 - (\omega/\omega_n)^2 + 2j\zeta(\omega/\omega_n)).$$

Let $r = \omega/\omega_n$ to simplify the form of the equations.

$$H(\omega) = 1/k/(1 - r^2 + 2j\zeta r)$$

Now separate $H(\omega)$ into real, imaginary and magnitude parts.

$$H(\omega) = \frac{1/k}{(1 - r^2 + 2j\zeta r)} + \frac{(1 - r^2 - 2j\zeta r)}{(1 - r^2 - 2j\zeta r)}$$

$$H(\omega) = \frac{1/k((1 - r^2) - 2j\zeta r)}{(1 - r^2)^2 + 4\zeta^2 r^2}$$

$$\mathrm{Re}[H(\omega)] = \frac{1/k\ (1 - r^2)}{(1 - r^2)^2 + 4\zeta r^2} \qquad \text{IV-10}$$

$$\mathrm{Im}[H(\omega)] = \frac{1/k\ (-2\zeta r)}{(1 - r^2)^2 + 4\zeta^2 r^2} \qquad \text{IV-11}$$

$$|H(\omega)| = \frac{1/k\sqrt{(1 - r^2)^2 + (2\zeta r)^2}}{(1 - r^2)^2 + 4\zeta^2 r^2} \qquad \text{IV-12}$$

Plots of the transfer functions above are shown in Figure 13 for damping ratios of 0.1 and 0.2. The data used to generate these plots is included in Appendix B.

Next, the applicability of the results from the

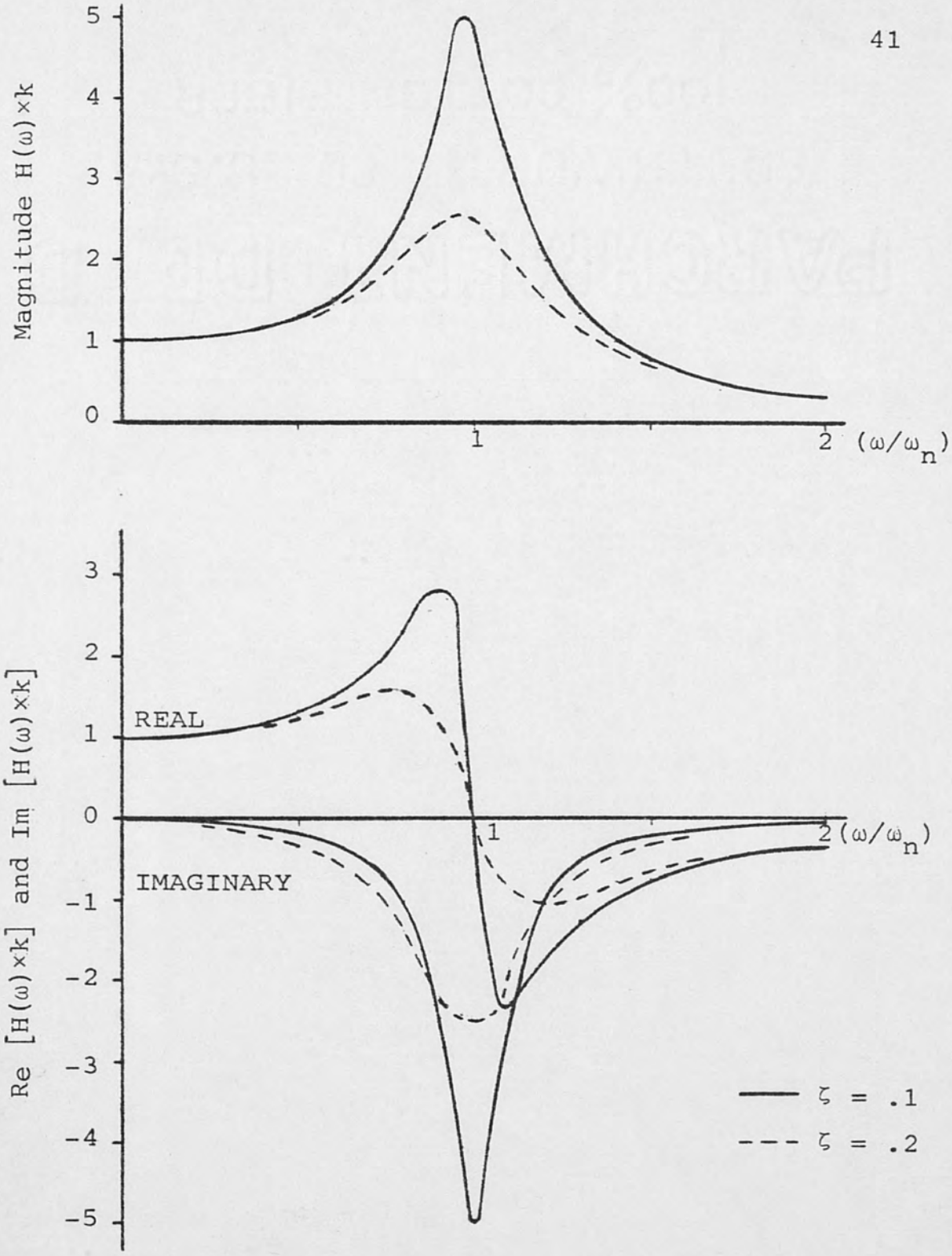

Figure 13. Magnitude, Real and Imaginary Parts of $H(\omega)\times k$ at $\zeta = .1$ and $.2$

single degree of freedom case should be verified for the multi-degree of freedom case. For this purpose the force response of an undamped two degree of freedom model will be investigated. Behavior of this model can be expressed by the matrix equation.

$$\begin{bmatrix} m_{11} & m_{12} \\ m_{21} & m_{22} \end{bmatrix} \begin{Bmatrix} \ddot{x}_1 \\ \ddot{x}_2 \end{Bmatrix} + \begin{bmatrix} k_{11} & k_{12} \\ k_{21} & k_{22} \end{bmatrix} \begin{Bmatrix} x_1 \\ x_2 \end{Bmatrix} = \begin{Bmatrix} f_1 \\ f_2 \end{Bmatrix} . \qquad \text{IV-13}$$

Taking Laplace transforms and assuming initial conditions zero,

$$\left(\begin{bmatrix} m_{11} & m_{12} \\ m_{21} & m_{22} \end{bmatrix} s^2 + \begin{bmatrix} k_{11} & k_{12} \\ k_{21} & k_{22} \end{bmatrix} \right) \begin{Bmatrix} X_1(s) \\ X_2(s) \end{Bmatrix} = \begin{Bmatrix} F_1(s) \\ F_2(s) \end{Bmatrix} . \qquad \text{IV-14}$$

As for the single degree of freedom case, the homogeneous case yields the characteristic equation as:

$$[B(s)] = [m]s^2 + [k] = 0$$

or

$$[B(s)] = 0$$

with roots s_1, s_2, s_3, and s_4

Again, define the transfer function as

$$[H(s)] = [B(s)]^{-1}$$

$$= \frac{\begin{bmatrix} (m_{22}s^2 + k_{22}) & -(m_{12}s^2 + k_{12}) \\ -(m_{21}s^2 + k_{21}) & (m_{11}s^2 + k_{11}) \end{bmatrix}}{(m_{11}s^2 + k_{11})(m_{22}s^2 + k_{22}) - (m_{21}s^2 + k_{21})(m_{12}s^2 + k_{12})} \qquad \text{IV-15}$$

where the denominator is the determinant of B(s), which can be expressed as

$$|B(s)| = A(s - s_1)(s - s_2)(s - s_3)(s - s_4),$$

and

$$\{X(s)\} = \frac{\begin{bmatrix} (m_{22}s^2 + k_{22}) - (m_{12}s^2 + k_{12}) \\ -(m_{21}s^2 + k_{21}) \quad (m_{11}s^2 + k_{11}) \end{bmatrix}}{|B(s)|}\{F(s)\}. \qquad \text{IV-16}$$

Then for:

$$H(s) = \begin{bmatrix} h_{11} & h_{12} \\ h_{21} & h_{22} \end{bmatrix},$$

taking only h_{11}:

$$h_{11}(s) = \frac{m_{22}s^2 k_{22}}{A(s - s_1)(s - s_2)(s - s_3)(s - s_4)}. \qquad \text{IV-17}$$

Then since:

$$[H(s)]\ \{F(s)\} = \{X(s)\}$$

which can be expanded to:

$$h_{11}F_1 + h_{12}F_2 = X_1$$

$$h_{21}F_1 + h_{22}F_2 = X_2.$$

Then for $F_2 = 0$

$$h_{11} = \frac{X_1}{F_1}$$

and

$$h_{21} = \frac{X_2}{F_1},$$

or in general

$$h_{ij} = \frac{X_i}{F_j},$$

which represents the transfer function for the response at i to a force at j with all other forces zero.

Returning to equation IV-17, noting that the coefficients of the characteristic equation are real, the roots will occur in conjugate pairs. Thus, the equation can be written as:

$$h_{11} = \frac{m_{22}s^2 + k_{22}}{A(s - p_1)(s - p_1^*)(s - p_2)(s - p_2^*)}.$$

Then from partial fraction expansion

$$h_{11} = \frac{A_1}{(s - p_1)} + \frac{A_2}{(s - p_1^*)} + \frac{A_3}{(s - p_2)} + \frac{A_4}{(s - p_2^*)}.$$

from which

$$A_1 = \frac{m_{22}p_1^2 + k_{22}}{A(p_1 - p_1^*)(p_1 - p_2)(p_1 - p_2^*)}$$

$$A_2 = A_1^*,$$

$$A_3 = \frac{m_{22}p_2^2 + k_{22}}{A(p_2 - p_1)(p_2 - p_1^*)(p_2 - p_2^*)} ,$$

$$A_4 = A_3^* .$$

Then

$$h_{11} = \frac{A_1}{(s - p_1)} + \frac{A_1^*}{(s - p_1^*)} + \frac{A_3}{(s - p_2)} + \frac{A_3^*}{(s - p_2)}$$

IV-18

which is a two degree of freedom transfer function represented as the sum of two single degree of freedom transfer functions. Rewriting as a summation yields

$$h_{11} = \sum_{k=1}^{2} \left[\frac{A_k}{(s - p_k)} + \frac{A_k^*}{(s - p_k^*)} \right] , \qquad \text{IV-19}$$

where A_k and A_k^* are the residues of the k^{th} pair of poles p_k and p_k^*, respectively. The other three transfer functions can be written the same way and $[H(s)]$ can be formed by substitution. Then in terms of partial fractions

$$|H(s)| = \frac{\begin{bmatrix} A_1 & C_1 \\ B_1 & D_1 \end{bmatrix}}{(s - p_1)} + \frac{\begin{bmatrix} A_2 & C_2 \\ B_2 & D_2 \end{bmatrix}}{(s - p_1^*)} + \frac{\begin{bmatrix} A_3 & C_3 \\ B_3 & D_3 \end{bmatrix}}{(s - p_2)} + \frac{\begin{bmatrix} A_4 & C_4 \\ B_4 & D_4 \end{bmatrix}}{(s - p_2^*)}$$

IV-20

where each of the A, B, C and D are constants and each matrix represents the residue matrix corresponding to

the associated pole. Examining only the first term in equation IV-20 and evaluating the constants as previously done for A_1,

$$B_1 = \frac{-(m_{21}p_1^2 + k_{21})}{A(p_1 - p_1^*)(p_1 - p_2)(p_1 - p_2^*)}$$

$$C_1 = \frac{-(m_{21}p_1^2 + k_{12})}{A(p_1 - p_1^*)(p_1 - p_2)(p_1 - p_2^*)}$$

$$D_1 = \frac{(m_{11}p_1^2 + k_{11})}{A(p_1 - p_1^*)(p_1 - p_2)(p_1 - p_2^*)}$$

which yields

$$\frac{\begin{bmatrix} A_1 & C_1 \\ B_1 & D_1 \end{bmatrix}}{(s - p_1)} = E\frac{\begin{bmatrix} (m_{22}p_1^2 + k_{22}) - (m_{12}p_1^2 + k_{12}) \\ -(m_{21}p_1^2 + k_{21}) \quad (m_{11}p_1^2 + k_{11}) \end{bmatrix}}{(s - p_1)} \qquad \text{IV-21}$$

where

$$E = \frac{1}{A(s - p_1^*)(s - p_2)(s - p_1^*)} .$$

An interesting conclusion can now be drawn. Equation IV-21 is identical to equation IV-16 evaluated at $s = p_1$. Also, the matrix in IV-16 is the adjoint matrix of $[B(s)]$. Then as stated by Richardson, Smith and Thornhill (5)

> Since the residue matrix is the same as the adjoint matrix evaluated at the r^{th} pole and because each row and column of the

adjoint matrix is proportional to the r^{th} mode shape vector, the conclusion is that each row and column of the residue matrix is also proportional to the r^{th} mode shape vector.

Next,determination of frequency response functions from experimental data will be investigated. As previously defined,the frequency response function $H(\omega)$ can be represented as the ratio of the Fourier transform of the output $Y(\omega)$ to the transform of the input $X(\omega)$ as shown in Figure 14a. This ratio could be used directly to calculate $H(\omega)$ from the transforms of measure impulse and response waveforms. However, the statistical variability of $Y(\omega)$ and $X(\omega)$ may cause degradation in the calculations. Therefore, better results can be obtained by calculating the frequency response function as the ratio of the cross-spectrum between the input and output to the power spectrum of the input (7). This is derived as follows:

$$H(\omega) = Y/X$$

$$H(\omega) = YX^*/XX^*$$

$$H(\omega) = G_{yx}/G_x \qquad \text{IV-22}$$

where:

X^* = complex conjugate of $X(\omega)$

$G_x(\omega) = XX^* \equiv$ input auto spectrum

$G_y(\omega) = YY^* \equiv$ output auto spectrum

$G_{yx}(\omega) = YX^* \equiv$ output-input cross-spectrum .

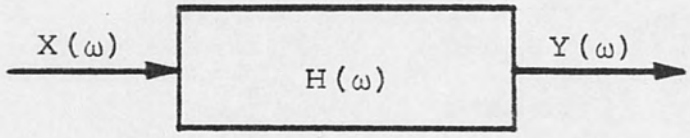

Figure 14a. Simple Linear System

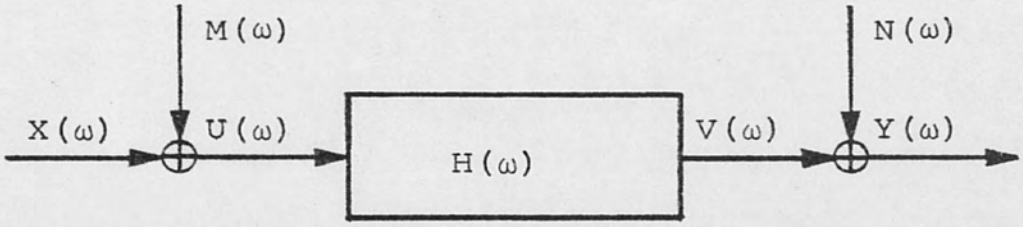

Figure 14b. System With Noise in Input and Output Measurement

To illustrate the advantages of this method of calculating $H(\omega)$, consider the system shown in Figure 14b. The quantities $M(\omega)$ and $N(\omega)$represent the transforms of the noise m(t) and n(t) in the input and output signals respectively. Computing the measured frequency response function

$$H'(\omega) = (V(\omega) + N(\omega)) \; / \; (U(\omega) + M(\omega)) \; . \qquad \text{IV-23}$$

Computing the frequency response function from equation IV-22

$$H'(\omega) = \frac{(G_{uv} + G_{un} + G_{mv} + G_{mn})}{(G_u + G_{um} + G_{mu} + G_m)} \qquad \text{IV-24}$$

Assuming measurement noise m(t) and n(t) are noncoherent with each other and the input signal u(t), the expected value of cross-spectrum terms involving m and n in equation IV-24 will equal zero. Thus, equation IV-24 reduces to:

$$H'(\omega) + G_{uv} \; / \; (G_u + G_m)$$

From equation IV-22 the true frequency response function is

$$H(\omega) = G_{uv} \; / \; G_u$$

Then $H'(\omega) = H(\omega) \; / \; (1 + (G_m \; / \; G_u)$

Therefore, for smaller values of $G_m \; / \; G_u$ better approximations of the true frequency response function are achieved from the measured one. However, some

additional error will occur during calculation of the cross-spectrum.

The accuracy of the measured frequency response function can be improved by averaging a number of input and response measurements. The accuracy of the calculated spectra will increase with the number of measurement averages. Large numbers of averages employed in some measurement techniques often reduce error due to noise to insignificant levels. However, many averages are usually not used in the impulse technique; otherwise the advantage of speed would be lost.

Use of the spectral method of calculating frequency response functions also provides a measurement of the noise contamination and nonlinear effects through the coherence function. The coherence function (γ^2) is defined as:

$$\gamma^2(\omega) = |G_{xy}|^2 / (G_x G_y)$$

$$\gamma^2(\omega) \equiv \frac{\text{response power caused by the measured input}}{\text{total measured response power}}$$

The range of γ^2 is from 0, for totally uncorrelated signals, to 1 for noiseless measurement of a linear system.

Since the previous derivation involved primarily the displacement frequency response function, the applicability of the velocity and acceleration frequency

response functions should be mentioned. The displacement frequency response function is the so called receptance, which is the ratio of the transformed displacement to the transformed force. The velocity frequency response function is the so called mobility and represents the ratio of the velocity to force transforms. Similarly, the acceleration frequency response function or inertiance is the acceleration transform to force transform ratio. All three functions contain the same information about the system and each can be determined from the other (5).

The general methods for obtaining and analyzing the frequency response functions as well as detailed description of the analysis performed on the shock tube are included in the next section.

Modal Analysis Method

In this section the general method of modal analysis via impulse testing is discussed and the investigation of shock tube dynamic characteristics is described. The general methods portion includes discussion of impulse test measurement technique and modal parameter identification from measured frequency response functions. The description of the shock tube analysis includes a summary of the equipment, configuration and procedures used to obtain impulse and response data, a description

of the methods used to obtain transfer function from measured data, and discussion of efforts to determine shock tube modal parameters.

General Methods

The general method of modal analysis through impulse or impact testing involves determining modal parameter from measured impulse/response data. The data is obtained by striking the structure under test with an impactor, which has a dynamic load cell attached so that the impulse can be measured and recorded. Simultaneously, the response at some point on the structure is measured and recorded from an attached transducer, usually an accelerometer. From the Fourier transforms of the impulse and response signals a frequency response function is formed. By changing the position of the impulse and/or response measurement on the structure elements of the transfer function matrix can be obtained. From one row or column of this matrix, modal parameters of the structure can be determined. Several apsects of the impulse test method will be discussed below, in more detail.

Various impactor configurations are available for impulse testing. The impactor consists of a hand held hammer-like instrument with a force transducer, several types of impact caps and extensions. Figure 15 is a

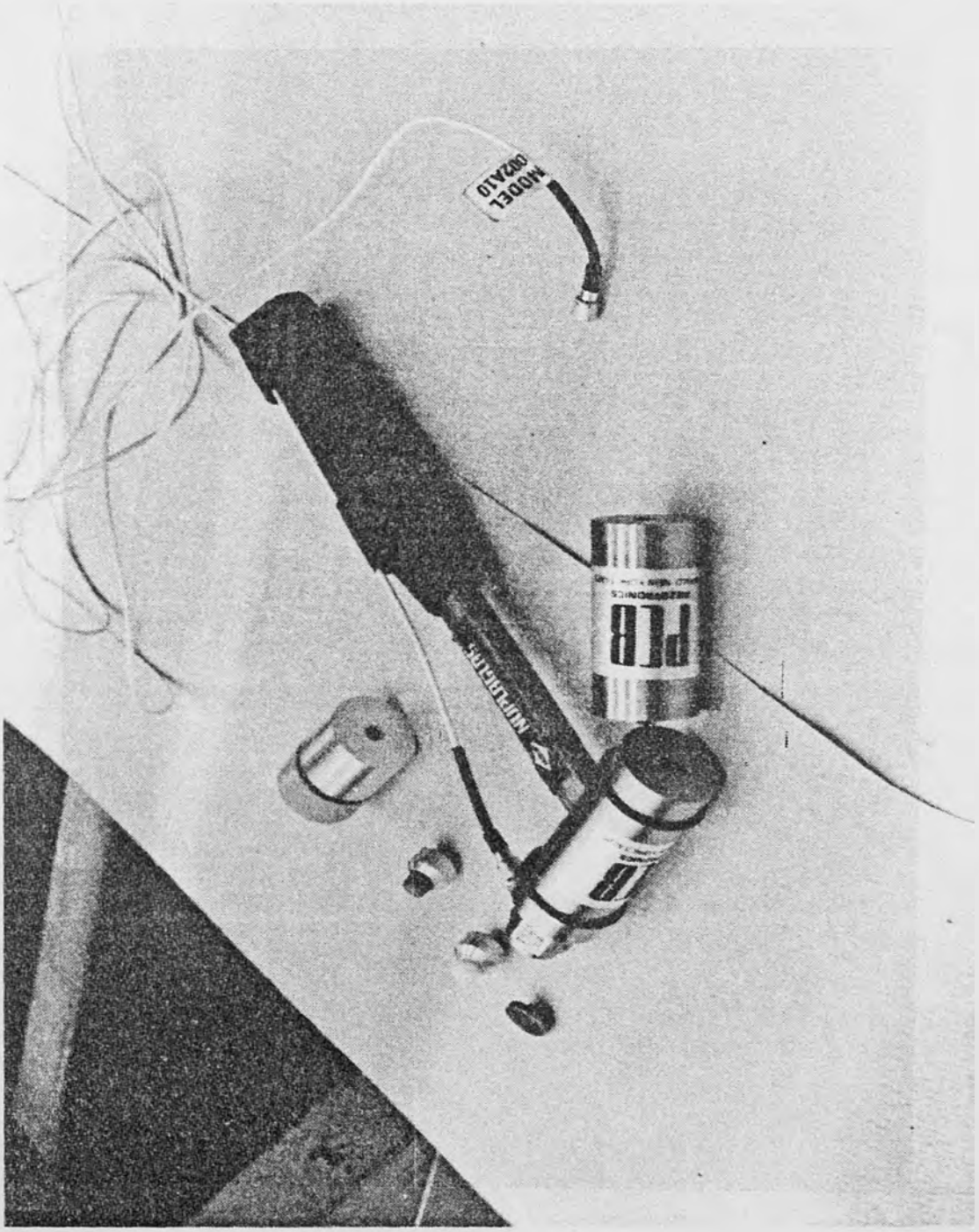

Figure 15. Impulse Hammer and Accessories

photograph of an impactor (impulse hammer) and accessories. The impact cap mounts on the transducer and is the point of contact between hammer and structure during tests. The extension can be connected to the opposite side of the hammer to increase its mass (7).

By varying the impact cap and hammer mass, different impulse shapes and corresponding impulse frequency contents can be obtained. For example, using a hard impact cap, such as a steel one, will yield a shorter duration impulse with faster rise and wider frequency range than will a softer impact cap, such as rubber or plastic. Also, addition of an extension will increase the pulse duration and amplitude and decreasing the frequency range from that obtained with the hammer's original mass. Thus, the impactor configuration must be selected to impart force pulses with frequency content in the range of interest (7).

Once impulse and response data are obtained, some windowing techniques are usually used to reduce the effects of noise and other digital signal processing problems. For example, a modified Hanning window (modified vers sine) can be applied to the impulse time domain waveform to reduce digitizer or bit noise. Also, an exponential window of the form:

$$X(t) = \exp(-at)$$

is often applied to the response waveform to reduce leakage problems, which result when a lightly damped response waveform does not decay to zero within the measured window. Anti-aliasing (low pass) filters may also be required if the impulse contains frequency content above the Nyquist folding frequency, which is defined as:

$$\frac{\omega_0}{2} = \frac{\pi}{(SA)}$$

where:

$\frac{\omega_0}{2}$ ≡ Nyquist folding frequency in radian/sec

SA ≡ sampling time in sec.

Processing of the impulse/response data is accomplished using a computer and FFT algorithm or a Fourier analyzer from which frequency response functions are obtained. Modal parameters of the structure under test are obtained from the frequency response function using one of several methods. For complex functions with closely coupled modes and/or high damping, a multiple mode curve fitting technique may be required. For data containing more distinct modes and lighter damping, a simpler, single mode technique may be adequate. Multimode methods involve assuming a curve shape based on an apparent number of natural frequencies in a frequency

band and fitting the assumed curve to the frequency response waveforms. Discussion of the details of these procedures are beyond the scope of this report. The single mode methods involve selecting values from the frequency response functions at or near an apparent pole and determining dynamic characteristics based on the assumption that the structure behaves as a single degree of freedom system at each resonant frequency. Two single mode techniques are discussed below (7).

From frequency response function data, structural dynamic characteristics can often be determined using one of two, simple, single mode methods. One technique, the half power method, involves determining the resonant frequency and damping from the magnitude of the frequency response function. This is illustrated in the upper plot Figure 16, which is the magnitude of a single degree of freedom frequency response function, $|H(\omega)|$. Since $|H(\omega)|$ is the square root of the magnitude squared where:

$$|H(\omega)|^2 = H(\omega)H(\omega)^*$$

$$|H(\omega)^2| = \frac{r^2}{(1 - (\omega/\omega_n)^2)^2 + (2\zeta(\omega/\omega_n))^2},$$

then

$$|H(\omega)| = \frac{r}{1 - (\omega/\omega_n)^2 + 2\zeta(\omega/\omega_n)}$$

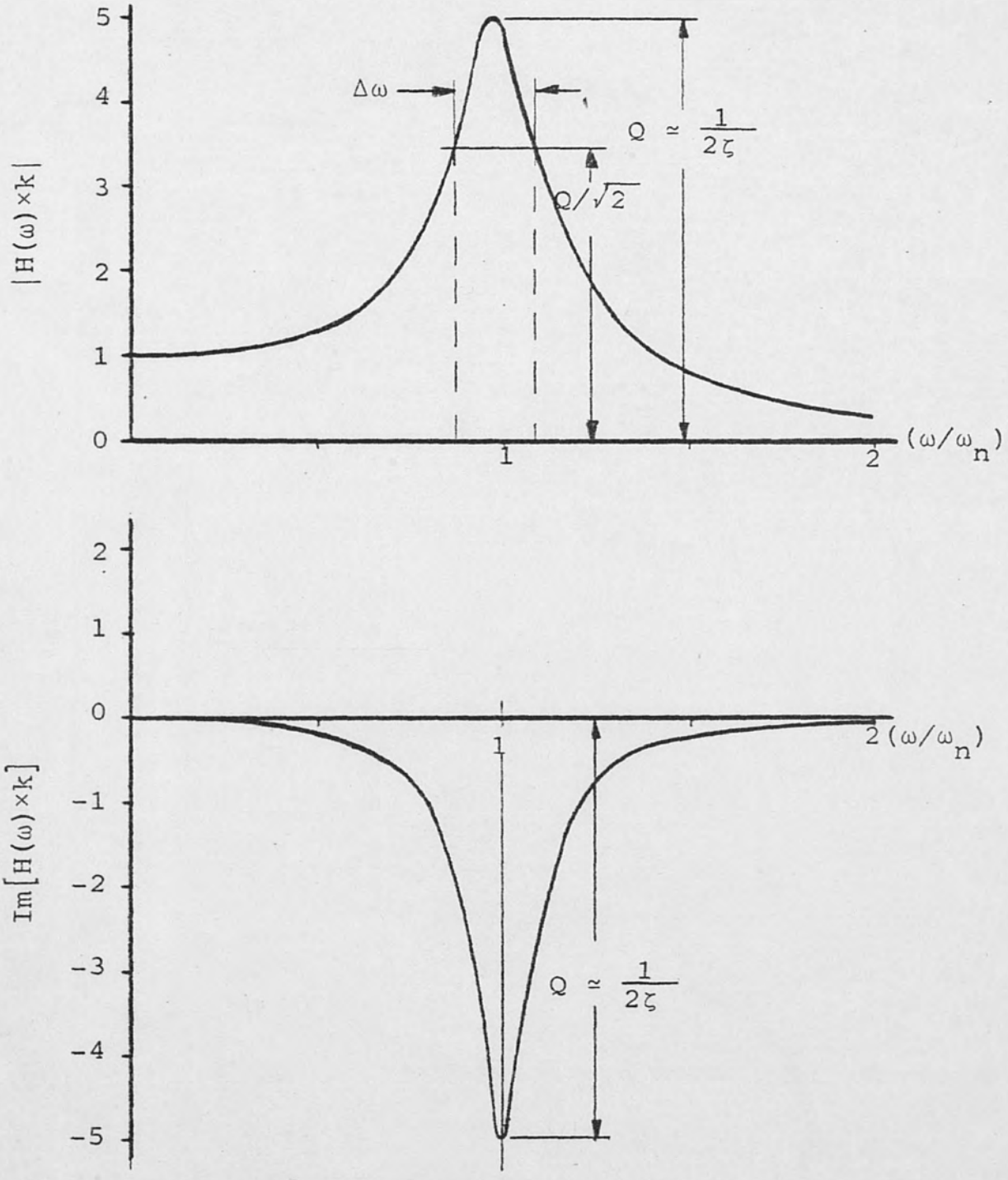

Figure 16. Single Mode Curve Fitting for Magnitude and Quadrature Transfer Functions

where:

r ≡ modal residue.

Differentiating $|H(\omega)|$ with respect to ω to determine the peak amplitude yields

$$\omega = \omega_n \sqrt{1 - 2\zeta^2} \quad .$$

Thus, the peak occurs at a frequency below both the natural frequency ω_n and the damped natural frequency ω_d. However, for $\zeta << 1$ (light damping) the peak occurs very near ω_n. This peak amplitude is known as the "Q" of the system, from which the damping ratio of the system can be determined from:

$$Q \simeq \frac{1}{2\zeta}$$

Also, ζ can be determined from the ratio of the half power point frequency bandwidth to resonant frequency as:

$$\zeta = \frac{\Delta\omega}{2\omega_n} \quad .$$

Both of these methods for obtaining ζ are shown in the upper plot in Figure 16.

The quadrature response, or quadrature picking, technique can also be used to determine resonant frequencies, damping coefficients, and mode shape vectors. This technique gets its name from the use of the imaginary part of the transfer function or quadrature

frequency response function. As shown in the lower plot of Figure 16 the damping ratio ζ can be determined from the amplitude at resonance. Also, from the transfer function described by:

$$H(s) = \frac{r}{2j(s - p)},$$

the real and imaginary parts are

$$Re(H(\omega)) = \tfrac{1}{2}\left\{\frac{r_1(\omega_d - \omega) + r_2\sigma}{(\omega_d - \omega)^2 + \sigma^2}\right\}$$

and

$$Im(H(\omega)) = \tfrac{1}{2}\left\{\frac{r_2(\omega_d - \omega) - r_1\sigma}{(\omega_d - \omega)^2 + \sigma^2}\right\}$$

where:

$r = r_1 + jr_2 \equiv$ complex residue

p and s are as defined previously.

At a modal resonance these expressions become:

$$Re(H(\omega)) = r_2/2\sigma$$

and

$$Im(H(\omega)) = r_1/2\sigma$$

However, in the case of light damping, resideus are usually real valued.

Therefore,

$$Re(H(\omega)) = 0.$$

Then the mode shape vector can be obtained by picking

the quadrature amplitude for each measurement at the modal resonant frequency.

From the above discussion it can be concluded that impulse testing is a useful tool for modal analysis of structures. The specific use of the technique in analysis of the shock tube is discussed below.

Shock Tube Dynamic Analysis

The following pages contain a detailed description of methods used to investigate shock tube dynamic characteristics. First, the instrumentation, test configuration and test procedure are discussed. Next, the impulse and response data obtained is described. The data processing procedure used to obtain frequency response functions is then summarized. Finally, the use and applicability of the single mode fitting technique is discussed.

The equipment used to conduct the investigation of shock tube dynamic characteristics is as follows:

1. Impulse Hammer - PCB Piezotronics model #086A05, with force tranducer model #208A05, S/N 1741, natural frequency 70 k Hz, assembly sensitivty 1000 lbf/volt

2. Response Accelerometer - PCB Piezotronics model #302A, S/N 4611, natural frequency > 35 k Hz, sensitivity 99.01 g's/volt, or model #308B, S/N 4624, natural frequency 26 k Hz, sensitivty 10.1 g's/volt

3. Transducer Power Supply - PCB Piezotronic model #480, 2 required

4. Trigger Amplifier - U.C.F. fabricated

5. DPO - Tektronic Inc., model #7704-A

6. Summing Amplifier - U.C.F. fabricated

7. Delay Circuit - U.C.F. fabricated

Any other equipment was obtained with performance parameter satisfying test configuration requirements.

Figure 17 illustrates the test configuration used. The impulse was applied to the tube by the impulse hammer. Figure 18 is a photograph of the hand held hammer and a pendulum mounted one. The response was measured from the accelerometer which was mounted to the structure at various points of interest. The transducer power supplies are the power sources for the tranducers' internal amplifiers. The delay circuit was used to delay the signal, allowing time for the DPO to be triggered. The trigger amplifier converts the impulse force signal to a trigger signal for the DPO. The summing amplifier could be used to add the impulse and response waveforms. The DPO displayed the waveforms which were digitized and stored in one of four memory locations. Figure 19 is a photograph of the signal processing electronics and DPO.

The procedure for obtaining impulse/response measurements, using the summing amplifier, was as follows:

1. Set up shock tube in desired configuration (empty or filled, etc.)

2. Install response accelerometer at desired location on tube.

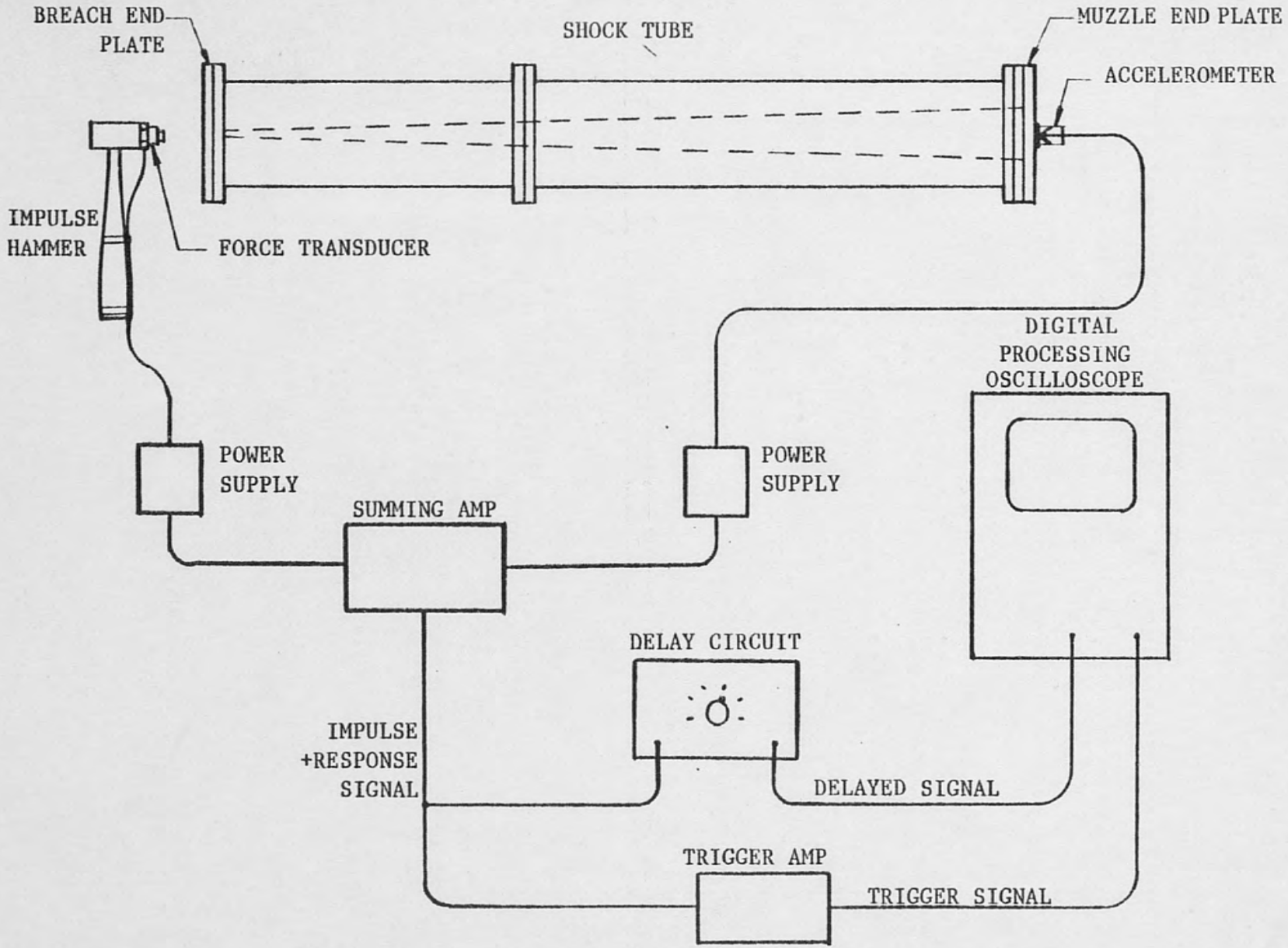

Figure 17.. Impulse Test Configuration

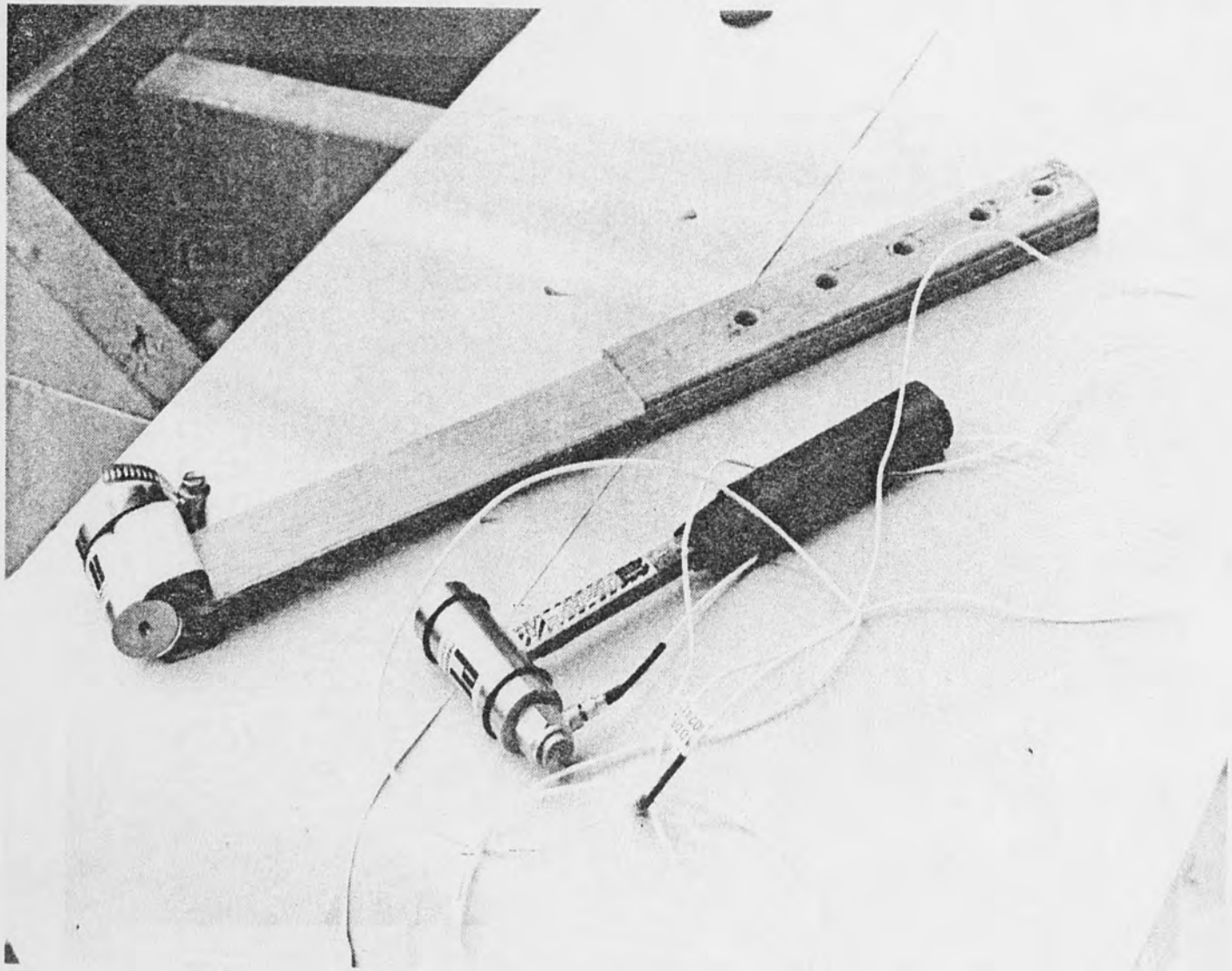

Figure 18. Hand Held and Pendulum Mounted Impulse Hammer

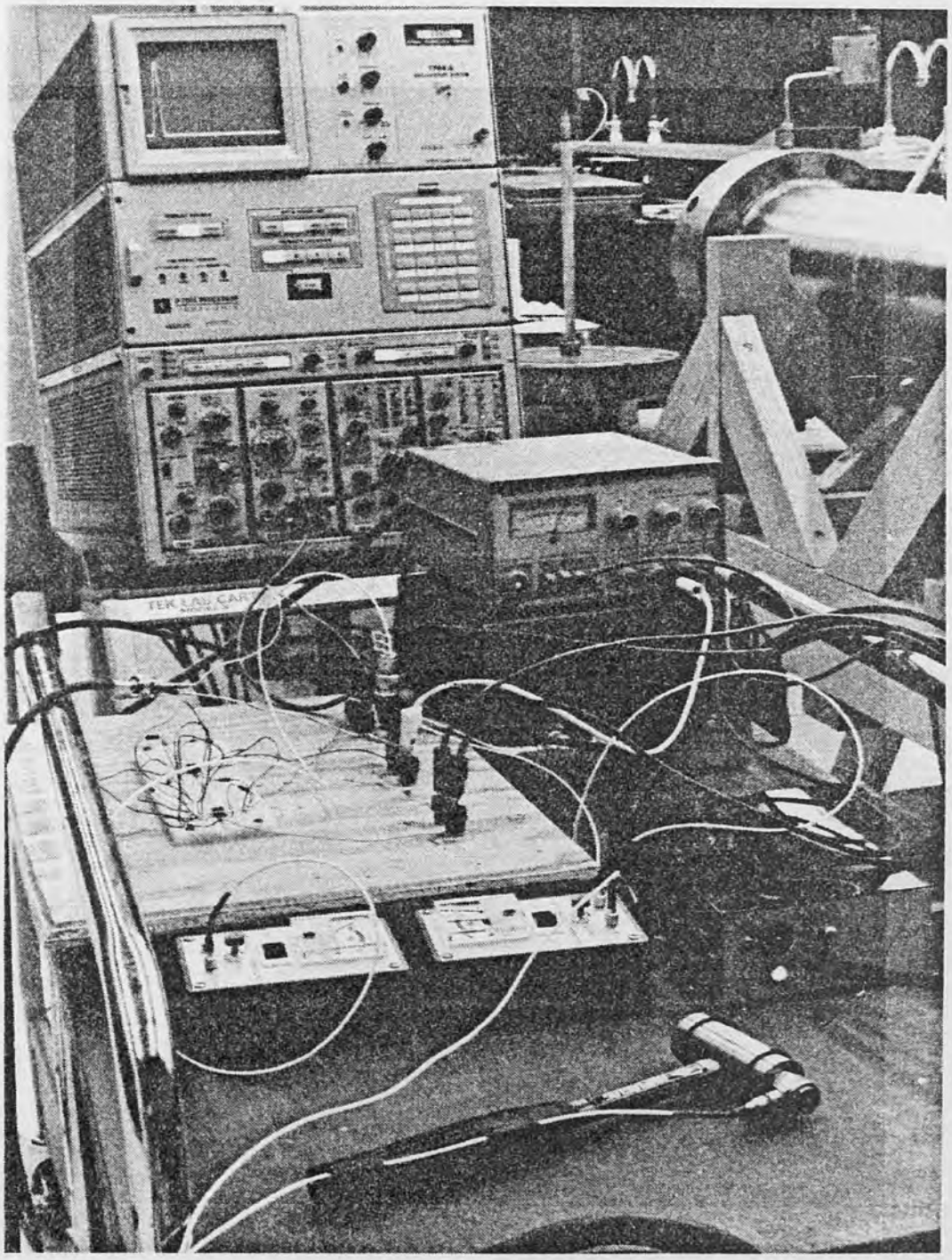

Figure 19. Signal Processing Electronics and DPO

3. Record impulse waveform alone by disconnecting accelerometer cable

4. Modify impulse hammer to obtain desired impulse shape (if required)

5. Re-connect response accelerometer

6. Obtain and record impulse and response waveforms on DPO

7. Adjust DPO as required

8. Record 2 separate impulse/response waveforms and visually compare to verify repeatability of data

9. Leave the data waveform in one memory location and move accelerometer or change tube configuration for next measurement

This procedure was used, with some exceptions, throughout the impulse testing.

The summing amplifier could only be used when the impulse and response measurement position were physically far enough apart to create a time lag separating the signals. When the summing amplifier was not used the above procedure was used except that the impulse and response were recorded as two separate waveforms and each was verified for repeatability separately. Also, in this case a pendulum mounted impulse hammer was used in order to obtain consistent scope triggering and therefore proper time correlation between impulse and response. The pendulum mounted impulse hammer and fixture are shown installed at the breach end of the tube in Figure 20.

Another exception to the procedure was that steps 3

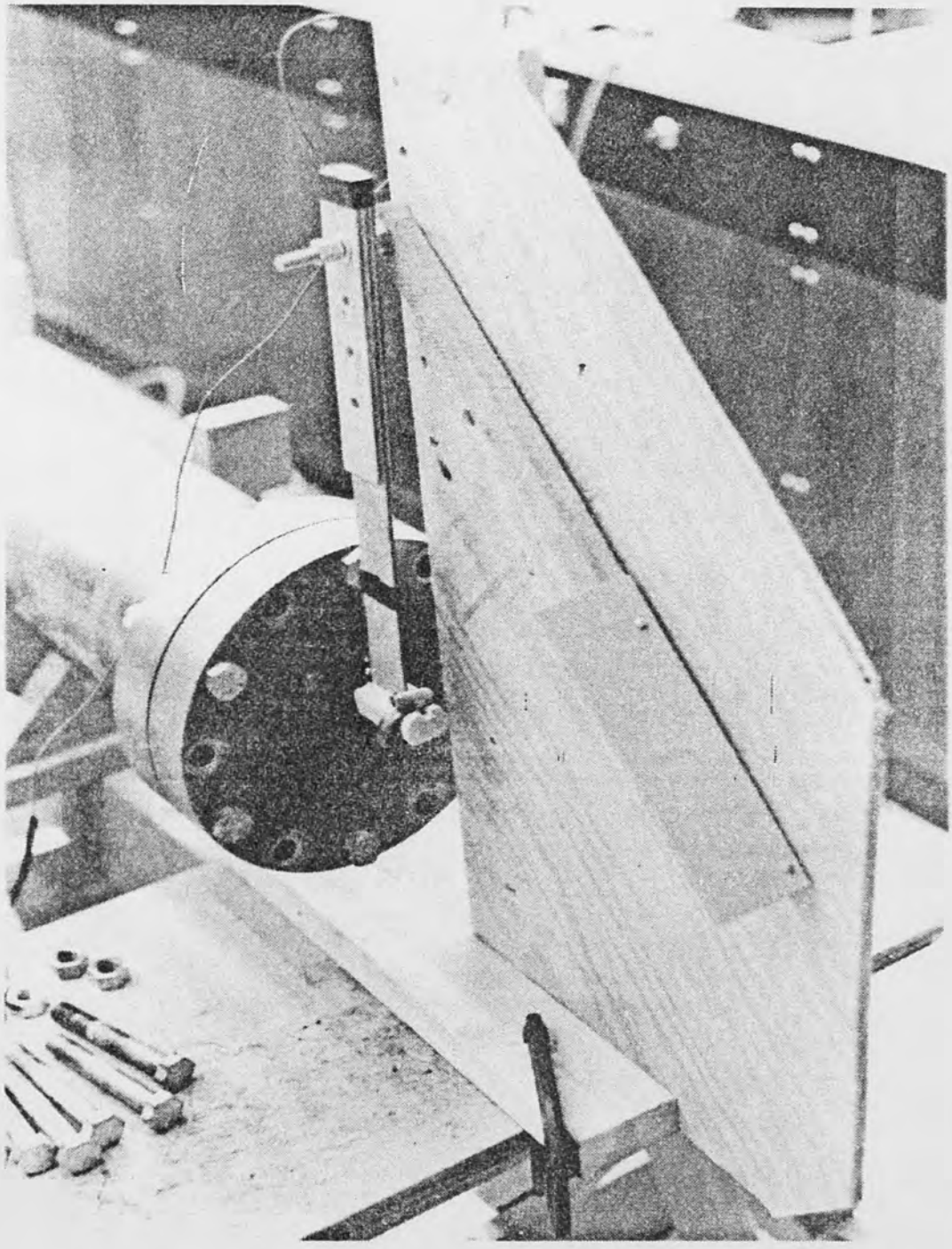

Figure 20. Pendulum Mounted Impulse Hammer

and 4 were only performed once, early in the investigation. Since a wide band of frequencies was to be investigated, the hammer was set up with a steel impact cap and no extension. This was done to yield the shortest possible pulse duration so that the widest range of frequencies could be excited in the shock tube structure.

Quite a number of impulse and response data waveforms were obtained during impulse testing. All impulse data were obtained from impacts near the center of the breach end plate. Response data waveforms were obtained from accelerometers mounted in a number of different positions and orientations on the shock tube. All data was obtained with the lenolium gasket in the flanged joint between the 4 and 6 foot tube sections. Two sets of impulse/response data waveforms were obtained from a response accelerometer mounted on the end of a dummy stinger, in the axial orientation. Figure 21 shows this configuration. Four sets of impulse/response data were obtained from an accelerometer mounted in the radial orientation, on the tube exterior, near the muzzle end. Details concerning these six sets of data waveforms are contained in Table 1. The data file names indicated in the table refer to the files on the floppy disk where each waveform was stored. The remainder of the impulse response data was obtained from an accelerometer mounted

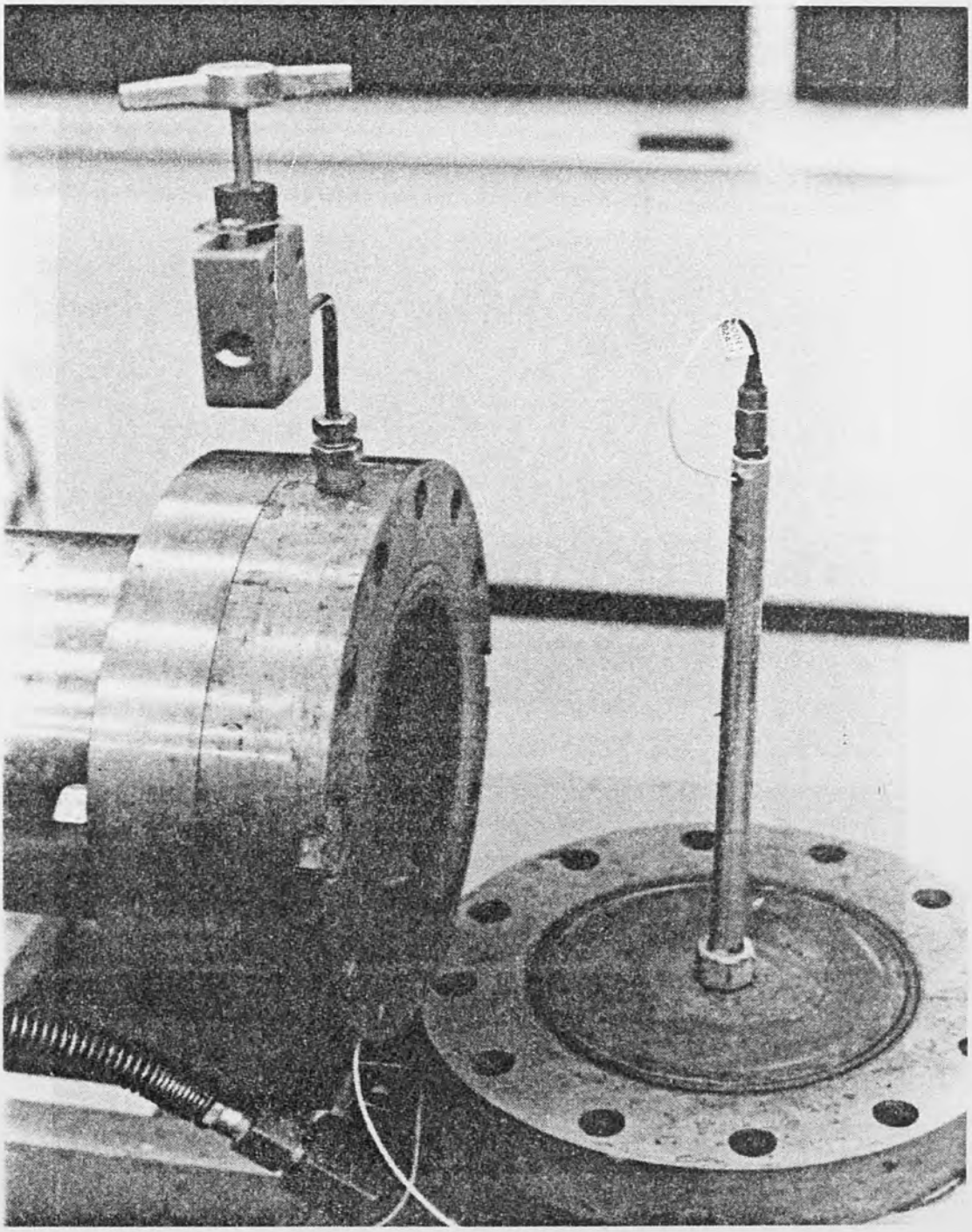

Figure 21. Response Accelerometer Mounted on Dummy Stinger

TABLE 1

Stinger and Radial Impulse Response Data Summary

DATA FILE NAME	ORIENTATION	TUBE FILLED	ACCELEROMETER MODEL	ACCELEROMETER POSITION
"IMT1.DAT" "RET1.DAT"	AXIAL AXIAL	NO	302A	End of Dummy Stinger
"IMT2.DAT" "RET2.DAT"	AXIAL AXIAL	YES	302A	End of Dummy Stinger
"IMPS1.DAT" "RESS1.DAT"	AXIAL RADIAL	YES	302A	Top Exterior of Tube, 32" From Muzzle
"IMPS2.DAT" "RESS2.DAT"	AXIAL RADIAL	YES	302A	North Side Exterior of Tube, 32" From Muzzle
"IMPS3.DAT" "RESS3.DAT"	AXIAL RADIAL	YES	302A	South Side Exterior of Tube, 32" From Muzzle
"IMPS4.DAT" "RESS4.DAT"	AXIAL RADIAL	YES	302A	Bottom Exterior of Tube, 32" From Muzzle

in the axial orientation at various positions along the length of the tube's exterior. These data were obtained to investigate the longitudinal modal characteristics of the shock tube. The test configuration is as illustrated schematically in Figure 22. Figure 23 shows the accelerometer mounted at the 6 ft. position. Details concerning these impulse/response measurements are summarized in Table 2. It should be noted from this table that an impulse waveform may be associated with several response waveforms. This is because the repeatability of the pendulum mounted hammer impulses allows multiple response measurements for a single impulse measurement.

All impulse/response data waveforms were taken directly from the DPO memory and stored in floppy disk data files on the PDP 11/34 computer. A procedure involving three special purpose computer programs was used to obtain frequency response functions from the data waveforms. The first step in the procedure was the use of program "DATS.BAS" to prepare impulse and response waveforms for later processing. Operations performed on waveforms in program "DATS.BAS" include multiplication by transducer sensitivities, correction of vertical and horizontal units and application of windows. The next step in the procedure was the use of program "IMX.BAS" to obtain FFTs of the prepared data waveforms. The final

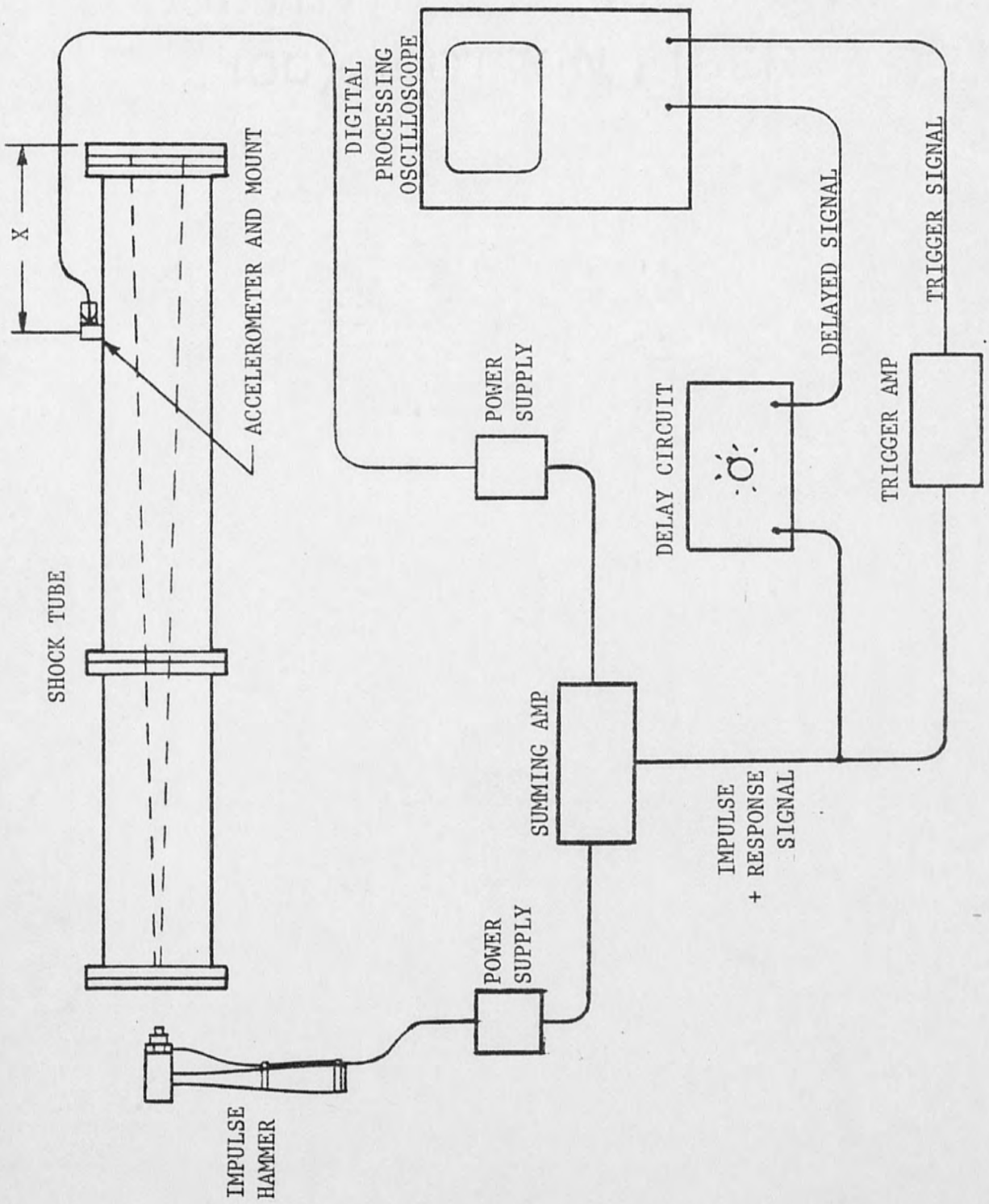

Figure 22. Longitudinal Mode Test Configuration

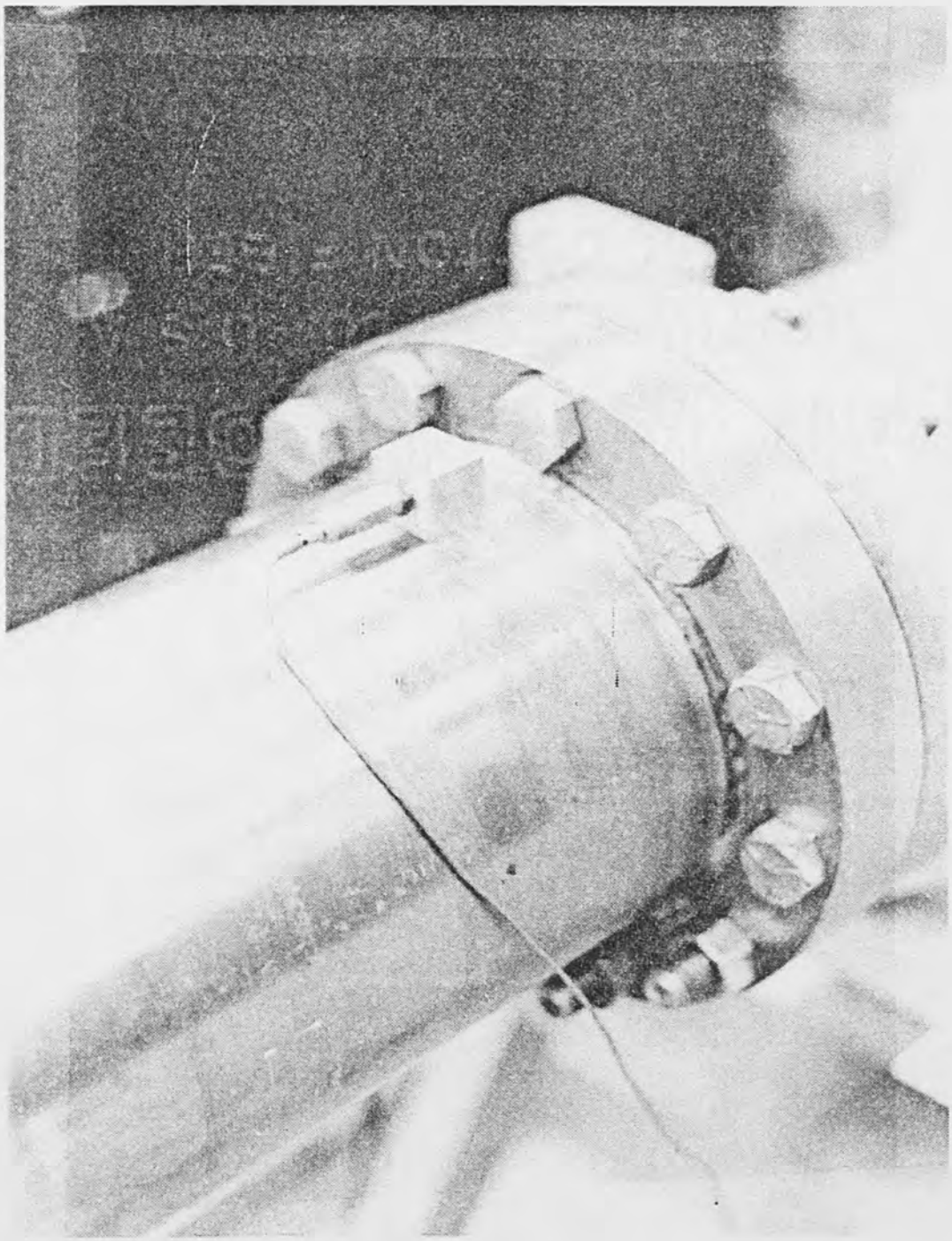

Figure 23. Response Accelerometer Mounted at the Six Foot Position

TABLE 2

Shock Tube Longitudinal Modal Analysis Data

DATA FILE NAME	TUBE FILLED	ACCELEROMETER MODEL	X DISTANCE FROM MUZZLE END PLATE
"IMP2.DAT" "RES2.DAT"	NO	302A	0.0 ft. (at center of plate)
"IMP4.DAT" "RES4.DAT"	YES	302A	0.0 ft. (at center of plate)
"IMM1.DAT" "RESM1.DAT"	YES	302A	1.0 ft.
"IMM2.DAT" "RESM2.DAT"	YES	302A	2.0 ft.
"IMM3.DAT" "RESM3.DAT"	YES	302A	3.0 ft.
"IMM4.DAT" "RESM4.DAT"	YES	302A	4.0 ft.
"IMM5.DAT" "RESM5.DAT"	YES	302A	5.0 ft.
"IMM6.DAT" "RESM6.DAT"	YES	308B	6.0 ft.

TABLE 2-Continued

DATA FILE NAME	TUBE FILLED	ACCELEROMETER MODEL	X DISTANCE FROM MUZZLE END PLATE
"IMM6.DAT" "RESM7.DAT"	YES	308B	7.0 ft.
"IM8.DAT" "REM8.DAT"	YES	302A	8.0 ft.
"IMM9.DAT"	YES	308B	8.0 ft.
"IMM9.DAT" "RESM9.DAT"	YES	308B	9.0 ft.
"IMM9.DAT" "RESM.DAT"	YES	308B	10.0 ft.

step in the procedure was the use of program "ADIM1.BAS" to obtain frequency response functions and a coherence function from transformed data waveforms. Descriptions and printouts of programs "DATS.BAS", "IMX.BAS", and "ADIM1.BAS" are included in Appendix A.

The investigation of shock tube dynamic characteristics from frequency response function data was accomplished in three basic steps. First, the frequency response of the stinger was investigated. Next, the radial or breathing modes of the tube were studied. Finally, the longitudinal mode shapes and frequencies of the shock tube were determined.

The investigation of the stinger's frequency response involved inspection and interpretation of the associated transfer function data. Of main interest were the frequencies of stinger vibration. This was determined from the resonant peaks indicated in the frequency response function imaginary and magnitude parts.

The investigation of shock tube radial modes consisted of inspecting the four radial transfer function waveforms. This was done to determine if these modes of vibration are radially symmetric in spite of gravitational loading and support conditions.

The investigation of longitudinal modes of shock tube vibration involved the use of a modified, single

mode, curve fitting methods to determine mode shapes at apparent resonant frequencies. The magnitude and imaginary parts of all longitudinal frequency response function waveforms were used to determine mode shapes (eigenvector) using the following procedure:

1. Identify apparent resonant frequencies from peaks in all the frequency response waveforms

2. Estimate the signed magnitude of the frequency response function at the resonant frequencies (from step 1) using both magnitude and imaginary parts of data (an attempt was made to take into account contributions from closely spaced modes)

3. Form the eigenvectors from the values determined in step 2 for each resonant frequency

4. Normalize the eigenvectors by dividing the values in each vector by the largest value in each

The results of this and the other two investigations are discussed in the next section.

Dynamic Analysis Results

This section contains discussions of the results obtained from the investigation of shock tube dynamic characteristics. First, a full set of typical modal analysis data, from impulse and response waveforms to frequency response functions is discussed. Next, some frequency response results are presented and interpreted. The longitudinal modal characteristics of the tube, estimated from frequency response function data, are then presented. Finally, predicted modal results from a

finite element model computer analysis, used as a verification tool, are discussed.

As mentioned in the previous section, a procedure consisting of the use of three computer programs was used to obtain frequency response function waveforms from impulse and response measurements. Figures 24 through 33 are the various plots obtained through this procedure, from programs "DATS.BAS", "IMX.BAS" and "ADMI1.BAS", for impulse and response waveforms from "IMP4.DAT" and "RES4.DAT". Figures 24 and 25 are plots of measured impulse and response data multiplied by the impulse hammer and response accelerometer sensitivities, respectively. Figure 26 is the response waveform of Figure 25 with the mean value subtracted from it. Figure 27 is a plot of the response waveform of Figure 26 multiplied by an exponential window. The window used was devised to decay from 1 to .25 in 5 m sec. These four plots were obtained using program "DATS.BAS". Figure 28 is a plot of the FFT magnitude of the impulse waveform for frequencies between 0 and 5 k Hz. Figure 29 is a plot of the FFT magnitude of the response waveform for 0 to 5 k Hz. These two plots were obtained using program "IMX.BAS". The next 3 figures, 30, 31 and 32, are the real and imaginary parts and magnitude of the frequency response function, respectively.

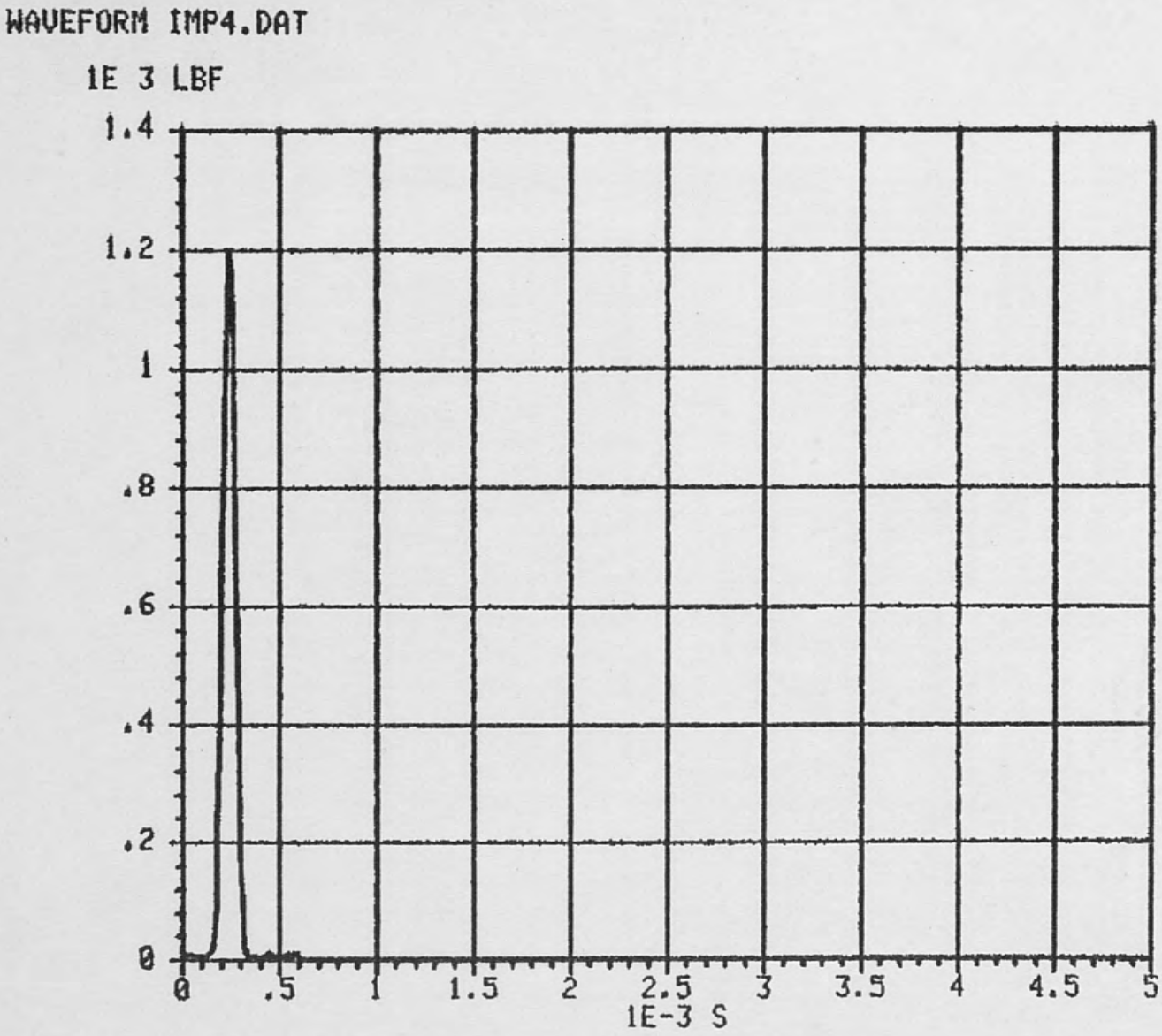

Figure 24. Impulse Waveform from "IMP4.DAT"

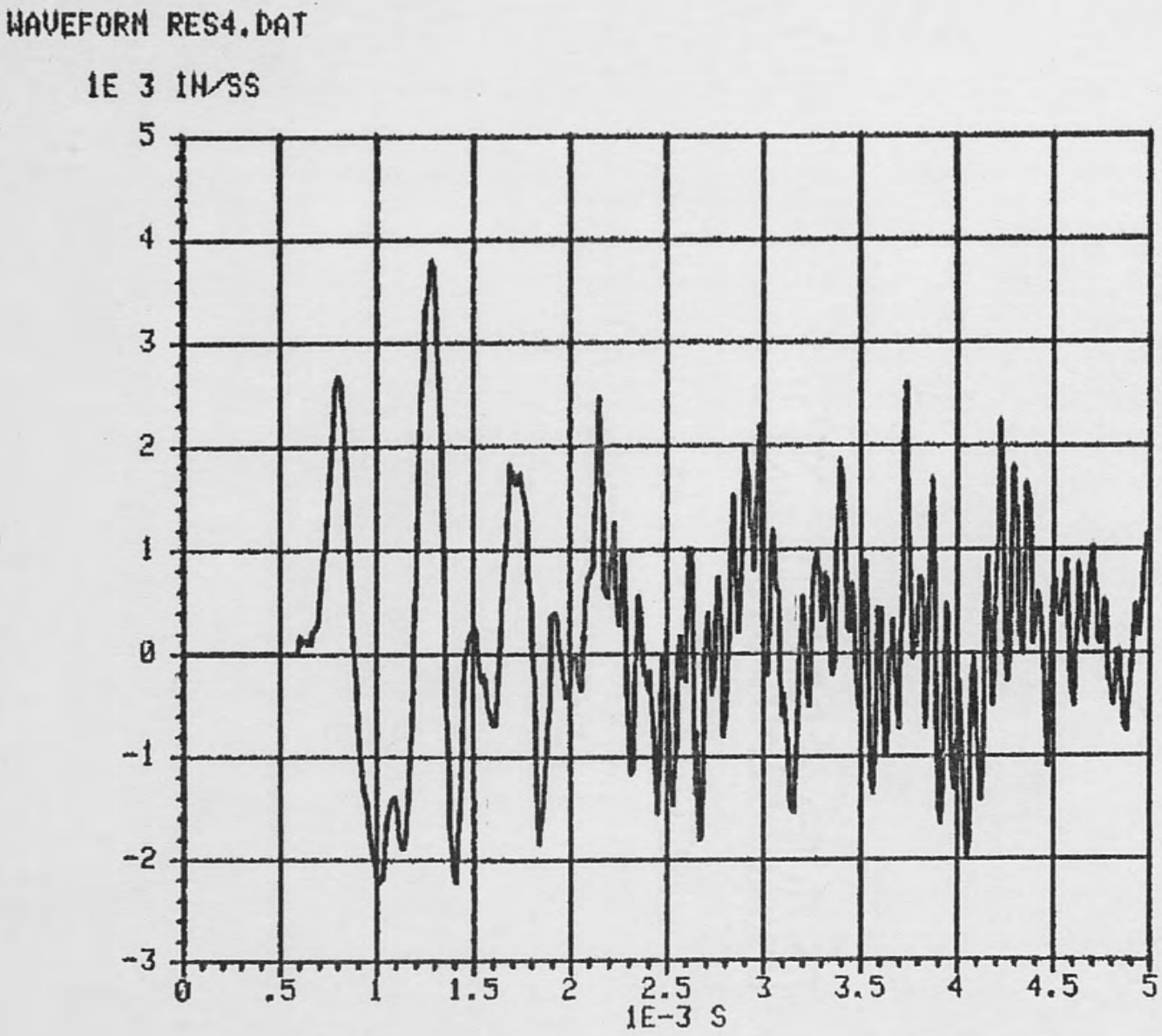

Figure 25. Response Waveform from "RES4.DAT"

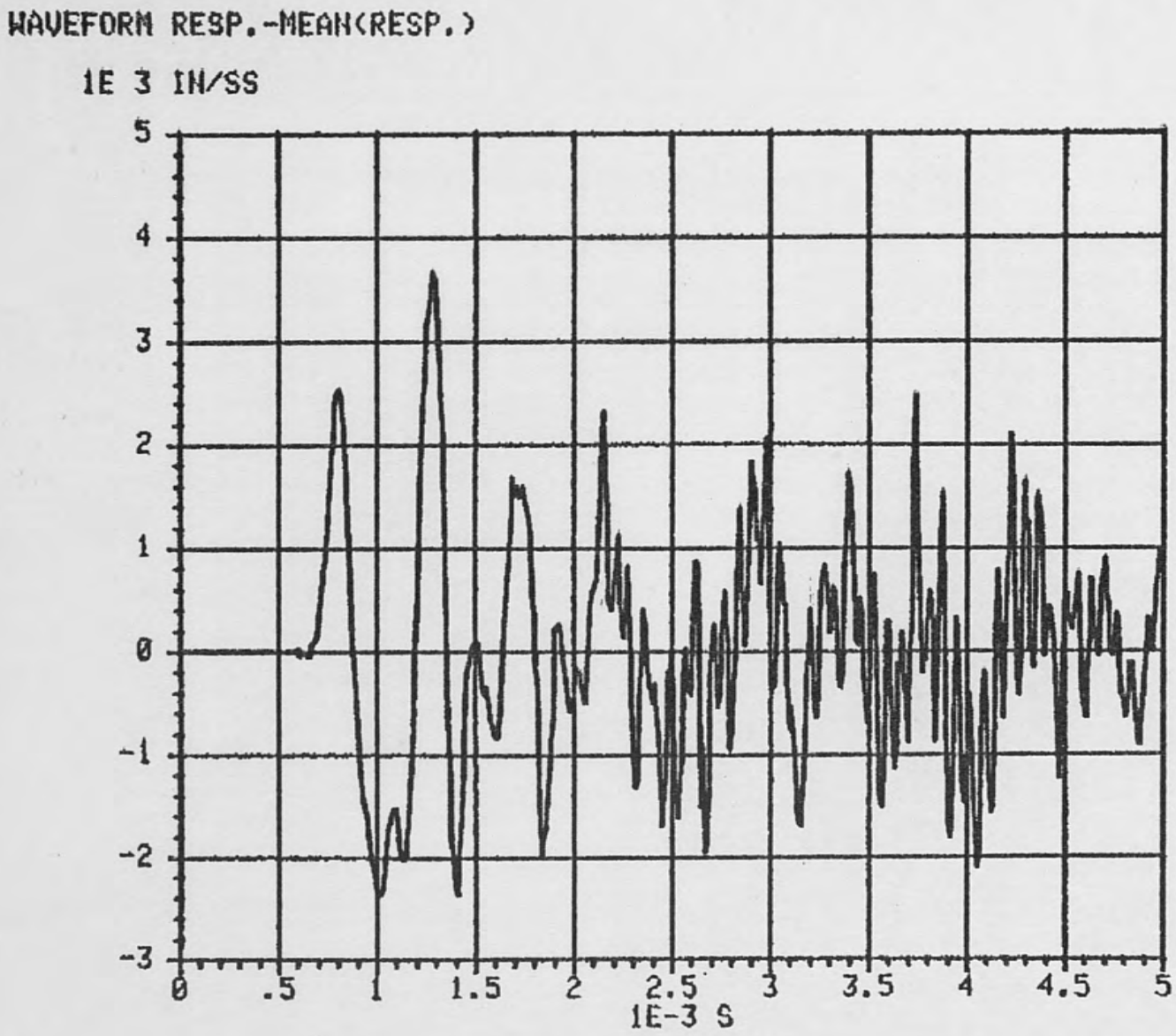

Figure 26. Response Waveform With Mean Value Removed

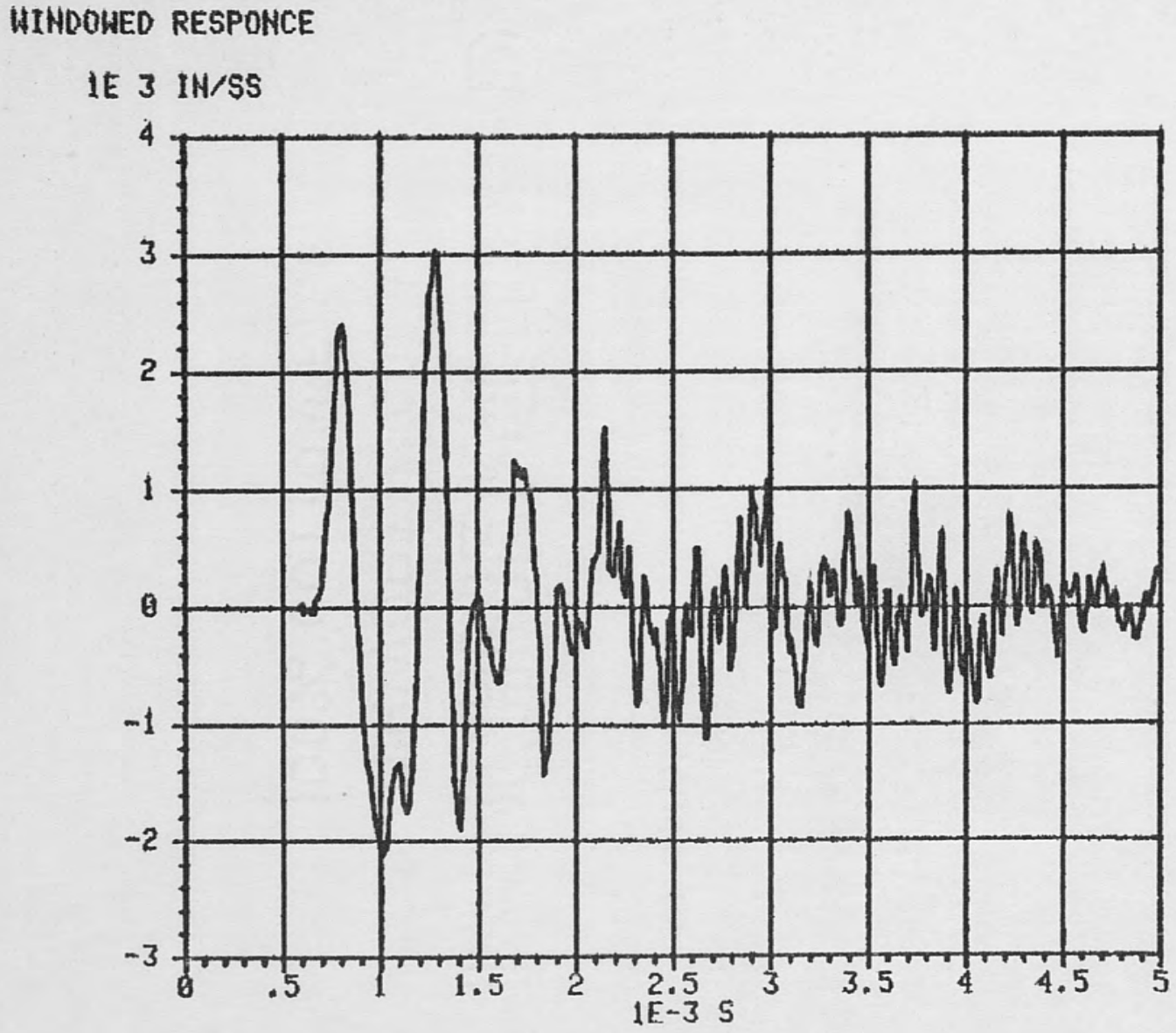

Figure 27. Windowed Response Waveform

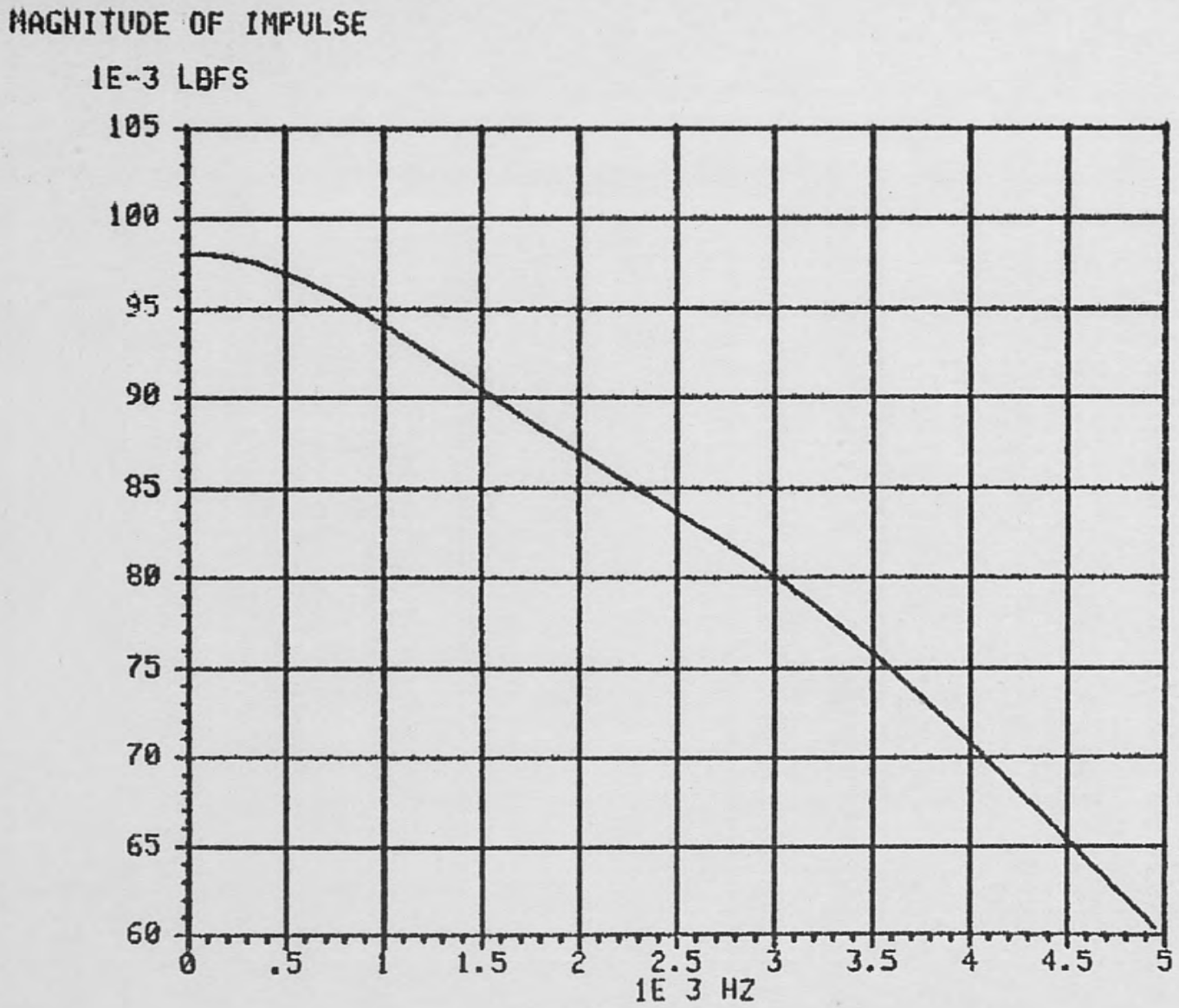

Figure 28. Magnitude of Impulse FFT

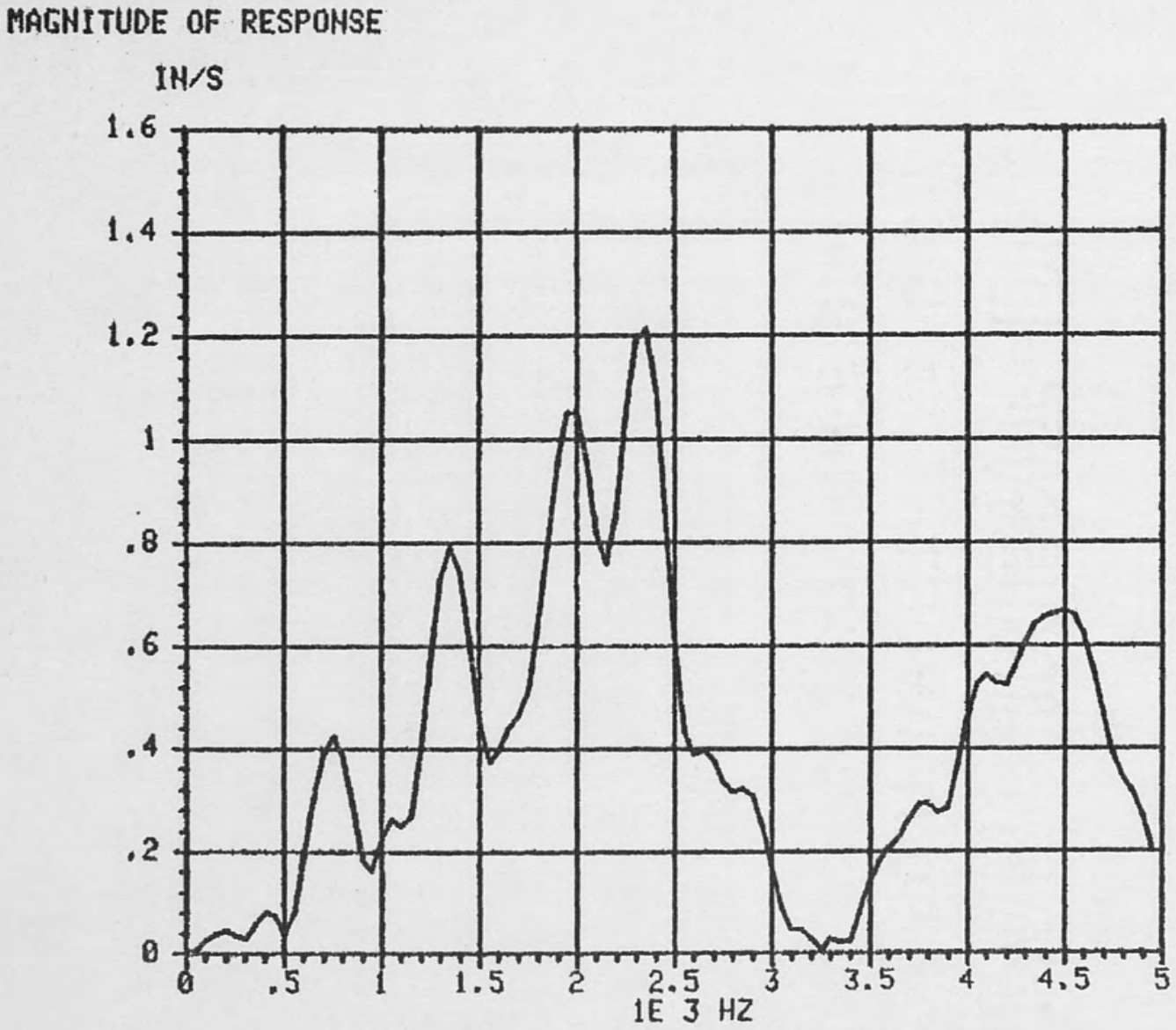

Figure 29. Magnitude of Response FFT

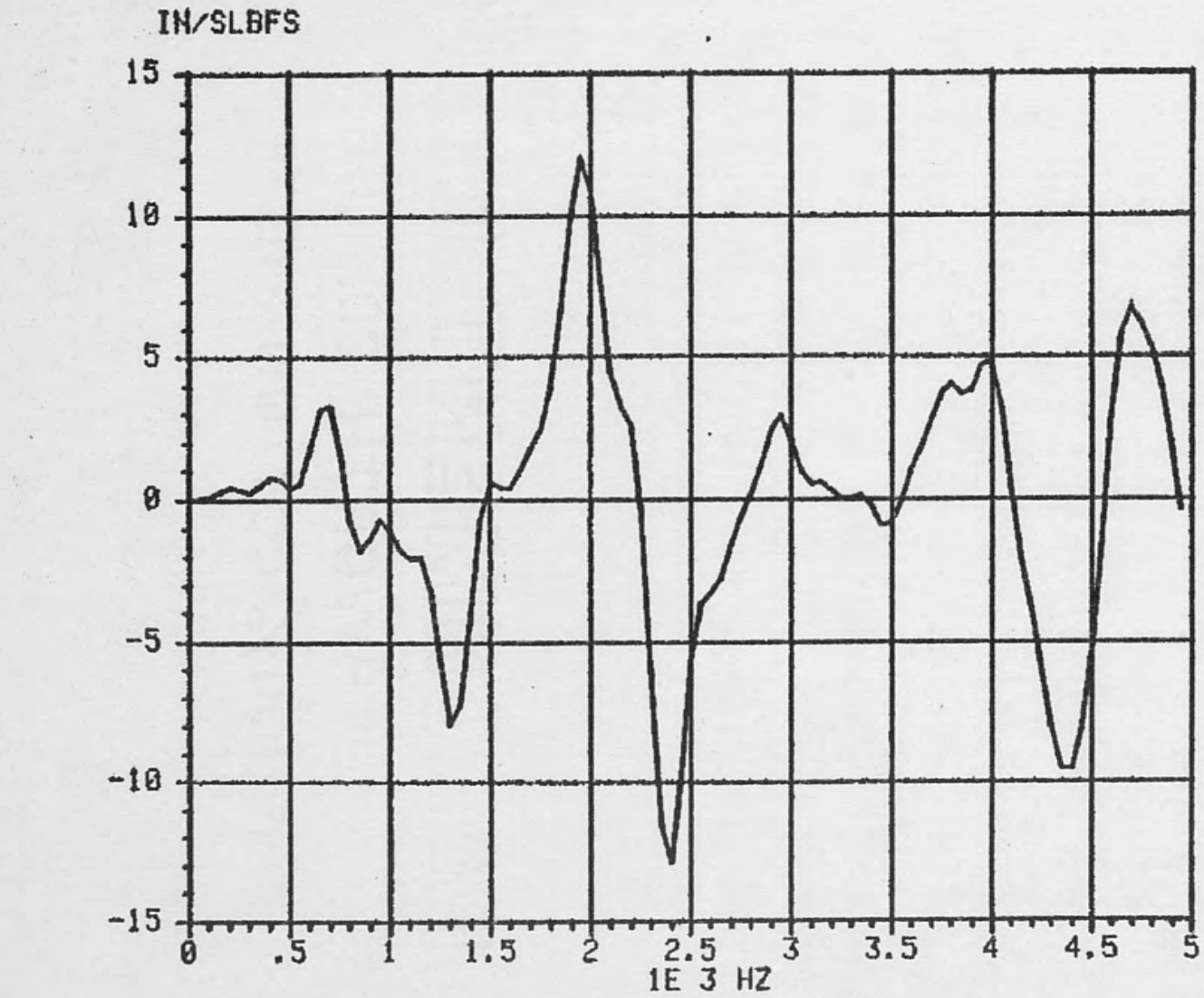

Figure 30. Real Part of Transfer Function

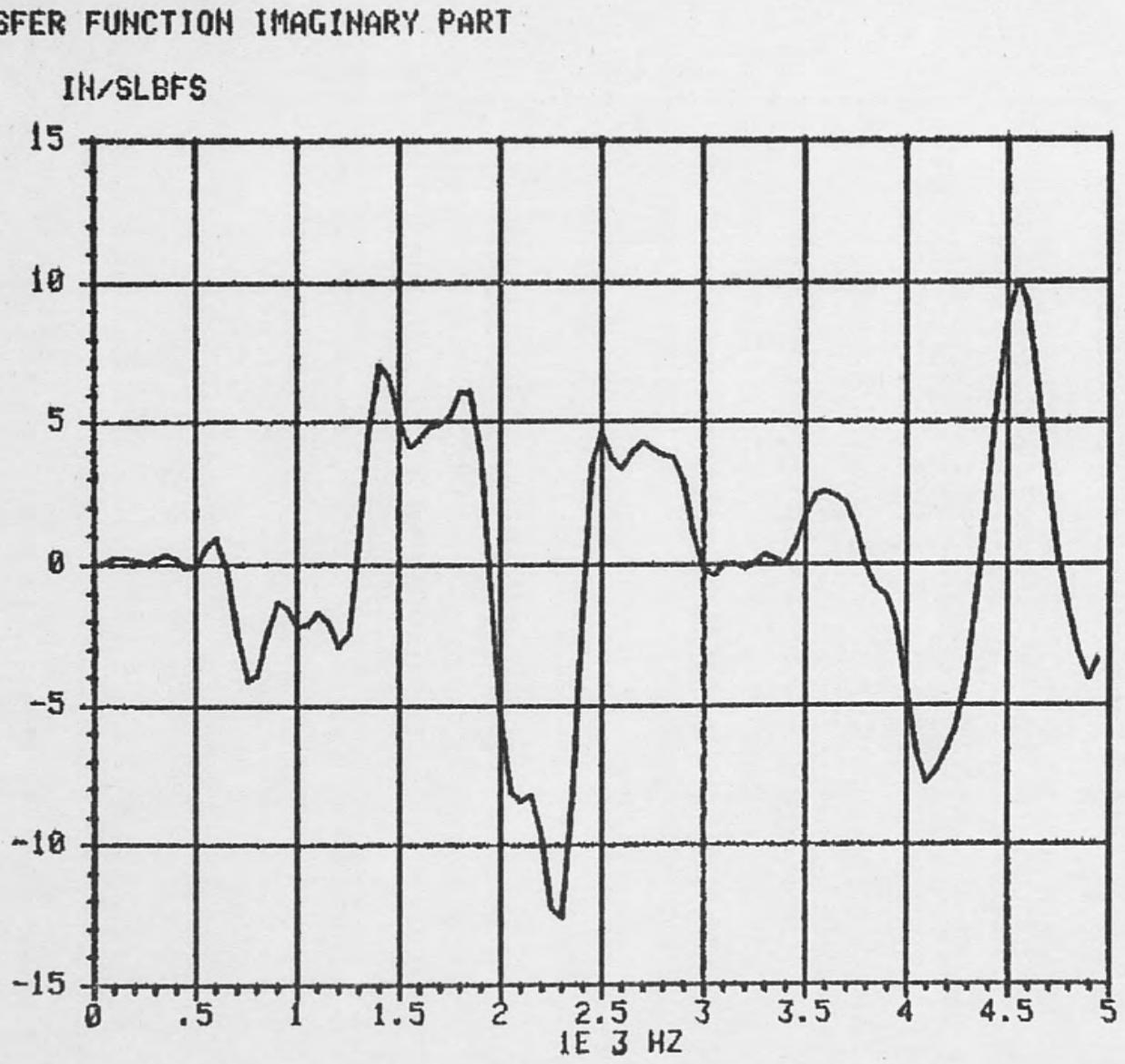

Figure 31. Imaginary Part of Transfer Function

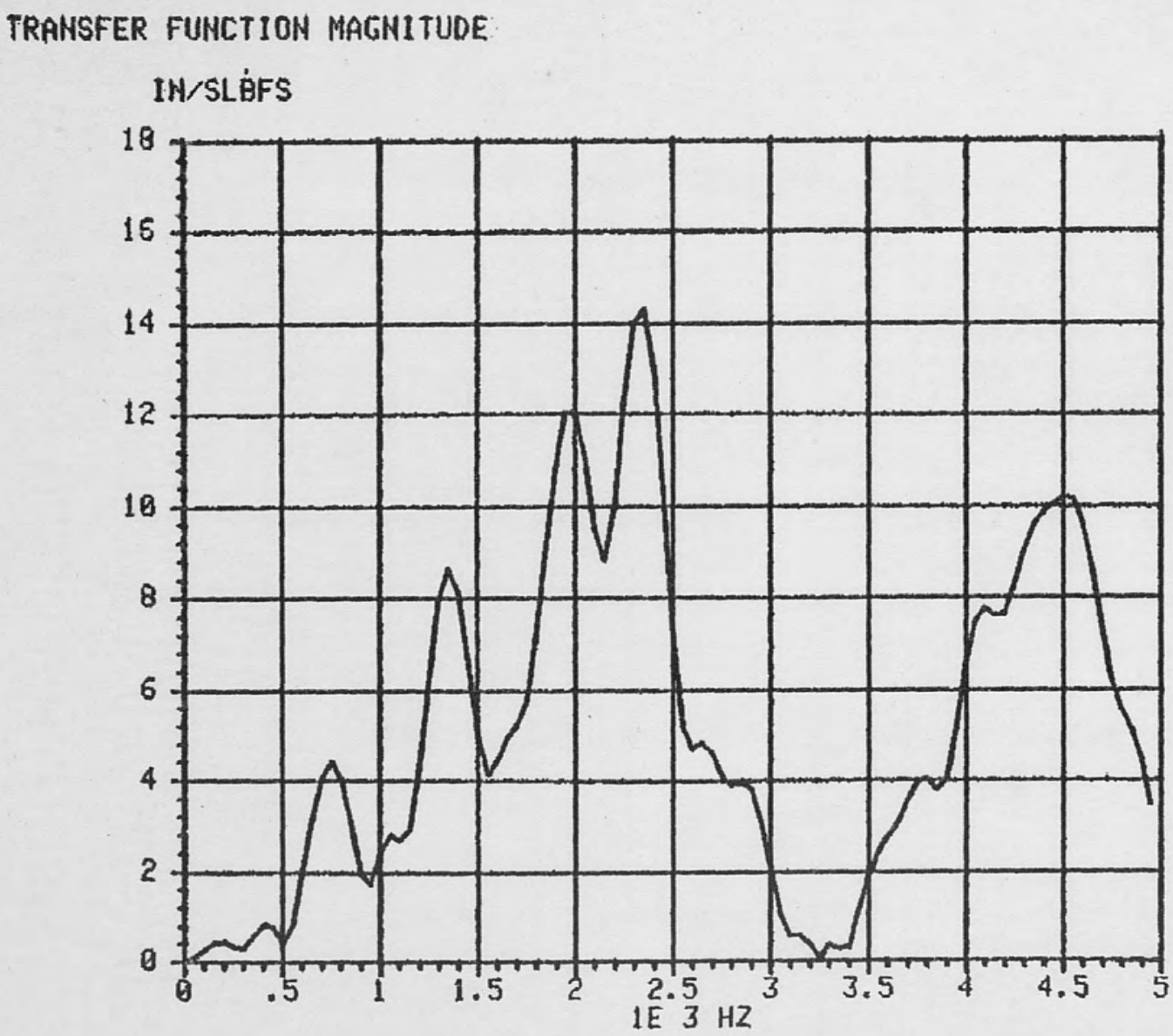

Figure 32. Magnitude of Transfer Function

Figure 33 is a plot of the coherence function, γ, associated with this frequency response function. These four plots were obtained from program "ADIM1.BAS".

Further explanation and interpretation of some of the plots in Figures 24 through 33 are required. For instance, Figure 28 illustrates the frequency content of the force impulse. From this plot the half power point (-3dB) can be estimated. This point is at approximately $68. \times 10^{-3}$ lbf sec amplitude or 4.2 k Hz frequency (8). Frequency response function up to this frequency should be sufficiently accurate to yield good estimates of modal parameters. From Figures 30 through 32, two conclusions can be drawn. First, four distinct resonant frequencies can be identified between 0 and 2.5 k Hz. These occur at approximately 700 Hz, 1350 Hz, 1900 Hz, and 2300 Hz. Also, some modal coupling is apparent, at least between the highest pair of modes. Figure 33, the coherence function, is a plot which contains only digitizer or bit noise. This is not what was expected, since it seems to indicate noiseless measurement of a perfect linear system. An error in the computer routine used to calculate γ was suspected. However, numerous attempts to determine the cause of this problem were unsuccessful.

Results of the investigations of the stinger dynamic characteristics and radial modes of the tube will

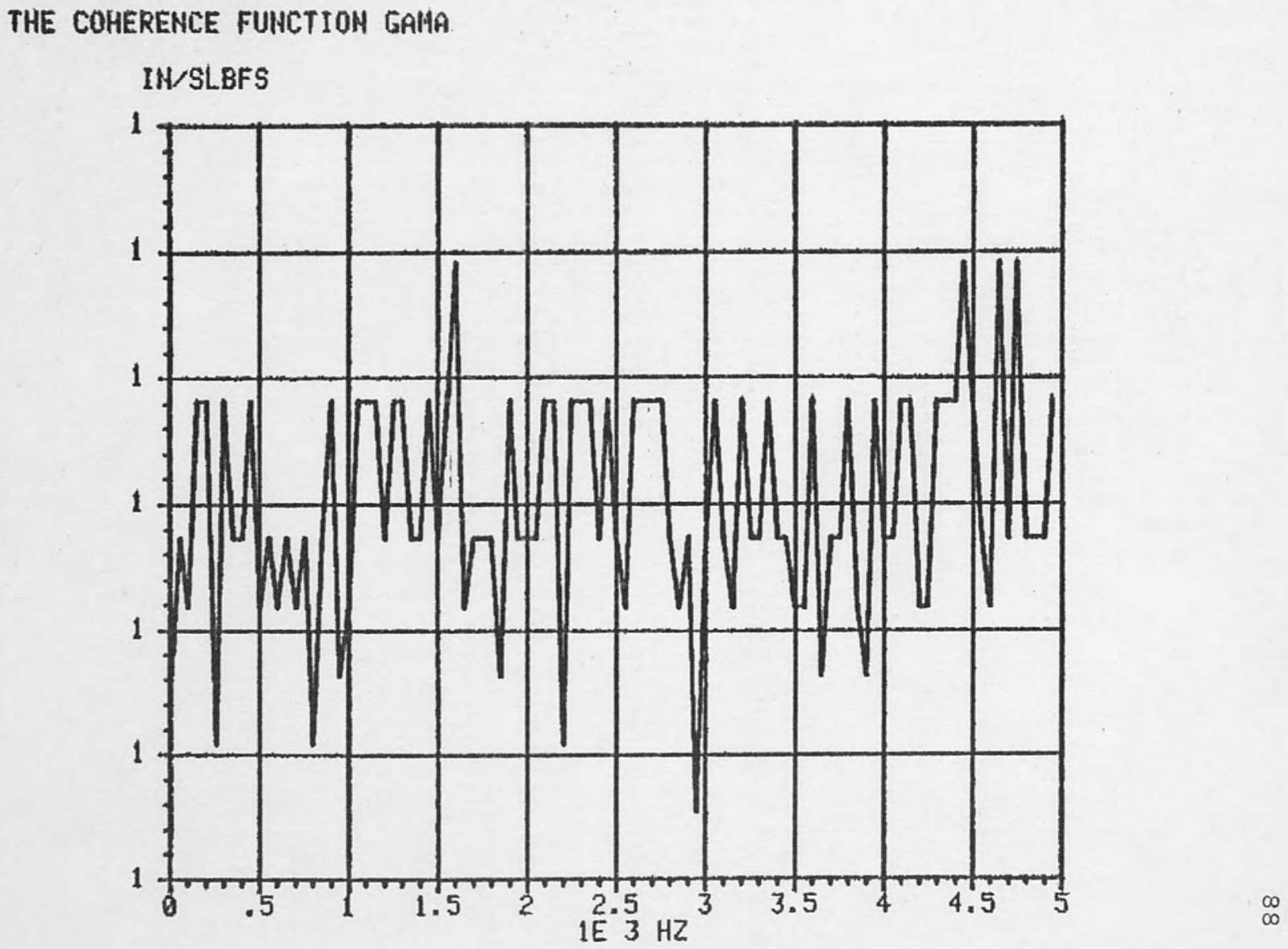

Figure 33. Coherence Function

now be discussed. Figures 33 and 35 are transfer function plots obtained from stinger mounted accelerometer impulse/response waveforms ("IMT2.DAT" and "RET2.DAT"). From these plots, it can be concluded that a major resonant frequency of the stinger occurs at approximately 2100 Hz. In Figure 34, the negative peaks at approximately 1900 Hz and 2300 Hz correspond to previously identified tube resonances. The negative values of these peaks are due to the fact that the response accelerometer was oriented in the negative direction with respect to previously discussed data. Another, conclusion that can be drawn from the stinger frequency response results is that since quite high amplification is indicated at 2100 Hz, very low damping must be associated with this stinger resonance.

The results of the investigation of shock tube radial modes are not so easily interpreted. Response waveforms obtained from radial mounted accelerometers are characterized by significantly lower signal levels than those for axial mounted sensors. Therefore, lower signal to noise ratios and noiser frequency response data are obtained. This data is not presented here because of problems in drawing clear conclusions from it. However, it should be sufficient to say that low frequency radial mode of the tube appeared to be

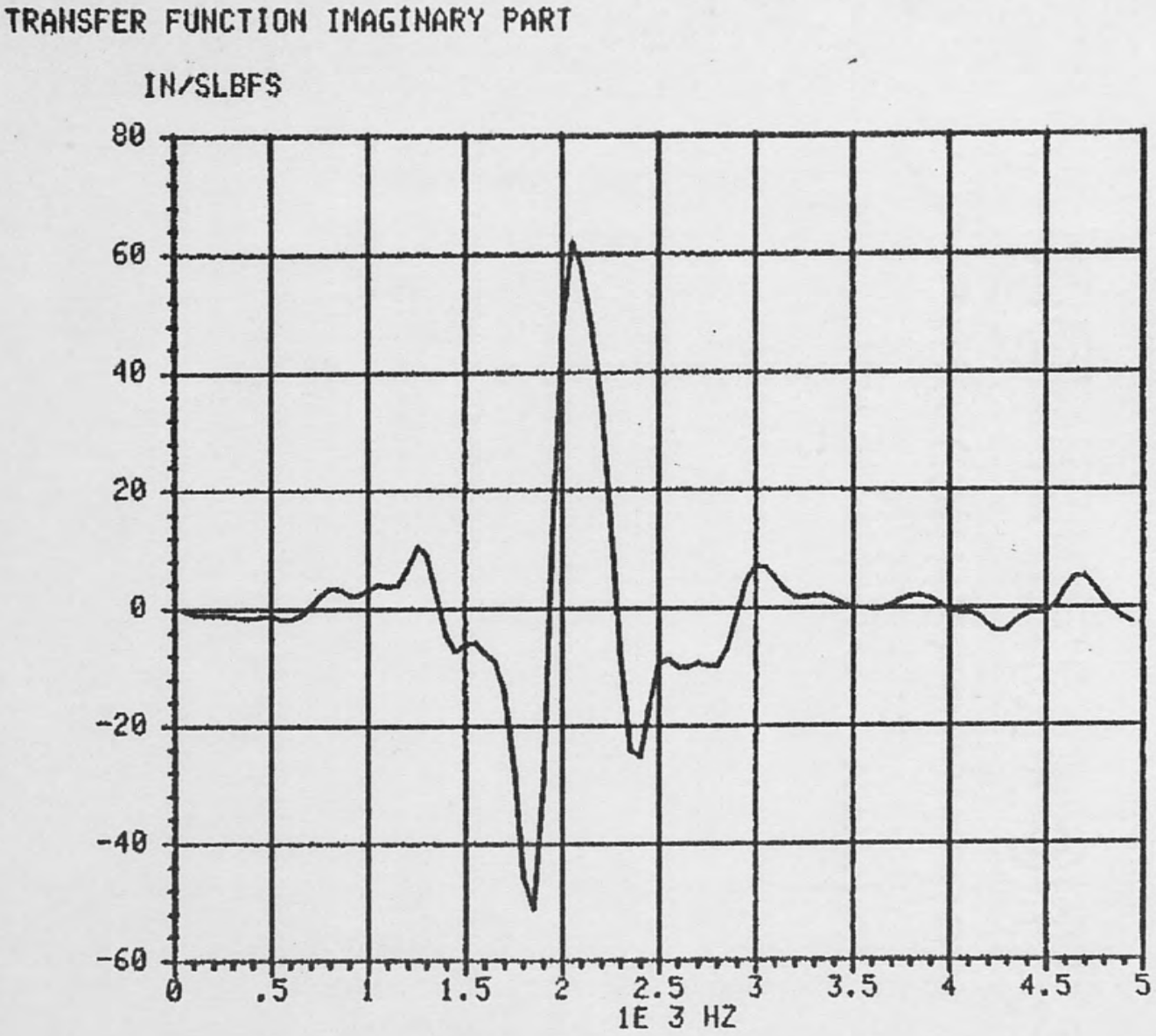

Figure 34. Imaginary Part of Transducer Function for Stinger

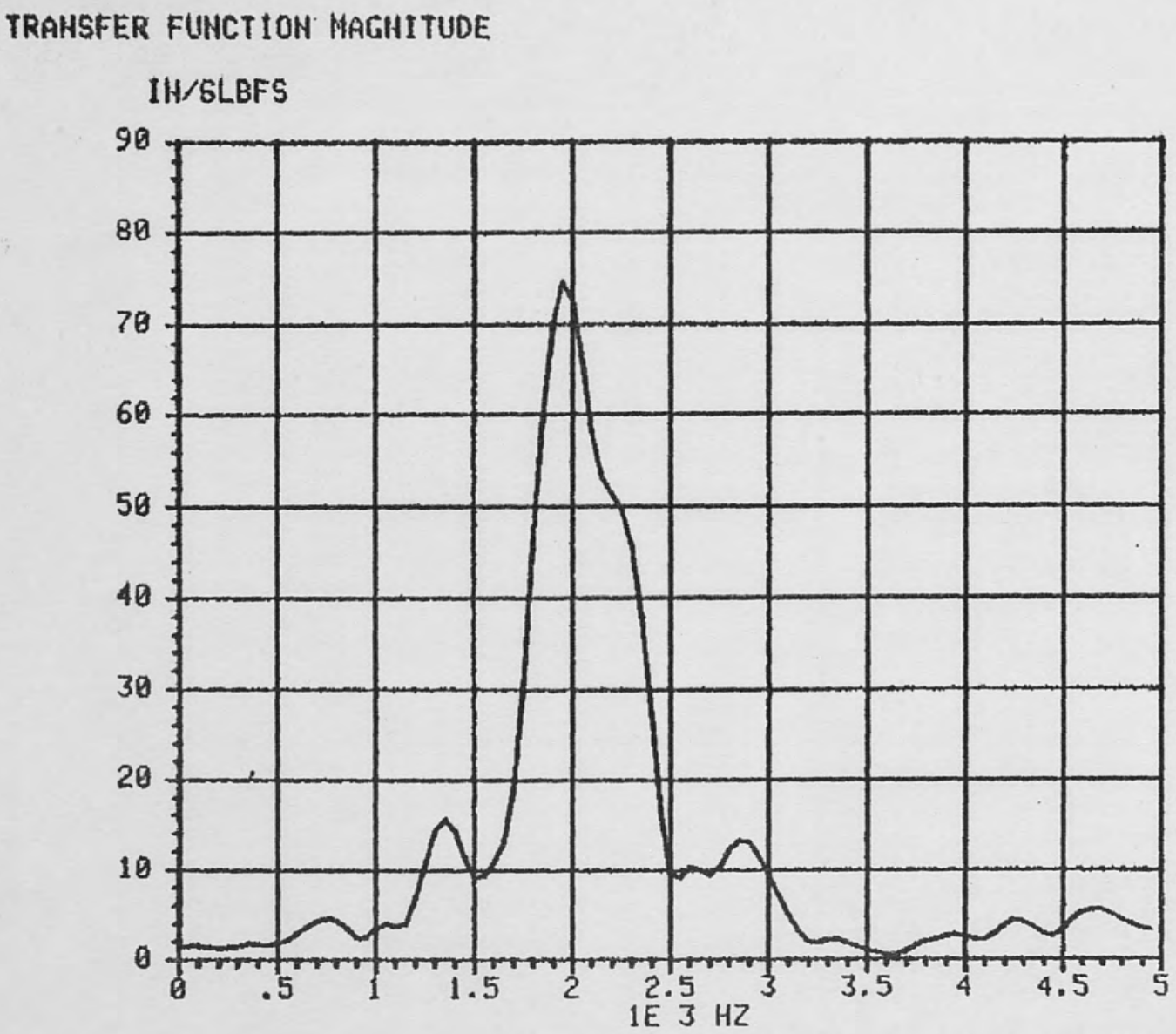

Figure 35. Magnitude of Transfer Function for Stinger

essentially symmetrical. Therefore, effect of gravitational and support structure loading were assumed to be negligible.

Next, results of the shock tube longitudinal mode investigation will be discussed. The frequency response function data used for this investigation includes that shown in Figures 31 and 32 and the waveforms contained in Appendix C. From these data, normalized eigenvectors were estimated using the procedure previously outlined in the methods section. Figure 36 is a set of plots of the first two estimated eigenvectors. Figure 37 shows the third estimated eigenvector. The results indicated in these figures have about the shape expected. The first mode has one node, or stationary point, and the maximum values occur at the ends. The second mode shape has two nodes and the third has three. Additional mode shapes would have been determined except that excessive data noise at frequencies above 2500 Hz degraded resolution. A method was sought to verify these results as is discussed below.

In an attempt to verify the shock tube longitudinal modal result, a finite element model was created and analyzed using the ANSYS, engineering analysis system. ANSYS is a large scale, proprietary, finite element program created and maintained by Swanson Analysis

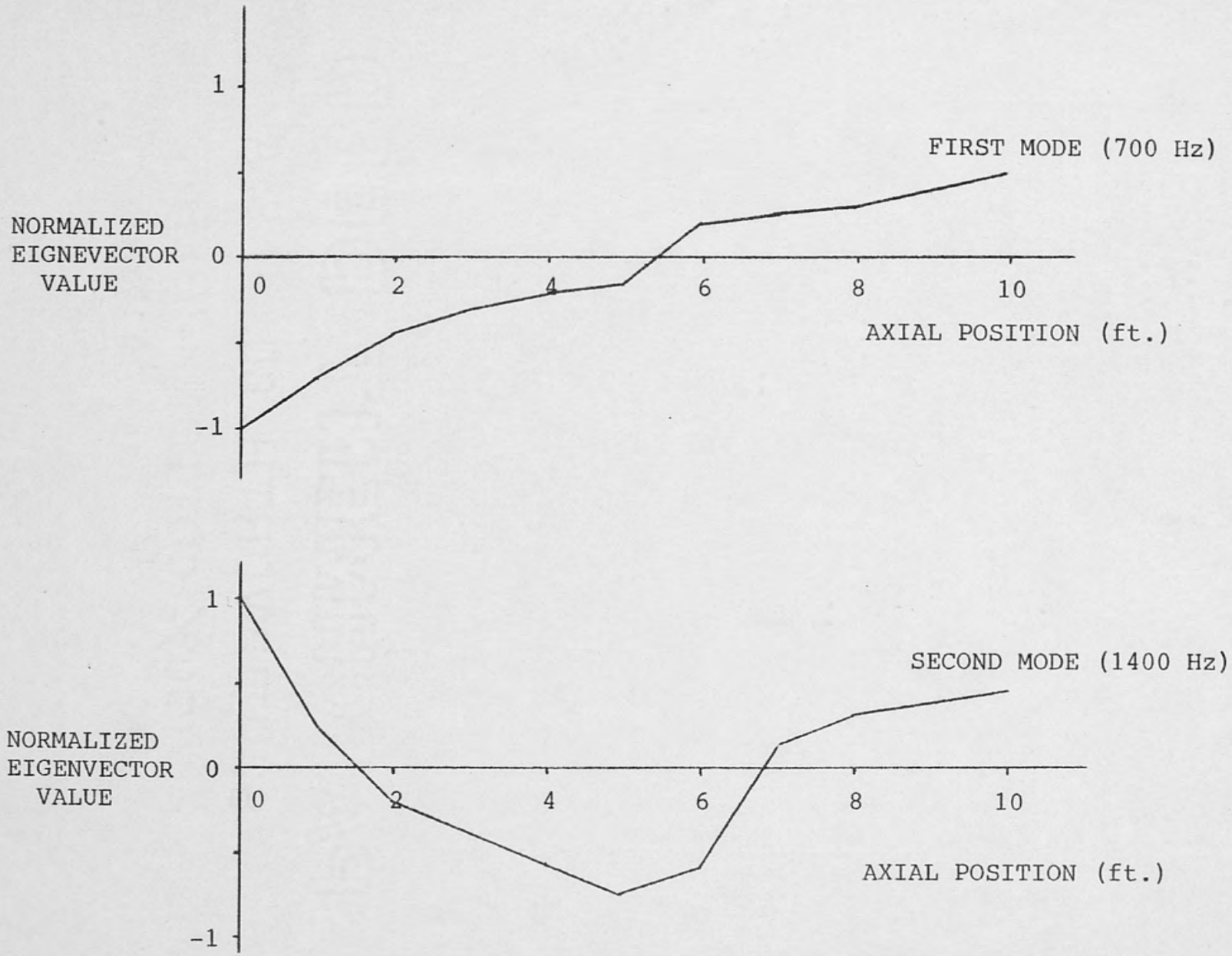

Figure 36. First Two Estimated Mode Shapes

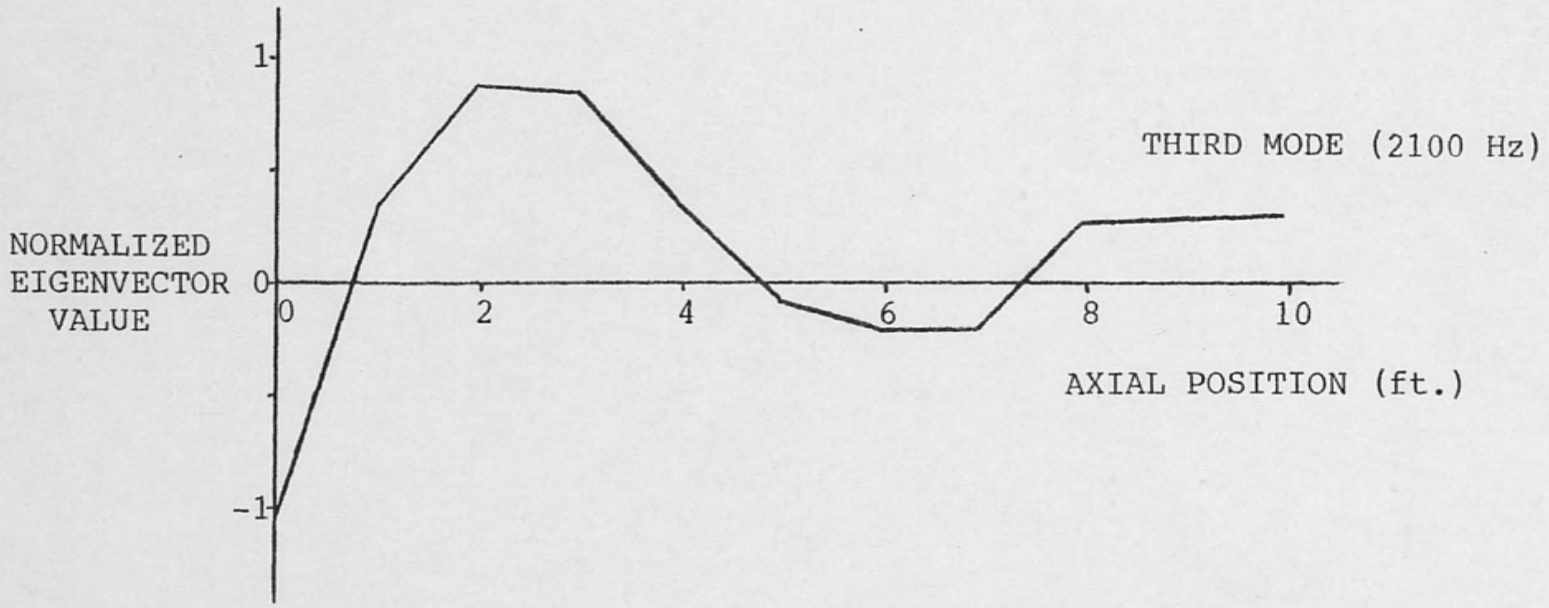

Figure 37. Third Estimated Mode Shape

Systems Inc., Houston, Pennsylvania (9). The model created consisted of 16 nodes and 15 bar-like elements. Figure 38 shows the model overlayed on a section view of the shock tube. Tapered elements were used to closely simulate the actual structure. Nodes were only allowed one degree of freedom, that of axial displacement. No longitudinal displacement constrains were applied. In other words, the model was solved as unconstrained axial vibration (free-free), of a nonuniform rod. The ANSYS modal analysis option was used to obtain solutions and the first 6 mode shapes were requested for printout. These printouts are included in Appendix D. The first mode for the free-free model represents rigid body displacement, as expected. The next three modes are predicted at frequencies of 752 Hz, 1423 Hz, and 2173 Hz. These resonances are very close to the first three estimated from frequency response data. Plots of the normalized predicted mode shape are shown in Figure 39, for the first two modes, and Figure 40 for the third.

Conclusions and recommendations based on all the above results are included in the next and final chapter.

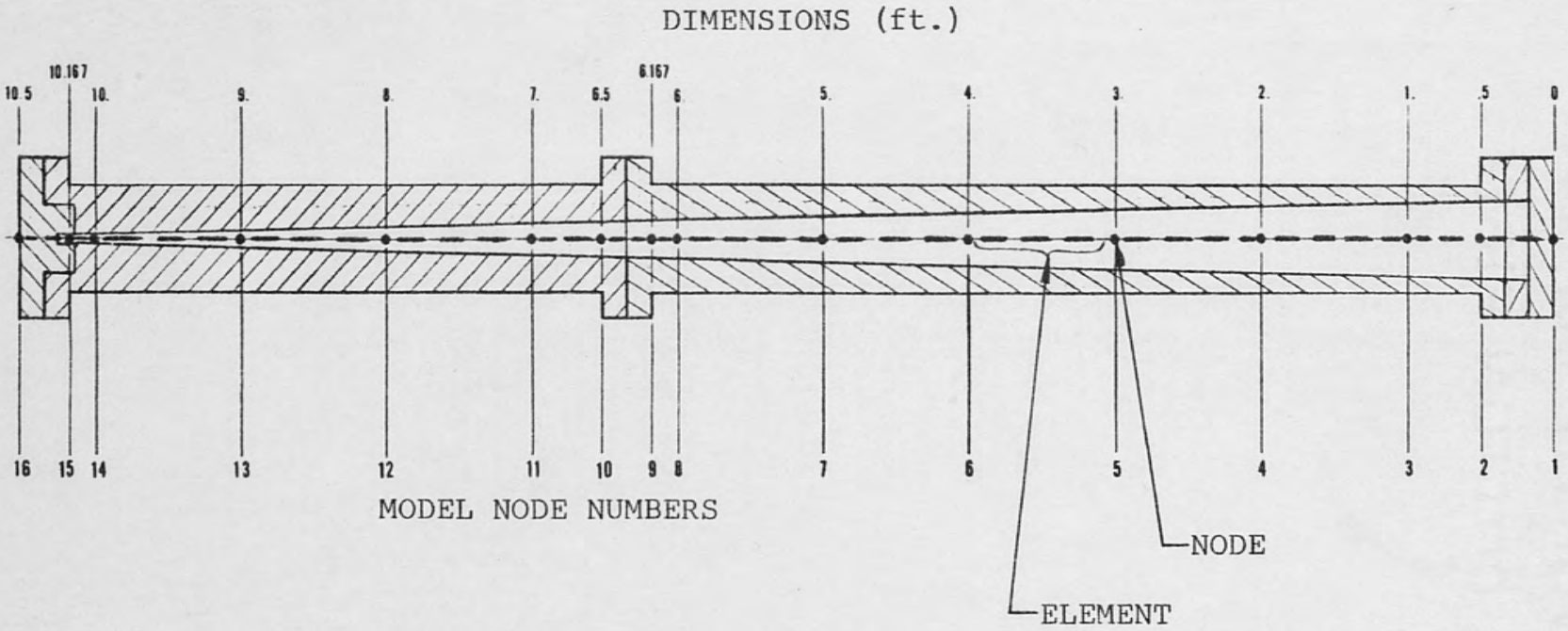

Figure 38. Finite Element Model and Shock Tube Section View

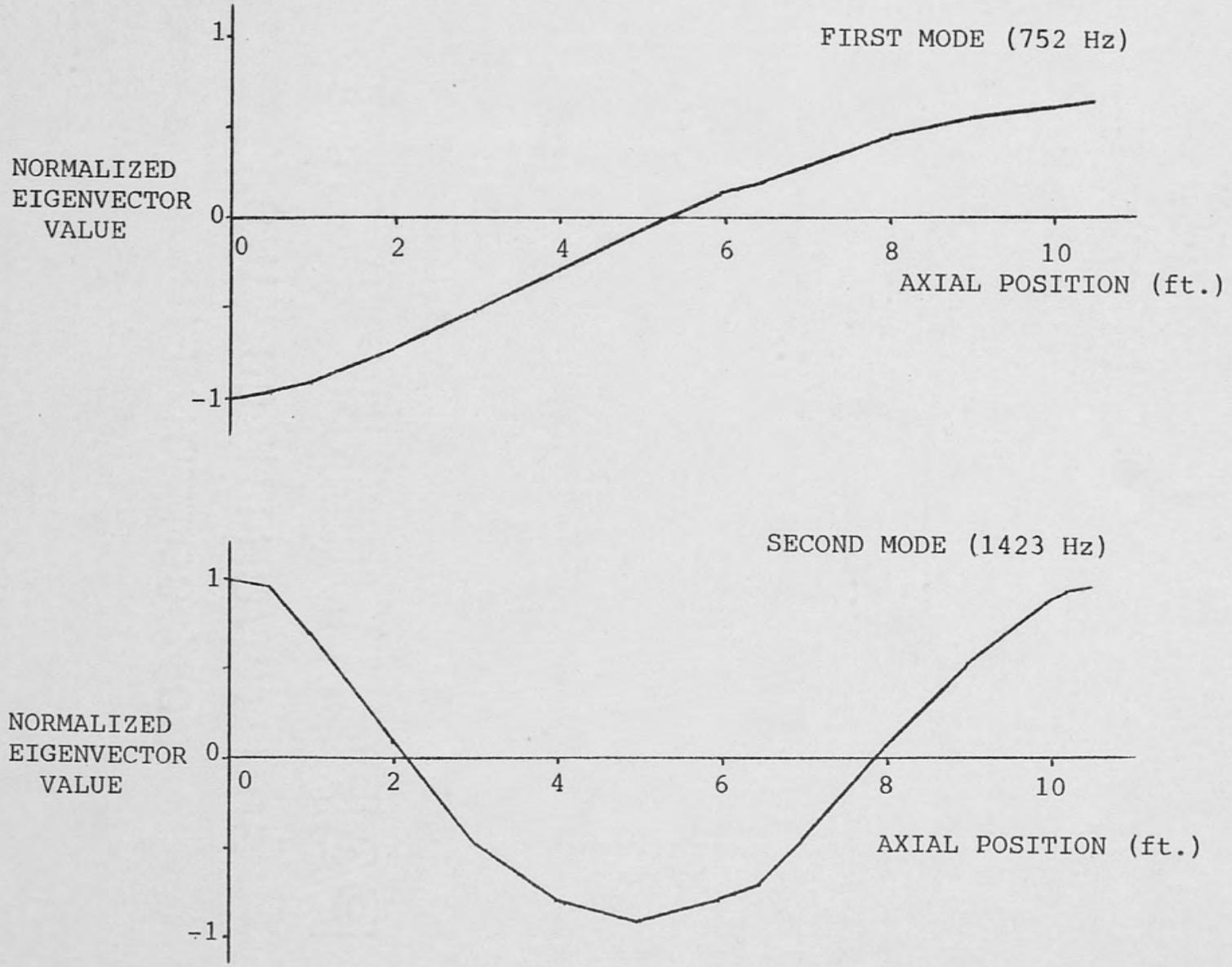

Figure 39. First Two Computer Predicted Mode Shapes

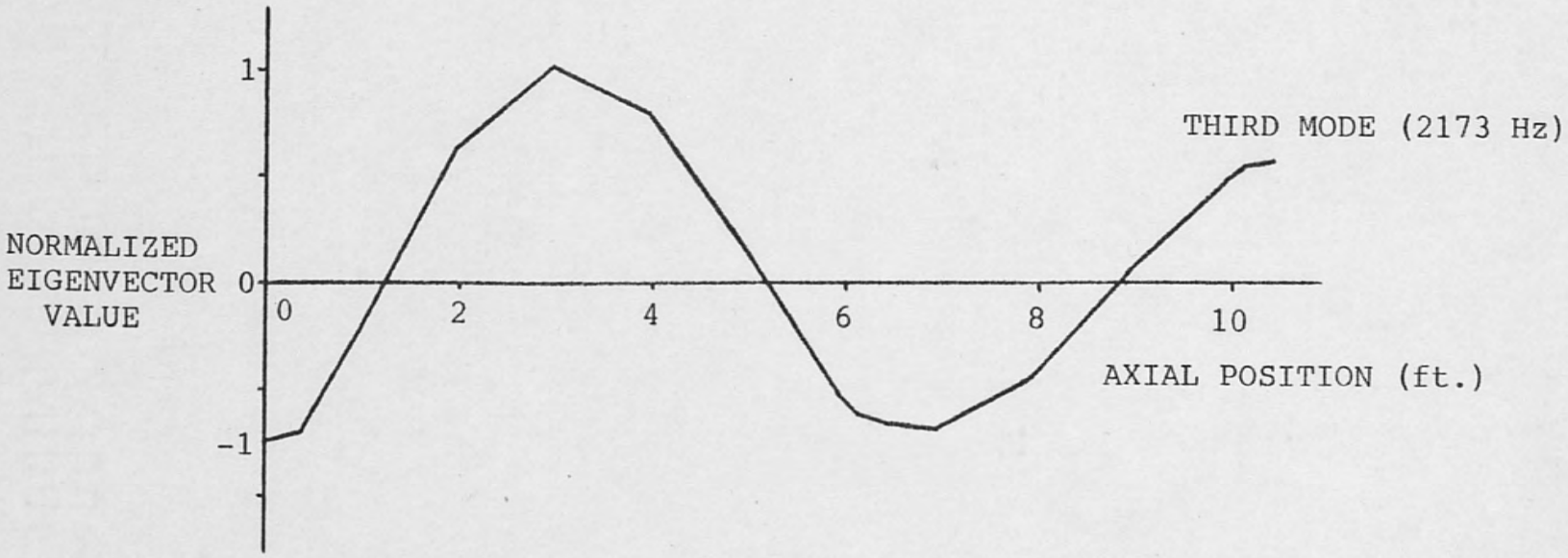

Figure 40. Third Computer Predicted Mode Shapes

V. CONCLUSIONS AND RECOMMENDATIONS

In summary of results obtained from shock wave curve fitting and analysis, several important points should be noted. First, from estimated peak pressures, an actual amplification (AF) and efficiency (η) of 5292 and 68.7%, respectively, were obtained. These values are approximately 49% higher than those predicted during initial calibration tests conducted by Connell (1). Also, an exponential decay time constant (θ) of approximately 101 μ sec was estimated in this analysis. This is about 38% less than the value calculated from the scaling laws, based on an AF value of 5292 and a range (R) of 9 feet. Another notable results was that, shock wave data noise was indicated to have major frequency content components in the range below 10 k Hz. However, the actual noise frequencies estimated from visual inspection of shock wave plots, appears to be in a much higher range.

Some qualifying comments should be made about these results. For instance, as previously mentioned, this analysis is based soley on two detonations of number 8 blasting caps. Therefore, it is impossible to predict shock tube performance for much larger

explosive weights from results obtained here. Also, it should be noted that the assumed shock wave equation used for curve fitting was slightly different than the theorectical form. The difference being that the discontinuous pressure rise in the theoretical equation was replaced by a linear rise with finite slope to better simulate the observed test data. No effort was made to determine the ramifications of this difference. Another qualifying point is that predicted low frequency noise content may be due to errors in fitting the exponential portion of the assumed curve to shock wave data. Although the curve fitting results appear visually to be very good, the shock wave data acutally falls above the fitted curve near the beginning of the exponential decay and below it at the end. This gives the appearance of a low frequency oscillation which is probably the source of the first peak in the noise frequency content plots. Two possible explanations for curve fitting errors are that either a proper fit of the assumed curve was not obtained, or a curve of a different shape should have been assumed. The latter seems more likely. Finally, from visual inspection of shock wave data plots, the frequency of noise appears to be on the order of 25 k Hz. This is believed to be above the frequency range where mechanical vibration of the shock tube would

render significant contribution.

Summarizing the results of shock tube dynamic characteristics analysis, several significant points should be mentioned. For instance, the stinger was determined to have a major resonant frequency of approximately 2100 Hz, at which very high amplification was observed. This might be interpreted as being a possible source of shock wave data noise, since longitudinal motion of the stinger mounted pressure transducer during passage of the shock wave would cause measurement variations. However, the period of the indicated stinger resonance is relatively large compared to the shock wave duration, which would seem to preclude this effect. Another significant result was that the first 3 longitudinal vibration modes of the shock tube structure were identified through impulse tests and verified via finite element analysis. These modes were determined to be at frequencies of approximately 700, 1400, and 2100 Hz and the corresponding mode shapes indicated were of generally expected form.

Some further comments on these results are required. First, it should be noted that the dummy stinger used during impulse tests did not exactly simulate the actual one used to support the pressure transducer. The difference being that, the potting used in fabrication

of the dummy stinger was a resilient, sealant-like, material instead of the relatively hard, expoxy-like, material used in the actual one. This would have the effect of making the dummy stinger less stiff, with lower natural frequencies and high damping, than the actual one. With regard to the modal analysis of the shock tube, two possible explanations could account for differences observed between experimentally determined and computer predicted mode shapes. First, variations in measured data, due to changes in instrumentation and experimental technique, may have caused errors in estimated mode shapes. Second, the differences in experimental and computer predicted mode shapes might be caused by the failure to include radial expansion capabilities and hydrodynamic effects in the finite element model. However, it could be argued that, since essentially the same resonant frequencies were indicated from test results and finite element analysis, the radial and hydrodynamic effects must be insignificant at the indicated resonances. Measurement errors are a more likely explanation of predicted mode shape differences. These errors may have results from replacement of the response accelerometer, due to damage, half way through the testing or from the required use of the pendulum mounted impulse hammer. Either of these might

have caused poor experimental mode shape estimates to be obtained for tube position from 6 to 10 feet.

Several conclusions and recommendations are in order based on the results of these analyses. First it is recommended that the shock tube performance parameters obtained here be verified and supported with the results of further analysis of shock tube performance for larger explosive weights. These data should then be used to conduct all future shock tube test operations. Furthermore, based on this analysis, it does not appear that shock wave data noise is caused by mechanical vibration of the shock tube structure or stinger. Therefore, further investigations should be performed to determine the source of the noise and energy losses. Areas which might be included in future research of the shock tube include the following: An investigation of shock wave reflection effects at the detonation site and as the wave propagates down the tube, an investigation of the after shock effects caused by expansion and contractions of the gas envelope of explosion products and a determination of the effects on calculated performance parameters due to truncation of the shock tube 1 foot from the vertex of the interior cone.

In spite of problems and limitations encountered during this research effort, the use of computer aided

analysis of shock wave data and shock tube modal analysis through impulse testing were very successfully demonstrated.

APPENDIX A

Computer Program Description and Printouts

Description of Program "NFIT.BAS"

Program "NFIT.BAS" is a SPS basic program written to obtain a curve fit for time domain shock wave data. The data is read as a digitized waveform from a file on floppy disk DX0 and plotted. The curve fitting is achieved in two parts. First, an exponential decay curve is fit to the data waveform. The time of the peak pressure value, and the times for the range of data to be fit are specified by the user. The curve fitting is accomplished through a linear least squares technique performed on the logarithm of the data waveform amplitude versus time curve. Following this process, data is printed indicating the equation of the linear curve fit, the equation of the exponential curve fit and the correlation coefficient of the linear fit. The next portion of the curve fitting process involves determining the linear rise time curve. This is accomplished by one of two methods. Either, a linear equation is fit between two user defined points on the data curve, or the line is fit from given initial point in the data curve with an assumed slope. The equation of the line is printed following calculation of its slope and intercept. Also, printed is the peak pressure for the fitted curve and its time of occurrence. Next the data waveform is again plotted. However, this graph includes

both the data waveform and the fitted curve plotted concurrently to allow for visual inspection of the fit quality. Following the plotting, the data waveform and the fitted waveform are stored in files "WAFIT.DAT" and "WBFIT.DAT" respectively of floppy disk DX0: for later processing.

The following pages contain a printout of the latest version of program "NFIT.BAS".

```
10 REM PROGRAM "NFIT.BAS" 6/26/81
20 REM PROGRAM TO OBTAIN TIME DOMAIN CURVE FIT FOR PRESSURE WAVEFORM
30 REM   OUTPUT- DX0:"WAFIT.DAT","WBFIT.DAT"
40 WAVEFORM WA IS AA(511),SA,HA$,VA$
50 OPEN #1 AS DX0:"SHOCK1.DAT" FOR READ
60 READ #1,WA
70 CLOSE #1
80 VA$="PSI"
90 PAGE
100 PRINT "ENTER PRESSURE TRANSDUCER SENSITIVITY IN PSI/VOLTS"
110 INPUT SS
120 AA=(AA+.8)*SS
130 PAGE
140 PRINT "DO YOU WANT TO PLOT WA (Y OR N)?"
150 INPUT N$
160 IF N$="N" THEN 210
170 PAGE
180 GRAPH WA
190 RELEASE "GRAPH"
200 WAIT
210 PAGE
220 PRINT "   ***EXPON. CURVE FIT***"
230 PRINT "  "
240 PRINT "ENTER STARTING TIME FOR EXPON. DECAY CURVE FIT."
250 INPUT TB
260 PRINT "ENTER INITIAL TIME FOR EXPON. CURVE FIT"
270 INPUT TI
280 PRINT "ENTER FINAL TIME FOR EXPON. CURVE FIT"
290 INPUT TF
300 NB=ITP(TB/SA)
310 NI=ITP(TI/SA)
320 NF=ITP(TF/SA)
330 N=NF-NI
340 DIM BB(511)
350 FOR I=0 TO 511
360 IF I<NI THEN 400
370 IF I>NF THEN 400
380 BB(I)=LOG(AA(I))
390 GOTO 410
400 BB(I)=0
410 NEXT I
420 DIM X(N),Y(N)
430 FOR I=0 TO N
440 X(I)=(NI+I-NB)*SA
450 Y(I)=BB(NI+I)
460 NEXT I
470 GOSUB 980
480 PRINT "   EXPON. EQN.-   Y = (";EXP(Q8);") EXP(";Q9;"X)"
490 BB=0
500 FOR I=NB TO 511
510 BB(I)=EXP(Q8)*EXP(Q9*(I-NB)*SA)
```

```
520 NEXT I
530 DELETE X,Y
540 PRINT "  "
550 PRINT "   ***LINEAR RISE TIME CURVE FIT***"
560 PRINT "  "
570 PRINT "ENTER STARTING TIME FOR RISE TIME CURVE FIT"
580 INPUT TA
590 NA=ITP(TA/SA)
600 PRINT "ENTER (0) FOR POINT TO POINT OR (1) FOR POINT SLOPE FIT "
610 INPUT II
620 PRINT
630 IF II=1 THEN 720
640 PRINT "ENTER FINAL TIME FOR RISE TIME CURVE FIT"
650 INPUT TE
660 NE=ITP(TE/SA)
670 N=NE-NA
680 TE=NE*SA
690 TA=NA*SA
700 M=(AA(NE)-AA(NA))/(TE-TA)
710 GOTO 740
720 PRINT "ENTER SLOPE OF LINEAR CURVE"
730 INPUT M
740 DIM Y(511)
750 FOR I=0 TO 511
760 IF I<NA THEN 780
770 Y(I)=AA(NA)+M*(I-NA)*SA
780 NEXT I
790 PRINT "  "
800 PRINT "  LINEAR EQN.  Y = (";AA(NA);") + X (";M;")"
810 FOR I=0 TO 511
820 IF I<NA THEN 860
830 IF I<NB THEN 850
840 IF BB(I)<Y(I) THEN 860
850 BB(I)=Y(I)
860 NEXT I
870 DELETE Y
880 PRINT
890 PRINT "  MAX PRESSURE = ";MAX(BB)
900 TM=(NA+ITP((MAX(BB)/M)/SA))*SA
910 PRINT "  AT TIME = ";TM
920 WAIT
930 PAGE
940 WAVEFORM WB IS BB,SA,HA$,VA$
950 GRAPH WA,WB
960 WAIT
970 GOTO 1240
980 REM ***LINEAR REGRESS. SUBROUTINE***
990 Q2=N+1
1000 Q3=0
1010 Q4=0
1020 Q5=0
1030 Q6=0
1040 Q7=0
```

```
1050 Q8=0
1060 Q9=0
1070 Q0=0
1080 FOR I=0 TO N
1090 Q3=Q3+X(I)
1100 Q4=Q4+Y(I)
1110 Q5=Q5+X(I)*Y(I)
1120 Q6=Q6+X(I)*X(I)
1130 Q7=Q7+Y(I)*Y(I)
1140 NEXT I
1150 Q9=(Q2*Q5-Q3*Q4)/(Q2*Q6-Q3*Q3)
1160 Q8=(Q4-Q3*Q9)/Q2
1170 Q0=(Q2*Q5-Q3*Q4)/SQR((Q2*Q6-Q3*Q3)*(Q2*Q7-Q4*Q4))
1180 PRINT
1190 PRINT "   LINEAR EQN.    Y =(";Q8;") + X (";Q9;")"
1200 PRINT
1210 PRINT "   LINEAR FIT CORRELATION COEFF. = ";Q0
1220 PRINT
1230 RETURN
1240 CANCEL DX0:"WAFIT.DAT"
1250 CANCEL DX0:"WBFIT.DAT"
1260 SQUISH DX0:
1270 OPEN #1 AS DX0:"WAFIT.DAT" FOR WRITE
1280 WRITE #1,WA
1290 CLOSE #1
1300 OPEN #1 AS DX0:"WBFIT.DAT" FOR WRITE
1310 WRITE #1,WB
1320 CLOSE #1
1330 SQUISH DX0:
1340 END
```

Description of Program "ADFFT1.BAS"

Program ADFFT1.BAS" is an SPS basic program written to obtain FFTs of time domain shock wave test data and generated waveforms from program "NFIT.BAS". The data waveforms are read in from storage files "WAFIT.DAT" and "WBFIT.DAT" of floppy disk DX0. The program produces graphical representations of the real part, the imaginary part and the magnitude of the transformed waveforms. The time domain waveforms transformed in the program include shock wave pressure versus time history from "WAFIT.DAT", the fitted curve from "WBFIT,DAT" and the noise or difference between the data and fitted curves.

Several important features of the program require further discussion. One feature, the time window expansion, was required to obtain adequate resolution in the transformed waveforms at low frequencies. This is accomplished by adding 3 additional 512 point arrays filled with zeros to the 512 window containing the data waveform. Thus the time domain waveform consists of a 2048 sample array with the first 512 occupied by the data and the remaining blocks empty or zero. The effect of this expansion process is to yield a frequency domain waveform with the same range of frequencies but 1024 samples instead a 256 sample waveform which would be

obtained from the original data. As an example of this process, consider a time domain waveform with 512 samples and a sample time increment of 9.76×10^{-7} seconds. This would be transformed to a frequency domain waveform with 256 samples and a sample frequency increment of 2000 Hz (10). By expanding the window of the time domain waveform to 2048 a transformed waveform is obtained with 1024 samples and a sample frequency increment of 500 Hz.

A 2048 sample waveform is the largest time domain signal which can be transformed due to free memory limitations of the computer used. Therefore, another method of improving frequency domain resolution was used. This method consisted of creating a new time waveform using only every second value from the data waveform. This yields a 256 sample waveform with twice the time sampling period,which is increased to a 2048 sample waveform by adding the appropriate number of zero windows. The frequency domain waveforms obtained using this method again have 1024 samples but the frequency range has been reduced by 1 half. Using the previous example to illustrate this, a transformed waveform can now be obtained with 1024 samples and a sample frequency increment of 250 Hz. A disadvantage of this method is that aliassing problems at high frequencies are

are increased. However, since this investigation is primarily concerned with low frequency signals, this should have little effect.

Another feature of the program, which should be discussed, is the transformation expansion subroutine. This subroutine causes the time domain waveforms to be transformed using the FFT and then isolated the low frequency portion of the frequency domain curve to be plotted. The portion of the waveform isolated is user specified by inputing the inverse of the waveform fraction desired. Again using the previous sample as an illustration, if a factor of 5 is input by the user the plotted frequency waveform would be one fifth of the original or 256 k Hz in range. The frequency sampling increment would remain unchanged.

The following pages are a printout of the latest version of program "ADFFT1.BAS".

```
10 REM PROGRAM "ADFFT1.BAS" 6/6/81
15 REM PROGRAM TO OBTAIN FFT-S OF WA, WB AND WA-WB FROM "NFIT.BAS"
20 WAVEFORM WA IS AA(511),SA,HA$,VA$
30 OPEN #1 AS DX0:"WAFIT.DAT" FOR READ
40 READ #1,WA
50 CLOSE #1
90 N$="WA"
100 J=0
110 J=J+1
120 PAGE
130 PRINT "DO YOU WISH TO PLOT ";N$;" (Y OR N) ?"
140 INPUT Q$
150 IF Q$="N" THEN 211
170 PAGE
180 PRINT "   WAVEFORM ";N$
190 GRAPH WA
200 WAIT
210 RELEASE "GRAPH"
211 DIM A(2047)
212 FOR I=0 TO 511
213 A(I)=AA(I)
214 NEXT I
215 DELETE WA,AA
216 WAVEFORM WA IS A,SA,HA$,VA$
220 GOSUB 450
230 IF J=2 THEN 310
240 IF J>2 THEN 440
250 WAVEFORM WA IS AA(511),SA,HA$,VA$
260 OPEN #1 AS DX0:"WBFIT.DAT" FOR READ
270 READ #1,WA
280 CLOSE #1
290 N$="WB"
300 GOTO 110
310 WAVEFORM WA IS AA(511),SA,HA$,VA$
315 WAVEFORM WT IS BB(511),SA,HA$,VA$
320 OPEN #1 AS DX0:"WAFIT.DAT" FOR READ
330 READ #1,WA
340 CLOSE #1
350 OPEN #1 AS DX0:"WBFIT.DAT" FOR READ
360 READ #1,WT
370 CLOSE #1
380 WA=WT-WA
390 AA=AA-MEA(AA)
410 DELETE WT,BB
411 FOR I=0 TO 511
412 IF I>255 THEN 415
413 AA(I)=AA(I*2)
414 GOTO 416
415 AA(I)=0
416 NEXT I
417 SA=SA*2
420 N$="WB-WA"
```

```
430 GOTO 110
440 GOTO 820
450 REM SUBROUTINE FFTEXPAND.
460 WAVEFORM WC IS CC(1024),SC,HC$,VC$
465 WAVEFORM WD IS DD(1024),SD,HD$,VD$
470 RFFT WA,WC,WD
480 RELEASE "RFFT"
490 DELETE A,WA
520 PAGE
530 PRINT "ENTER EXPANSION FACTOR (IE 2 FOR 1/2 MAX. FREQ.)"
540 INPUT P
550 DP=ITP(1024/P)
560 DIM EE(DP),FF(DP)
580 EE=CC(0:DP)
590 FF=DD(0:DP)
610 DELETE CC,DD,WC,WD
612 WAVEFORM WE IS EE,SC,HC$,VC$
618 WAVEFORM WF IS FF,SD,HD$,VD$
620 PAGE
630 PRINT "REAL PART FFT FOR ";N$;" EXPANDED BY ";P
650 GRAPH WE
660 WAIT
670 PAGE
680 PRINT "IMAG. PART FFT FOR ";N$;" EXPANDED BY ";P
700 GRAPH WF
710 WAIT
730 POLAR WE,WF
740 PAGE
750 PRINT "MAGN. OF FFT FOR ";N$;" EXPANDED BY ";P
770 GRAPH WE
780 WAIT
790 RELEASE "GRAPH"
800 DELETE EE,FF,WC,WD
810 RETURN
820 END
```

Description of Program "DATS.BAS"

Program "DATS.BAS" is an SPS basic program written to prepare impulse test data for analysis in program "IMX.BAS" and "ADIM1.BAS". A number of operations are performed on the impulse and response waveforms as they are processed in program "DATS.BAS". First, the impulse waveform is read from a user specified data file. Next, the vertical scale and units of the impulse waveform are modified according to a user input impulse hammer load cell sensitivity. Then, the waveform is plotted for inspection. Next, the user is given an opportunity to change the horizontal unit, the vertical units and shift the waveform in time. The waveform is again plotted for inspection. Next, the user is given the opportunity to remove any constant term from the waveform or multiply it by a window. These steps are not particularly applicable to the impulse waveform. The processed impulse waveform is then stored in a temporary data file, "WIM.DAT", for later use in program "IMX.BAS".

The response waveform is processed through program "DATS.BAS" in a similar manner. First, the response waveform is read from a user selected data file. The program then applies a user input accelerometer sensitivity and plots the waveform. User modifications to units and user specified time scale shifts are applied

to the waveform and it is again plotted. Next, the user is given the option of removing a constant value from the waveform. If selected, this process is accomplished by subtracting the mean value of the waveform array from each value in the array. Next, the program gives the user the option of multiplying the waveform by a window. If this option is selected, the waveform is multiplied by a window characterized by a discontinuous rise in amplitude to one followed by an exponential decay. The user is required to input the time of the initial rise in the window and the decay time constant. At this point the final response waveform is plotted for inspection. The response waveform is then stored in temporary file "WRE.DAT" for later use in program "IMX.BAS".

The following pages contain a printout of the latest version of program "DATS.BAS".

```
10 REM PROGRAM "DATS.BAS" 6/13/81
20 REM PREPARES IMPULSE AND RESPONCE WAVEFORMS FOR "IMX.BAS".
30 WAVEFORM WA IS A(511),SA,HA$,VA$
40 PAGE
50 PRINT "ENTER DESIRED FILE NAME FOR IMPULSE (IE IMP1.DAT)"
60 INPUT N$
70 PRINT "ENTER CALIBRATION FACTOR FOR IMPULSE HAMMER IN LBF/VOLT"
80 INPUT CF
90 T$="LBF"
100 CHANGE 110,"IMP1.DAT",N$
110 OPEN #1 AS DX1:"IMP1.DAT" FOR READ
120 READ #1,WA
130 CLOSE #1
140 PAGE
150 A=A*CF
160 VA$=T$
170 PRINT "WAVEFORM ";N$
180 GRAPH WA
190 WAIT
200 PAGE
210 PRINT "   HA$= ";HA$
220 PRINT "ENTER NEW VALUE FOR HA$"
230 INPUT HA$
240 PRINT "   VA$= ";VA$
250 PRINT "ENTER NEW VALUE FOR VA$"
260 INPUT VA$
270 PRINT "ENTER OFFSET VALUE"
280 INPUT T
290 IT=ITP(T/SA)
300 DIM B(511)
310 FOR I=0 TO 511
320 IF I>=IT THEN 350
330 B(I)=0
340 GOTO 360
350 B(I)=A(I-IT)
360 NEXT I
370 A=B
380 PAGE
390 PRINT "WAVEFORM ";N$
400 GRAPH WA
410 WAIT
420 PAGE
430 PRINT "IS REMOVAL OF DC DESIRED (Y OR N)?"
440 INPUT Q2$
450 IF Q2$="N" THEN 470
460 GOSUB 1150
465 PAGE
470 PRINT "IS WINDOWING DESIRED (Y OR N)?"
480 INPUT Q$
490 IF Q$="N" THEN 560
500 PRINT "ENTER 0 FOR IMPULSE, 1 FOR RESPONSE"
510 INPUT Q1
```

```
520 IF Q1=1 THEN 550
530 GOSUB 770
540 GOTO 570
550 GOSUB 900
560 IF L=1 THEN 720
570 CANCEL DX1:"WIM.DAT"
580 OPEN #1 AS DX1:"WIM.DAT" FOR WRITE
590 WRITE #1,WA
600 CLOSE #1
610 PAGE
620 PRINT "ENTER DESIRED FILE NAME FOR RESPONCE (IE RES1.DAT)"
630 INPUT N$
640 PRINT "ENTER SENSITIVITY OF ACCELEROMETER IN G-S/VOLT"
650 INPUT CF
660 CF=CF*386.4
670 T$="IN/SS"
680 CHANGE 690,"RES1.DAT",N$
690 OPEN #1 AS DX1:"RES1.DAT" FOR READ
700 L=1
710 GOTO 120
720 CANCEL DX1:"WRE.DAT"
730 OPEN #1 AS DX1:"WRE.DAT" FOR WRITE
740 WRITE #1,WA
750 CLOSE #1
760 GOTO 1350
770 REM SUBROUTINE IMWIN
780 REM APPLIES A RECTANGULAR WINDOW OF DURATION TE TO INPULSE
790 PRINT "ENTER TIME DURATION OF IMPULSE WINDOW"
800 INPUT TE
810 NE=ITP(TE/SA)
820 FOR I=NE TO 511
830 A(I)=0
840 NEXT I
850 PAGE
860 PRINT "WINDOWED IMPULSE"
870 GRAPH WA
880 WAIT
890 RETURN
900 REM SUBROUTINE REWIN
910 REM APPLIES AN EXPONENTIAL WINDOW TO RESPONCE WAVEFORM
920 PAGE
930 PRINT "ENTER TA FOR WINDOW=EXP(-T/TA)  (IE 1.086E-3)"
940 INPUT TA
950 PRINT "ENTER OFFSET TIME FOR EXP. WINDOW"
960 PRINT " THIS SHOULD BE THE SAME TIME AS THE LAG IN RESPONCE "
970 INPUT TQ
980 WAVEFORM WC IS CC(511),SA,HA$,VC$
990 CC=0
1000 NS=ITP(TQ/SA)
1010 FOR I=NS TO 511
1020 T=I*SA-TQ
1030 CC(I)=EXP(-T/TA)
1040 NEXT I
```

```
1050 PAGE
1060 PRINT "EXPONENTIAL WINDOW"
1070 GRAPH WC
1080 WAIT
1090 WA=WA*WC
1100 PAGE
1110 PRINT "WINDOWED RESPONCE"
1120 GRAPH WA
1130 WAIT
1140 RETURN
1150 REM SUBROUTINE MEAN
1160 PRINT "ENTER RESPONCE WAVEFORM LAG TIME."
1170 INPUT TQ
1180 NS=ITP(TQ/SA)
1190 PQ=511-NS
1200 DIM TT(PQ)
1210 FOR I=0 TO PQ
1220 TT(I)=A(I+NS)
1230 NEXT I
1240 TT=TT-MEA(TT)
1250 A=0
1260 FOR I=NS TO 511
1270 A(I)=TT(I-NS)
1280 NEXT I
1290 DELETE TT
1300 PAGE
1310 PRINT "WAVEFORM RESP.-MEAN(RESP.)"
1320 GRAPH WA
1330 WAIT
1340 RETURN
1350 END
```

Description of Program "IMX.BAS"

Program "IMX.BAS" is an SPS basic program written to obtain FFTs of impulse and response data waveforms for use in transfer function calculations of program "ADIM1.BAS". This process is accomplished in several steps. First, the impulse waveform is read from a temporary file "WIM.DAT" on floppy disk DX1, where it was stored after processing in program "DATS.BAS". Next, an FFT and expansion subroutine, similar to that in program "ADFFT1.BAS", is used to obtain the real and imagingary parts of the transformed impulse waveform. The transformed waveforms are plotted for inspection. They are then stored in temporary files "TEMI1.DAT" (for the real part) and "TEMI2.DAT" (for the imaginary part) on DX1. Finally, the magnitude of the transformed impulse is calculated and plotted for inspection. These same steps are repeated for the response waveform except that the time domain waveform is read from file "WRE.DAT" and the real and imaginary parts of the transform are stored in files "TEMR1.DAT" and "TEMR2.DAT", respectively. At the end of the run, the dimension, N, of the array in the stored waveforms, is printed out for input into program "ADIM1.BAS".

The following pages are a printout of the latest version of program "IMX.BAS".

```
10 REM PROGRAM "IMX.BAS" 6/28/81
20 REM PROGRAM TO OBTAIN FFT-S FROM IMPULSE &RESPONSE
70 WAVEFORM WA IS AA(511),SA,HA$,VA$
80 OPEN #1 AS DX1:"WIM.DAT" FOR READ
90 READ #1,WA
100 CLOSE #1
110 N$="IMPULSE"
120 J=0
130 J=J+1
140 PAGE
150 PRINT "DO YOU WISH TO PLOT THE ";N$;" WAVEFORM (Y OR N)?"
160 INPUT Q$
170 IF Q$="N" THEN 220
180 PAGE
190 PRINT "  ";N$;" WAVEFORM"
200 GRAPH WA
210 WAIT
220 DIM A(2047)
230 FOR I=0 TO 511
240 A(I)=AA(I)
250 NEXT I
260 DELETE WA,AA
270 WAVEFORM WA IS A,SA,HA$,VA$
280 GOSUB 670
290 IF J=2 THEN 530
300 CANCEL DX1:"TEMI1.DAT","TEMI2.DAT"
310 OPEN #1 AS DX1:"TEMI1.DAT" FOR WRITE
320 WRITE #1,WE
330 CLOSE #1
340 OPEN #1 AS DX1:"TEMI2.DAT" FOR WRITE
350 WRITE #1,WF
360 CLOSE #1
370 POLAR WE,WF
380 PAGE
390 PRINT "MAGNITUDE OF ";N$
400 GRAPH WE
410 WAIT
420 DELETE WE,WF,EE,FF
470 WAVEFORM WA IS AA(511),SA,HA$,VA$
480 OPEN #1 AS DX1:"WRE.DAT" FOR READ
490 READ #1,WA
500 CLOSE #1
510 N$="RESPONSE"
520 GOTO 130
530 CANCEL DX1:"TEMR1.DAT","TEMR2.DAT"
540 OPEN #1 AS DX1:"TEMR1.DAT" FOR WRITE
550 WRITE #1,WE
560 CLOSE #1
570 OPEN #1 AS DX1:"TEMR2.DAT" FOR WRITE
580 WRITE #1,WF
590 CLOSE #1
600 POLAR WE,WF
```

```
610 PAGE
620 PRINT "MAGNITUDE OF ";N$
630 GRAPH WE
640 WAIT
650 DELETE WE,WF,EE,FF
660 GOTO 910
670 REM SUBROUTINE FFTEXPAND.
680 WAVEFORM WB IS BB(1024),SB,HB$,VB$
690 WAVEFORM WC IS CC(1024),SC,HC$,VC$
700 RFFT WA,WB,WC
710 DELETE WA,A
720 RELEASE "RFFT."
730 REM P IS EXPANSION FACTOR
740 P=10.25
750 DP=ITP(1024/P)
760 DIM EE(DP),FF(DP)
770 EE=BB(0:DP)
780 FF=CC(0:DP)
790 DELETE WB,WC,BB,CC
800 WAVEFORM WE IS EE,SB,HB$,VB$
810 WAVEFORM WF IS FF,SC,HC$,VC$
820 PAGE
830 PRINT "REAL PART OF ";N$
840 GRAPH WE
850 WAIT
860 PAGE
870 PRINT "IMAGINARY PART OF ";N$
880 GRAPH WF
890 WAIT
900 RETURN
910 PAGE
920 PRINT
930 PRINT "  WAVEFORM ARRAY DIM., N = ";DP
940 END
```

Description of Program "ADIM.BAS"

Program "ADIM.BAS" is an SPS basic program written to obtain frequency response function waveforms from the transformed inpulse response waveforms generated in program "IMX.BAS". This process is accomplished in several steps. First, the proper value of N, the waveform array dimension, must be input by the user. Next, the real and imaginary parts of the impulse and response transformed waveforms are read from temporary storage files "TEMI1.DAT", "TEMI2.DAT", "TEMR1.DAT" and "TEMR2.DAT". Then the real part of the frequency response function is calculated and plotted from:

$$Re(H(\omega)) = \frac{R_r F_r + R_i F_i}{(F_r^2 + F_i^2)}$$

where:

R_r = real part of response transform

R_i = imaginary part of response transform

F_r = real part of impulse transform

F_i = imaginary part of impulse transform.

The imaginary part is then calculated and plotted from:

$$Im(H(\omega)) = \frac{R_i F_r + R_r F_i}{(F_r^2 + F_i^2)}$$

The magnitude of the frequency response function is calculated from:

$$|H(\omega)| = Re(H(\omega))^2 + Im(H(\omega))^2.$$

Finally, the coherence function γ^2 is calculated and plotted from:

$$\gamma^2 = \frac{((R_r F_r + R_i F_i)^2 + (R_i F_r - R_r F_i)^2)^2}{(F_r^2 + F_i^2)(R_r^2 + R_i^2)}$$

Details of how these expressions were derived are discussed in the Theory portion of Section IV.

The following page is a printout of the latest version of program "ADIM1.BAS".

```
10 REM PROGRAM "ADIM1.BAS" 6/12/81
20 REM PROGRAM TO OBTAIN RE, IM, MAG & GAMA OF XFER FUNCTION
30 PRINT " ENTER NUMBER OF SAMPLES IN WAVEFORMS ( N )"
40 INPUT N
50 WAVEFORM WA IS A(N),SA,HA$,VA$
60 WAVEFORM WB IS B(N),SB,HB$,VB$
70 WAVEFORM WC IS C(N),SC,HC$,VC$
80 WAVEFORM WD IS D(N),SD,HD$,VD$
90 OPEN #1 AS DX1:"TEMI1.DAT" FOR READ
100 READ #1,WA
110 CLOSE #1
120 OPEN #1 AS DX1:"TEMI2.DAT" FOR READ
130 READ #1,WB
140 CLOSE #1
150 OPEN #1 AS DX1:"TEMR1.DAT" FOR READ
160 READ #1,WC
170 CLOSE #1
180 OPEN #1 AS DX1:"TEMR2.DAT" FOR READ
190 READ #1,WD
200 CLOSE #1
210 WAVEFORM WE IS E(N),SE,HE$,VE$
220 WAVEFORM WF IS F(N),SF,HF$,VF$
230 N$="TRANSFER FUNCTION REAL PART"
240 WE=(WC*WA+WD*WB)/(WA*WA+WB*WB)
250 GOSUB 390
260 N$="TRANSFER FUNCTION IMAGINARY PART"
270 WF=WE
280 WE=(WD*WA-WC*WB)/(WA*WA+WB*WB)
290 GOSUB 390
300 E=SQR(E*E+F*F)
310 N$="TRANSFER FUNCTION MAGNITUDE"
320 GOSUB 390
330 F=(C*A+D*B)*(C*A+D*B)+(D*A-C*B)*(D*A-C*B)
340 N$="THE COHERENCE FUNCTION GAMA"
350 E=F/((A*A+B*B)*(C*C+D*D))
360 GOSUB 390
370 DELETE WA,WB,WC,WD,WE,A,B,C,D,E
380 GOTO 450
390 REM SUBROUTINE GRAPH WE
400 PAGE
410 PRINT N$
420 GRAPH WE
430 WAIT
440 RETURN
450 END
```

APPENDIX B

Transfer Function Data for Single Degree of Freedom System

This appendix contains two tables of transfer function data calculated for a single degree of freedom system. The first column represents the frequency ratio (ω/ω_n). The second, third, and fourth columns are the calculated transfer function real and imaginary parts and magnitude, respectively. The first table of values were calculated for damping ratio, ζ, of .1. The second table is for ζ = .2.

0	1	0	1
0.02	1.00038414111	-0.004003137819 55	1.00039215055
0.04	1.00153826005	-0.00802514631447	1.00157041156
0.06	1.00346746147	-0.0120851159551	1.00354023151
0.08	1.0061803127	-0.0162025815249	1.00631075981
0.1	1.00968893422	-0.0203977562468	1.00989495114
0.12	1.01400912872	-0.0246917807317	1.01430971461
0.14	1.01916055101	-0.0291069924809	1.01957611082
0.16	1.02516692209	-0.0336672224003	1.02571960107
0.18	1.03205629131	-0.0383981257619	1.03277035419
0.2	1.03986135182	-0.0433275563258	1.0407636178
0.22	1.04861981533	-0.0484859939832	1.04974016247
0.24	1.05837485373	-0.0539070383904	1.05974680929
0.26	1.06917561652	-0.0596279837614	1.07083705362
0.28	1.0810778346	-0.0656904934219	1.08307180066
0.3	1.09414452327	-0.0721413971384	1.0965202319
0.32	1.1084467993	-0.0790336398785	1.11126082586
0.34	1.12406482992	-0.0864274179494	1.1273825617
0.36	1.14108893446	-0.0943915478871	1.14498634082
0.38	1.15962086307	-0.103005125752	1.16418666974
0.4	1.1797752809	-0.112359550562	1.18511365785
0.42	1.20168149032	-0.122561006784	1.20791539628
0.44	1.22548542839	-0.133733528892	1.23276080079
0.46	1.25135198074	-0.146022808509	1.25984302209
0.48	1.27946765633	-0.159620955052	1.28938355366
0.5	1.31004366812	-0.174672489083	1.32163720091
0.52	1.34331946022	-0.191481940602	1.35689811916
0.54	1.37956670855	-0.210323552405	1.3955071838
0.56	1.41909379118	-0.231553765461	1.43786102752
0.58	1.46225066379	-0.255607409583	1.48442317133
0.6	1.50943396226	-0.283018867925	1.53573779208
0.62	1.56109194882	-0.314449970198	1.59244681432
0.64	1.61772855129	-0.35072705719	1.65531118956
0.66	1.67990509667	-0.392890632106	1.7252374279
0.68	1.74823719416	-0.442262385428	1.80331065117
0.7	1.82338219521	-0.500536288881	1.89083558415
0.72	1.90600905766	-0.569903040496	1.98938684108
0.74	1.99673601632	-0.653220447424	2.10086926575
0.76	2.09600995922	-0.754246008054	2.22758721262
0.78	2.20388081124	-0.877950476389	2.37231694113
0.8	2.31958762887	-1.03092783505	2.53836541283
0.82	2.44080962162	-1.22189492657	2.72957484246
0.84	2.56233149885	-1.46220004011	2.95018163293
0.86	2.6737265094	-1.76605591251	3.20433564615
0.88	2.75554235327	-2.14971389262	3.49489391553
0.9	2.77372262774	-2.62773722628	3.8208035995
0.92	2.6736776436	-3.20284301056	4.17214039699
0.94	2.38071084263	-3.84513435063	4.52248187289
0.96	1.82280816618	-4.46401999881	4.82183618142
0.98	0.99039219531	-4.9019411687	5.00099029413
1	7.105427358E-13	-5	5
1.02	-0.934143787851	-4.71696368123	4.80857265583
1.04	-1.63453156248	-4.16645300241	4.47560320516
1.06	-2.05244154195	-3.52036898781	4.07498639181
1.08	-2.2382149375	-2.90537515926	3.66753472001

1.1	-2.27027027027	-2.37837837838	3.28797974611
1.12	-2.21418863216	-1.94960005348	2.95018163293
1.14	-2.11366732852	-1.60853187884	2.65611829196
1.16	-1.99465137926	-1.3390020833	2.40240727269
1.18	-1.87147881547	-1.12555810513	2.18387591332
1.2	-1.75159235669	-0.955414012739	1.99521721117
1.22	-1.63853820384	-0.818598119855	1.83164142978
1.24	-1.53373112963	-0.707524777061	1.68905964612
1.26	-1.4374558929	-0.616471894166	1.56407066347
1.28	-1.3494245161	-0.541122612973	1.4538776451
1.3	-1.26908221446	-0.478204892404	1.35618936221
1.32	-1.19577273721	-0.425220908705	1.26912775568
1.34	-1.12882549255	-0.380247903472	1.19114879873
1.36	-1.06759934505	-0.341792634007	1.12097750477
1.38	-1.01150258732	-0.30868500011	1.05755563137
1.4	-0.96	-0.28	1
1.42	-0.912613110512	-0.255000121394	0.947569391332
1.44	-0.868917062579	-0.23309250561	0.899638248304
1.46	-0.828535985992	-0.213796843328	0.855675738993
1.48	-0.791137894484	-0.196721116236	0.815229026509
1.5	-0.756429652042	-0.18154311649	0.777909841584
1.52	-0.724152273219	-0.16799625386	0.743383653385
1.54	-0.694076669948	-0.155850569805	0.711360891213
1.56	-0.665999873936	-0.144944168993	0.681589791742
1.58	-0.639741720142	-0.135096487279	0.65385054054
1.6	-0.615141955836	-0.1261829653	0.627950449129
1.62	-0.592057731417	-0.118090805823	0.603719964678
1.64	-0.570361427667	-0.110723572606	0.581009352507
1.66	-0.54993877624	-0.10399844709	0.55968592497
1.68	-0.530687233911	-0.0978440027404	0.539631716181
1.7	-0.512514575481	-0.0921983892399	0.520741522311
1.72	-0.495337674607	-0.0870078431703	0.502921242997
1.74	-0.479081445963	-0.0822254602462	0.486086471915
1.76	-0.463677925847	-0.0778101782504	0.470161294405
1.78	-0.449065471642	-0.073725930596	0.455077257906
1.8	-0.435188063413	-0.0699409387628	0.440772487177
1.82	-0.421994693364	-0.0664271183119	0.427190921339
1.84	-0.409438830992	-0.0631595782214	0.414281653764
1.86	-0.397477953581	-0.0601161972402	0.401998359142
1.88	-0.386073133171	-0.0572772640752	0.39029879469
1.9	-0.375188672465	-0.0546251707037	0.379144364616
1.92	-0.364791783194	-0.0521441500695	0.368499738769
1.94	-0.354852301422	-0.049820051003	0.358332517791
1.96	-0.345342435025	-0.047640144714	0.348612938363
1.98	-0.336236539278	-0.0455929562917	0.339313613062
2	-0.327510917031	-0.0436681222707	0.330409300228

0	1	0	1
0.02	1.00033608731	-0.00800589105487	1.00036812317
0.04	1.00134539741	-0.0160472018815	1.0014739725
0.06	1.00303107858	-0.0241597208811	1.00332200051
0.08	1.00539839033	-0.0323799803648	1.00591967194
0.1	1.0084547214	-0.0407456453092	1.00927753008
0.12	1.01220961415	-0.0492959227671	1.01340929095
0.14	1.01667479398	-0.0580719996562	1.01833196643
0.16	1.02186420247	-0.0671175174036	1.0240660181
0.18	1.02779403195	-0.0764790929104	1.03063554361
0.2	1.03448275862	-0.0862068965517	1.03806849817
0.22	1.04195117029	-0.0963552994802	1.04639695384
0.24	1.05022238325	-0.106983604406	1.05565739987
0.26	1.05932184134	-0.118156876339	1.06589108776
0.28	1.06927728736	-0.129946892561	1.07714442493
0.3	1.08011869436	-0.142433234421	1.08946942141
0.32	1.09187813939	-0.155704547507	1.10292419386
0.34	1.10458959725	-0.169860001387	1.11757353156
0.36	1.11828862372	-0.185010985541	1.13348952827
0.38	1.13301188778	-0.201283084318	1.15075228346
0.4	1.14879649891	-0.218818380744	1.16945067431
0.42	1.16567905702	-0.237778146648	1.18968319775
0.44	1.18369432879	-0.258345984458	1.21155887669
0.46	1.2028734211	-0.280731493509	1.23519821836
0.48	1.22324127913	-0.305174539492	1.26073420138
0.5	1.24481327801	-0.331950207469	1.2883132528
0.52	1.26759059937	-0.361374512978	1.31809615212
0.54	1.29155398083	-0.393810925832	1.35025876435
0.56	1.31665529044	-0.429677717159	1.38499245285
0.58	1.34280620109	-0.469456055837	1.42250394799
0.6	1.3698630137	-0.513698630137	1.46301433995
0.62	1.39760639699	-0.563038314576	1.50675671048
0.64	1.42571448	-0.61819598049	1.55397170141
0.66	1.45372737347	-0.679985872778	1.60490001668
0.68	1.4810008745	-0.749315918644	1.65977044684
0.7	1.50664697194	-0.82717872969	1.71878147212
0.72	1.52945911009	-0.914626710352	1.78207384491
0.74	1.54782152674	-1.01272142333	1.84969082819
0.76	1.55960527808	-1.12244319256	1.92152214246
0.78	1.56206022181	-1.24454236263	1.99722753559
0.8	1.55172413793	-1.37931034483	2.07613699634
0.82	1.52438910898	-1.52625038994	2.15712827814
0.84	1.47519113346	-1.68364205449	2.23849043954
0.86	1.39891576507	-1.84803004295	2.31779644434
0.88	1.29062257436	-2.01373735007	2.39182874481
0.9	1.14665057333	-2.1726010863	2.45662431346
0.92	0.965934702814	-2.31421855883	2.50771557161
0.94	0.75133148332	-2.42698142378	2.54061760783
0.96	0.510408159864	-2.49995833403	2.55153055273
0.98	0.255101777879	-2.52524992244	2.53810245811
1	1.776356839E-13	-2.5	2.5
1.02	-0.240338625225	-2.42718215574	2.4390522487
1.04	-0.454053361063	-2.31478184071	2.35889368662
1.06	-0.633674054472	-2.1737686011	2.26424661608

1.08	-0.77643461226	-2.01574370491	2.16010957847
1.1	-0.88346655448	-1.85107278082	2.05109326769
1.12	-0.958468764769	-1.68786952286	1.94102186985
1.14	-1.00639524541	-1.53176312385	1.83279285725
1.16	-1.03245740157	-1.38616965952	1.72841968602
1.18	-1.04150697247	-1.2527810678	1.6291707024
1.2	-1.03773584906	-1.1320754717	1.53573779209
1.22	-1.02458982002	-1.02375068012	1.44839557937
1.24	-1.00480391969	-0.92705123543	1.36713383037
1.26	-0.980493976737	-0.840995514424	1.29175922435
1.28	-0.953264704646	-0.764523071395	1.22196936288
1.3	-0.924313462827	-0.696584058942	1.15740430651
1.32	-0.89452059865	-0.636189218868	1.09768111199
1.34	-0.864523852948	-0.582434370513	1.04241608212
1.36	-0.834777556149	-0.534509169662	0.991238427777
1.38	-0.805598672048	-0.491696668477	0.943798089741
1.4	-0.777202072539	-0.453367875648	0.899769688436
1.42	-0.749727283381	-0.418973924597	0.858853974165
1.44	-0.723258617449	-0.388037410256	0.820777716237
1.46	-0.697840252255	-0.360143785186	0.785292661162
1.48	-0.673487477478	-0.334933288531	0.752173975943
1.5	-0.650195058518	-0.312093628088	0.721218445975
1.52	-0.627943436941	-0.291353487225	0.692242598021
1.54	-0.606703312561	-0.272476844953	0.66508085261
1.56	-0.586439016626	-0.255258054112	0.639583766531
1.58	-0.567110982937	-0.239517603058	0.615616397721
1.6	-0.548677546427	-0.225098480585	0.593056806651
1.62	-0.531096240707	-0.211863065734	0.571794696998
1.64	-0.51432472281	-0.19969047003	0.551730191593
1.66	-0.498321420927	-0.1884742672	0.532772735743
1.68	-0.483045976817	-0.178120553348	0.514840118137
1.7	-0.468459536498	-0.168546288264	0.49785759874
1.72	-0.454524929356	-0.159677875509	0.481757133142
1.74	-0.441206765697	-0.151449945219	0.466476683237
1.76	-0.428471475239	-0.143804309005	0.451959604812
1.78	-0.416287303328	-0.136689061045	0.438154103394
1.8	-0.404624277457	-0.130057803468	0.425012750574
1.82	-0.39345415341	-0.123868977548	0.412492053783
1.84	-0.382750347992	-0.118085285095	0.400552073324
1.86	-0.372487863462	-0.112673186866	0.38915608111
1.88	-0.362643207436	-0.107602466853	0.378270256262
1.9	-0.353194311	-0.102845853012	0.367863413246
1.92	-0.344120446993	-0.0983736864543	0.35790675879
1.94	-0.335402149848	-0.0941786323208	0.348373674247
1.96	-0.327021137939	-0.090225426571	0.339239520485
1.98	-0.318960239075	-0.0865206537964	0.330481462744
2	-0.311203319502	-0.0829875518672	0.3220783132

APPENDIX C

Frequency Response Function Data

This appendix contains a number of plots of frequency response function data waveforms. Both imaginary part and magnitude are included. The distance from the muzzle end plate to the response accelerometer position corresponding to each plot is noted below it.

TRANSFER FUNCTION IMAGINARY PART

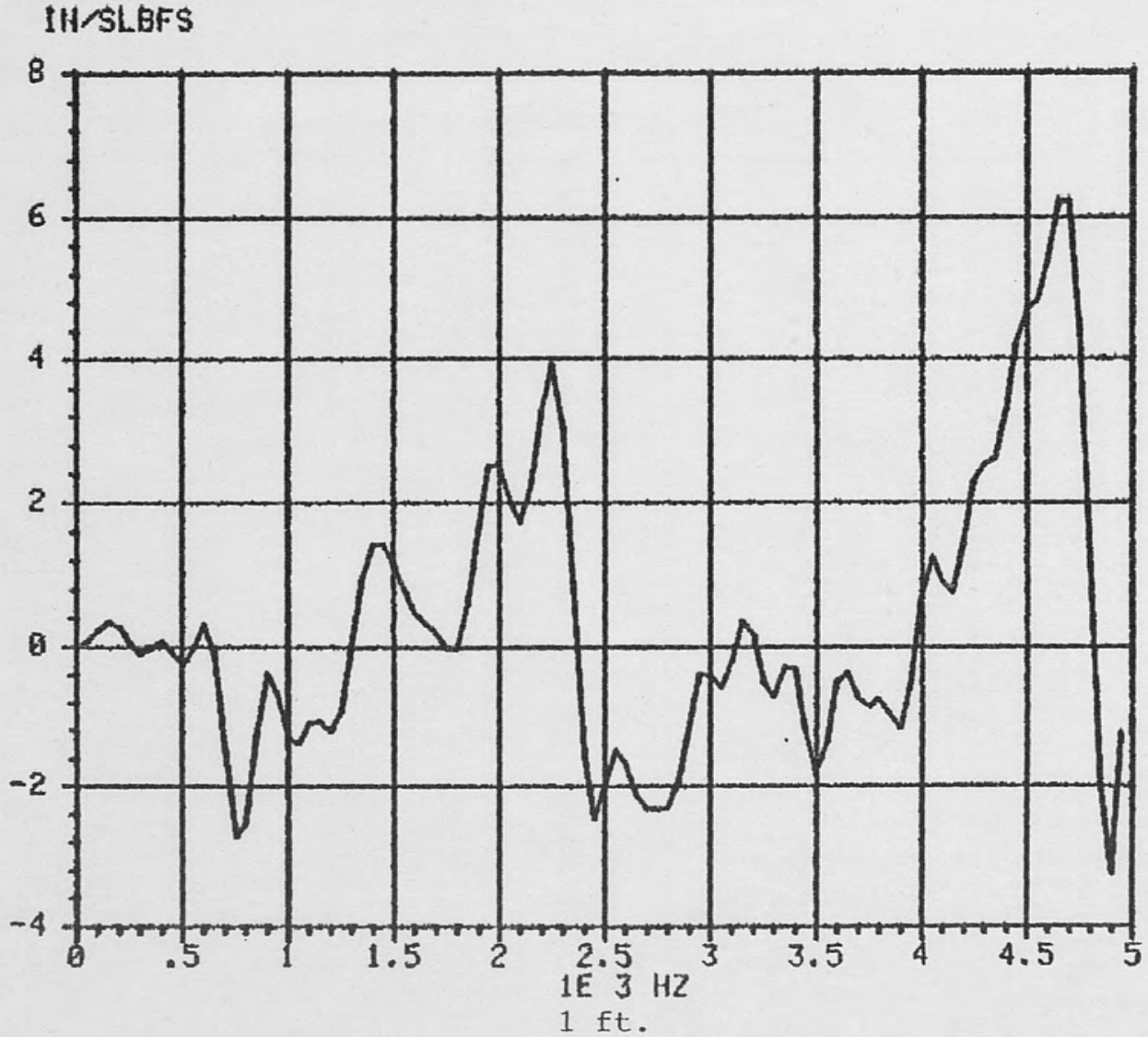

TRANSFER FUNCTION MAGNITUDE

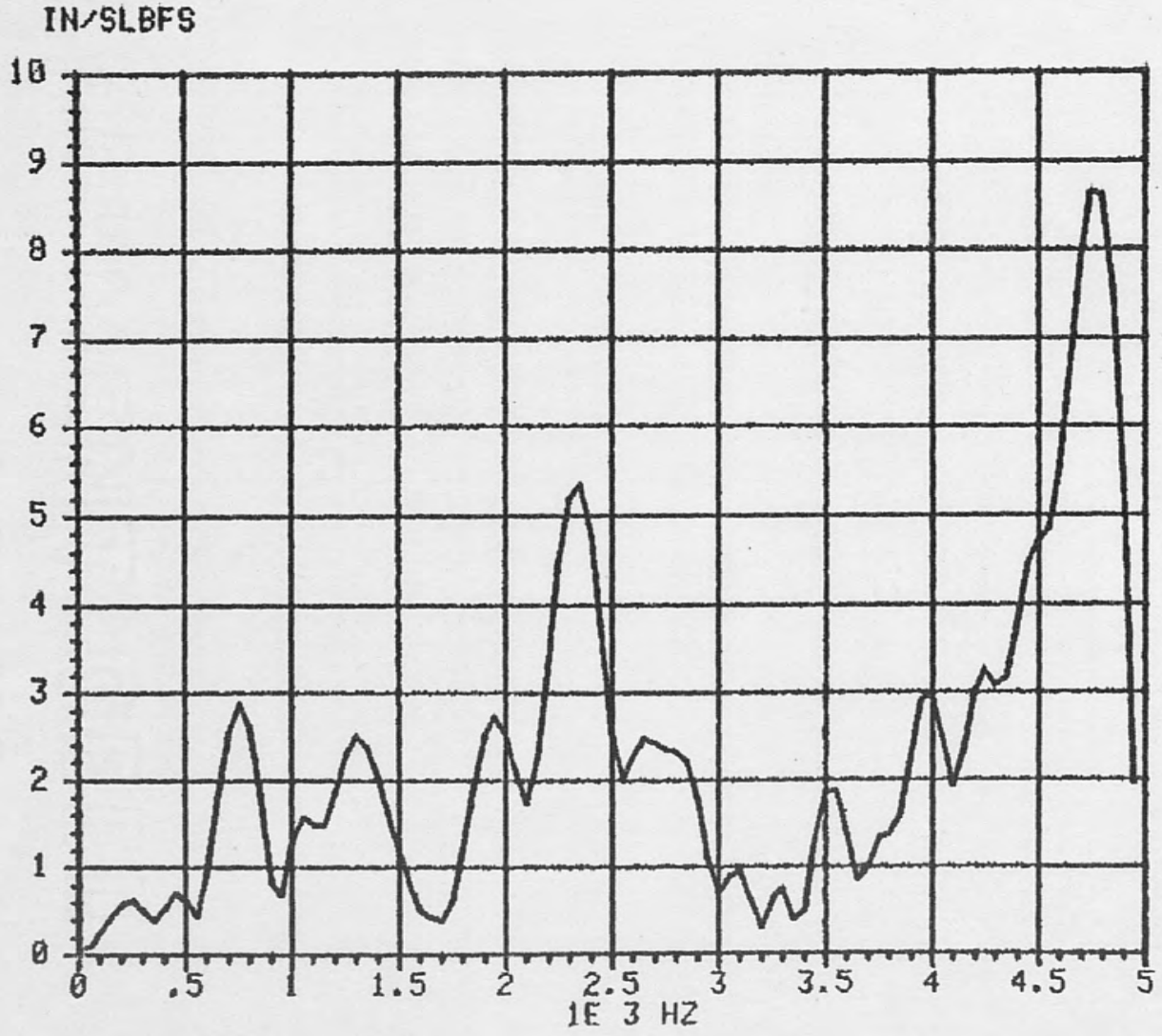

1 ft.

TRANSFER FUNCTION IMAGINARY PART

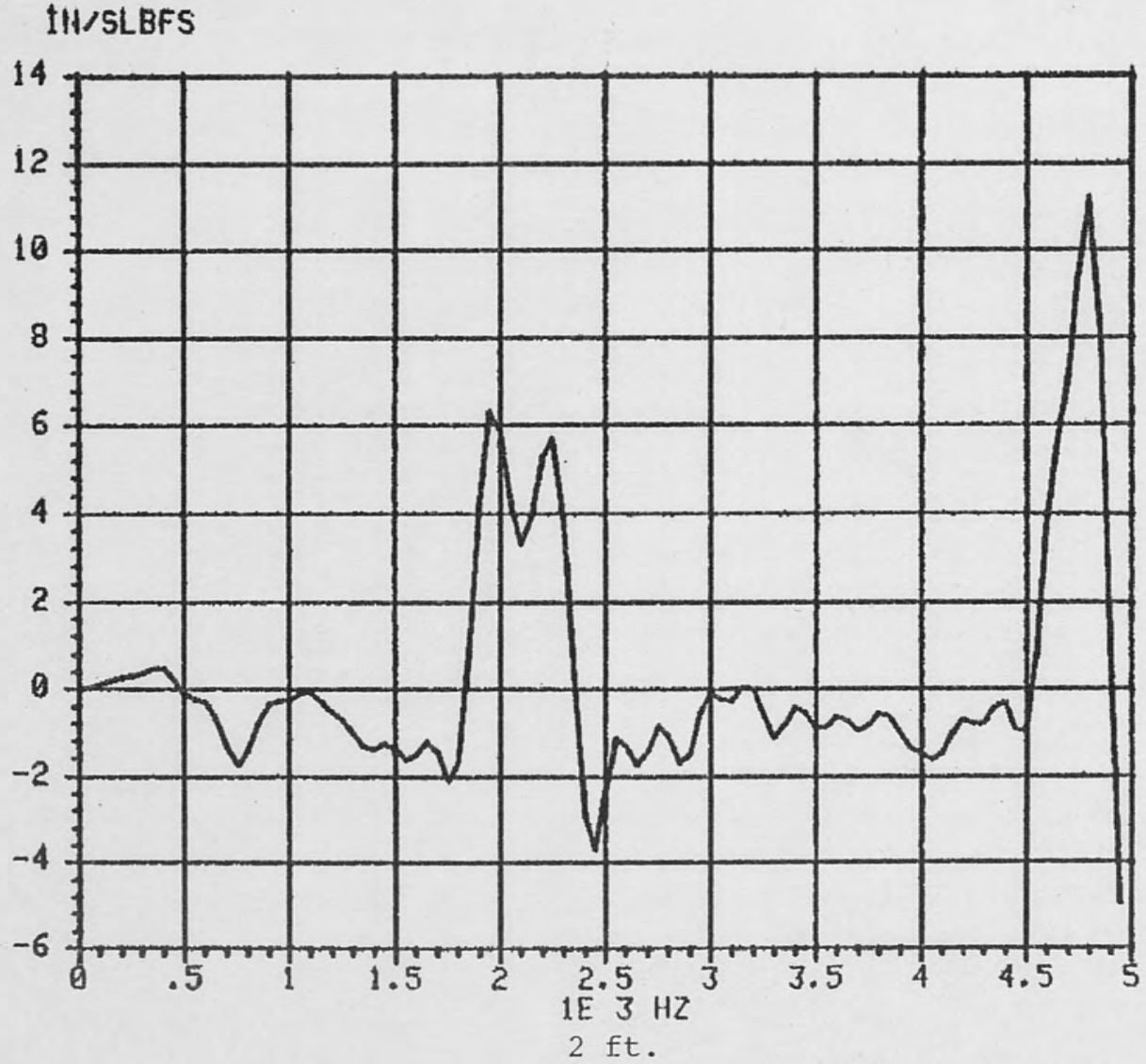

2 ft.

TRANSFER FUNCTION MAGNITUDE

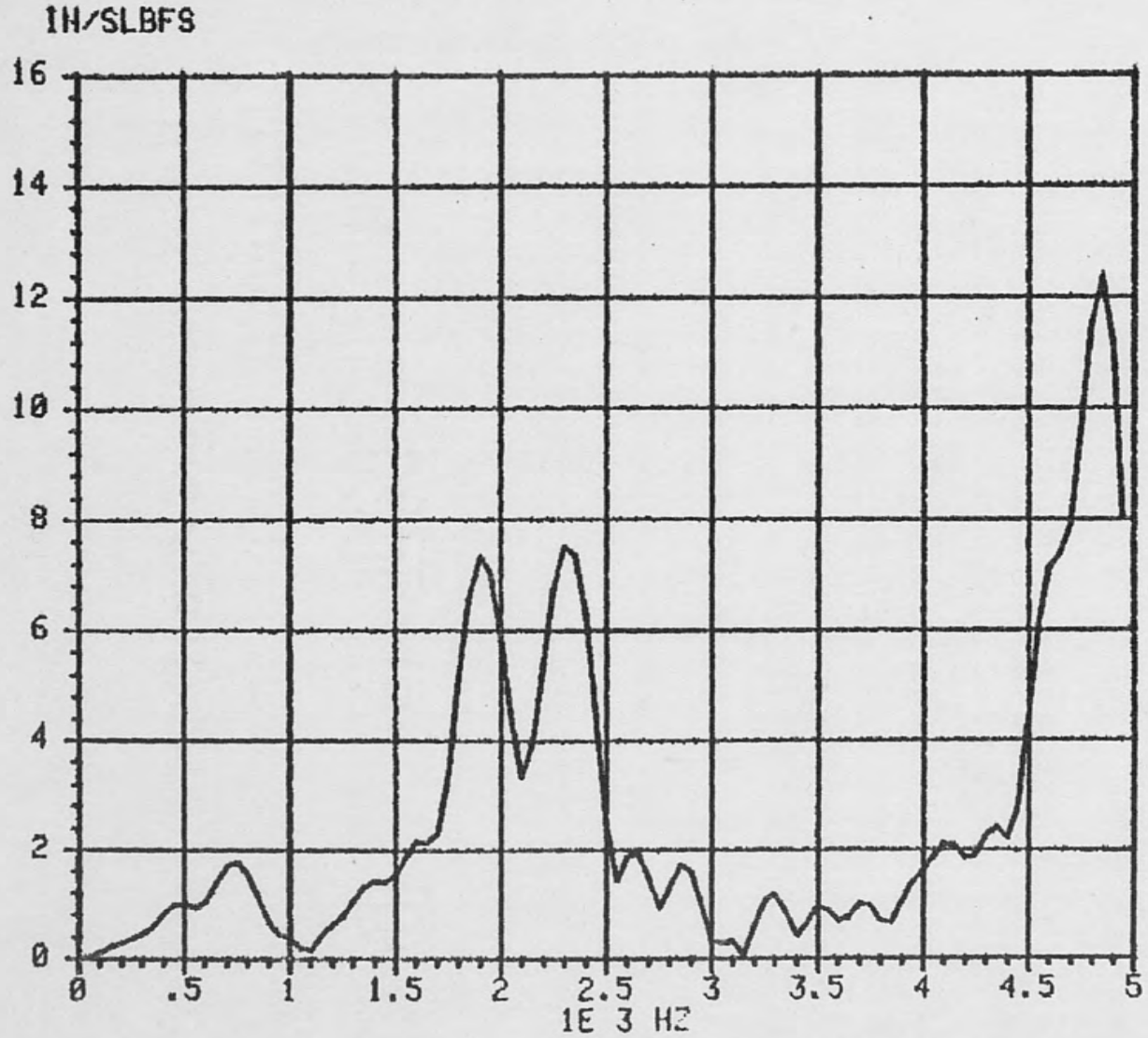

2 ft.

TRANSFER FUNCTION IMAGINARY PART

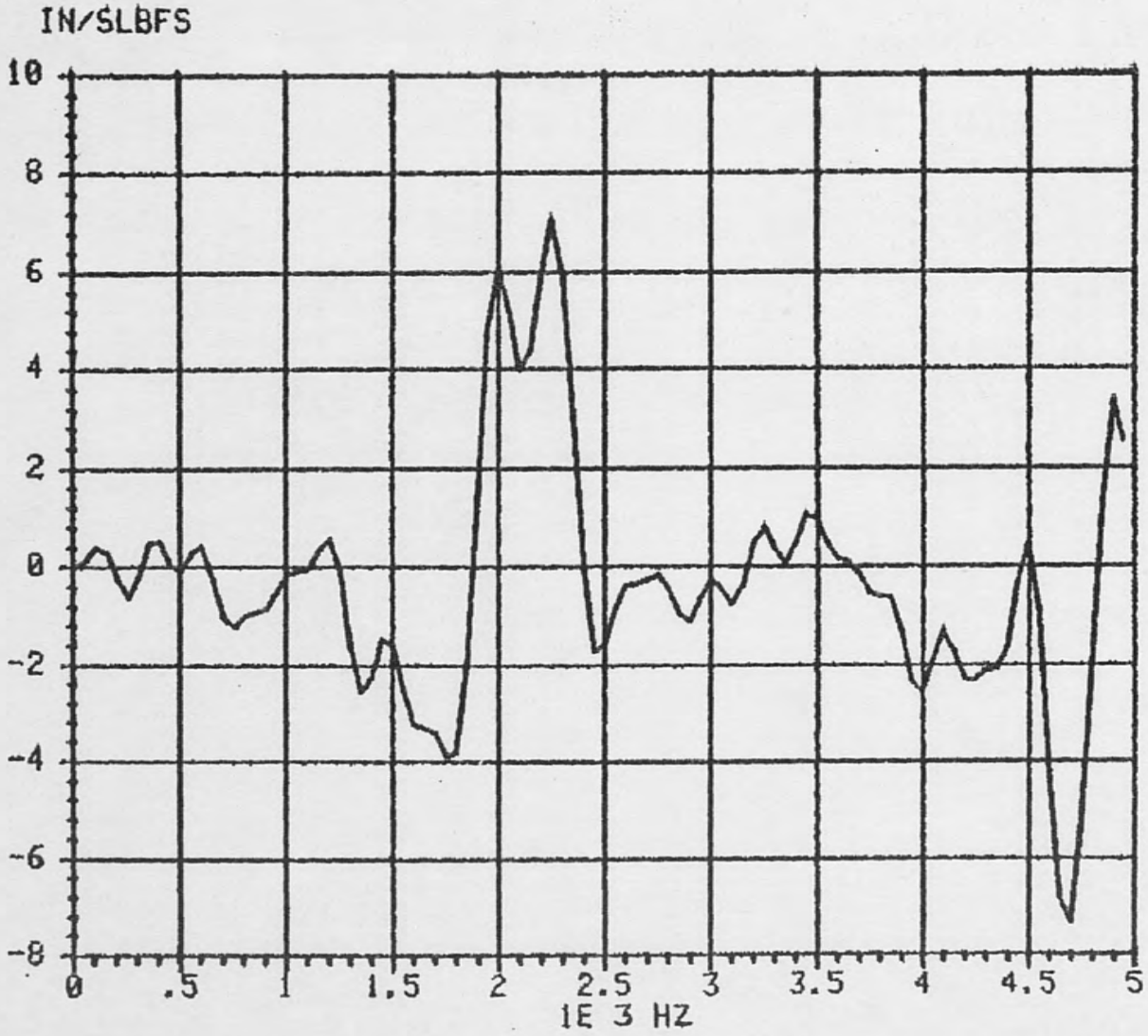

3 ft.

TRANSFER FUNCTION MAGNITUDE

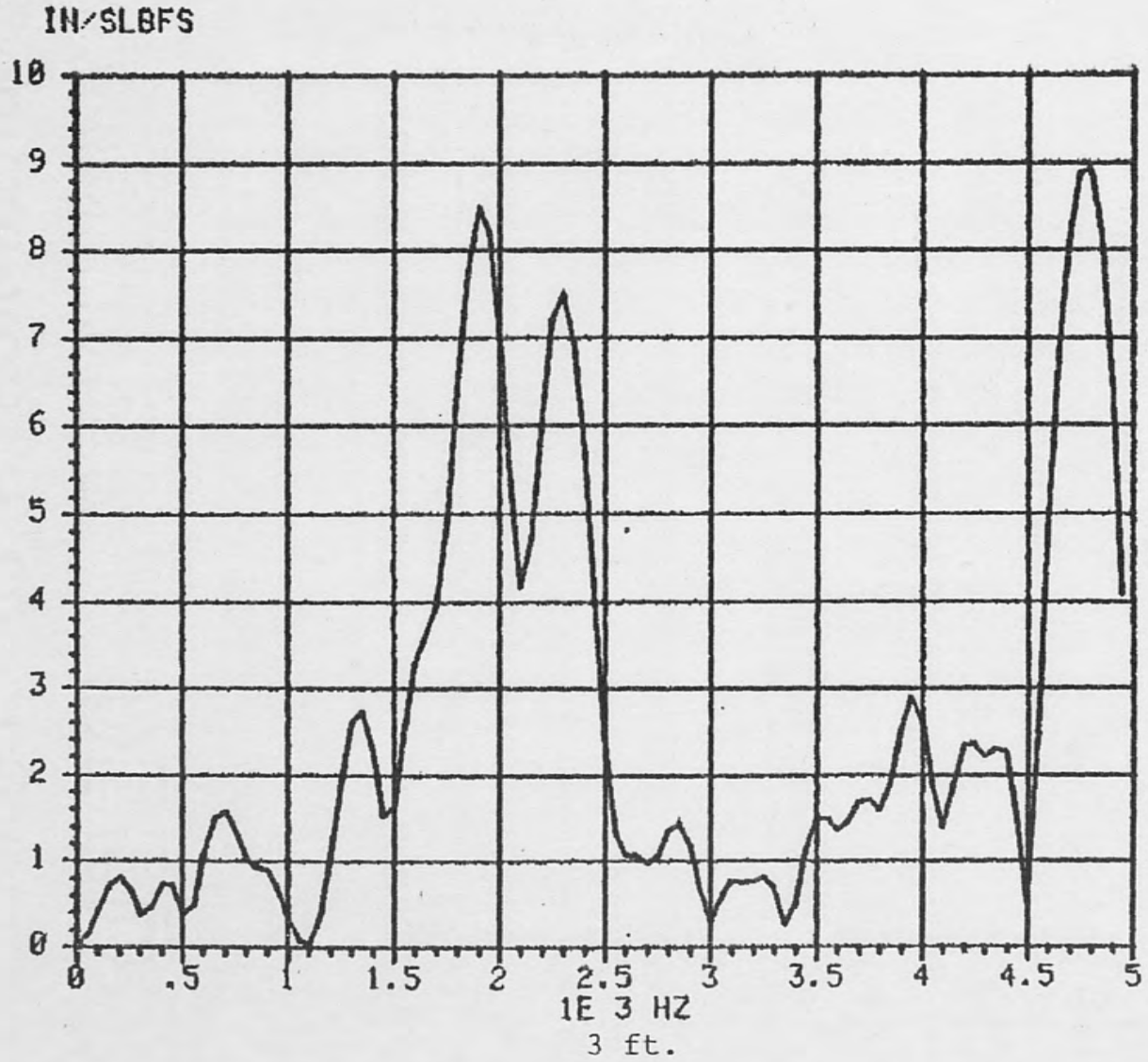

3 ft.

TRANSFER FUNCTION IMAGINARY PART

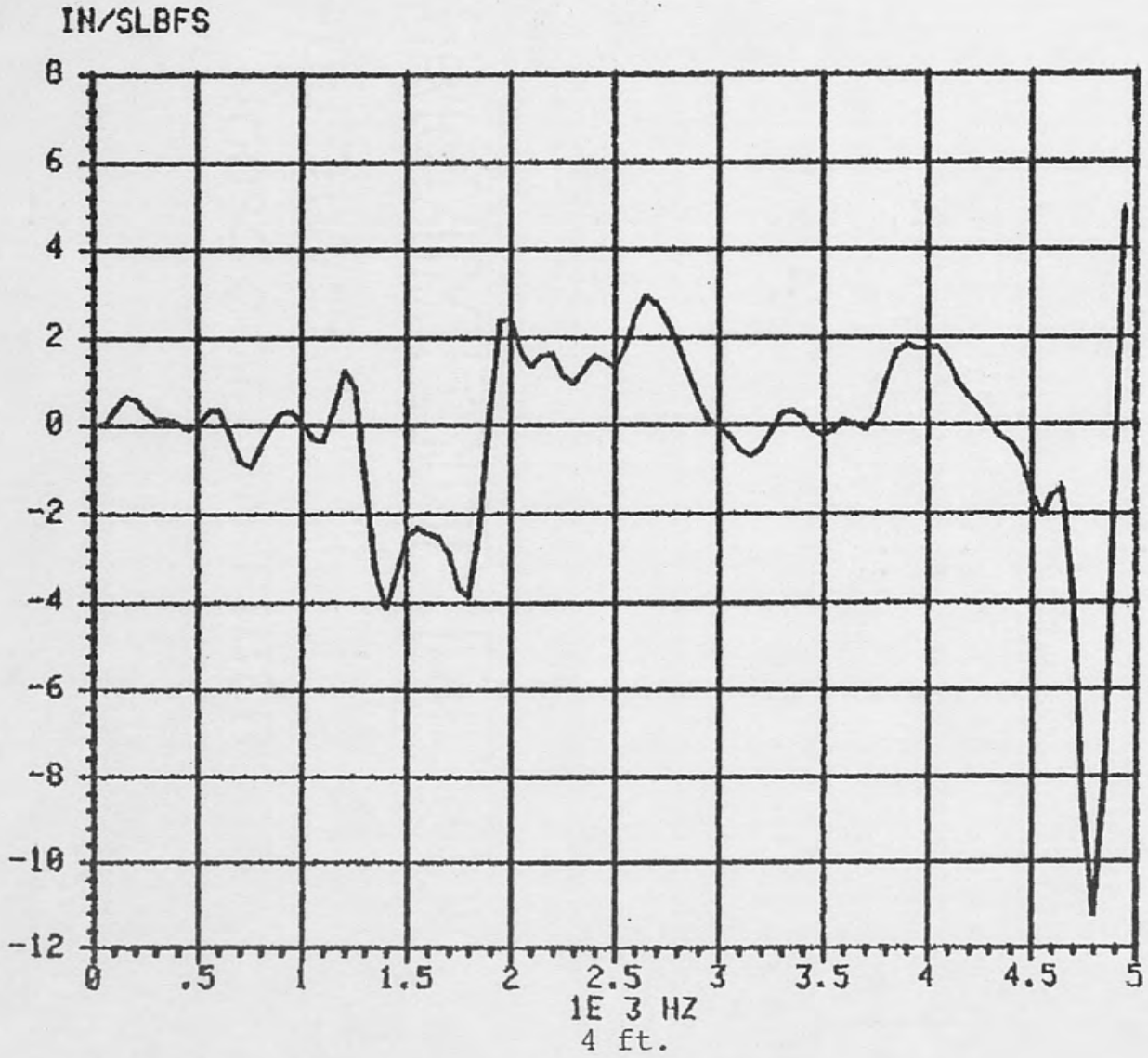

TRANSFER FUNCTION MAGNITUDE

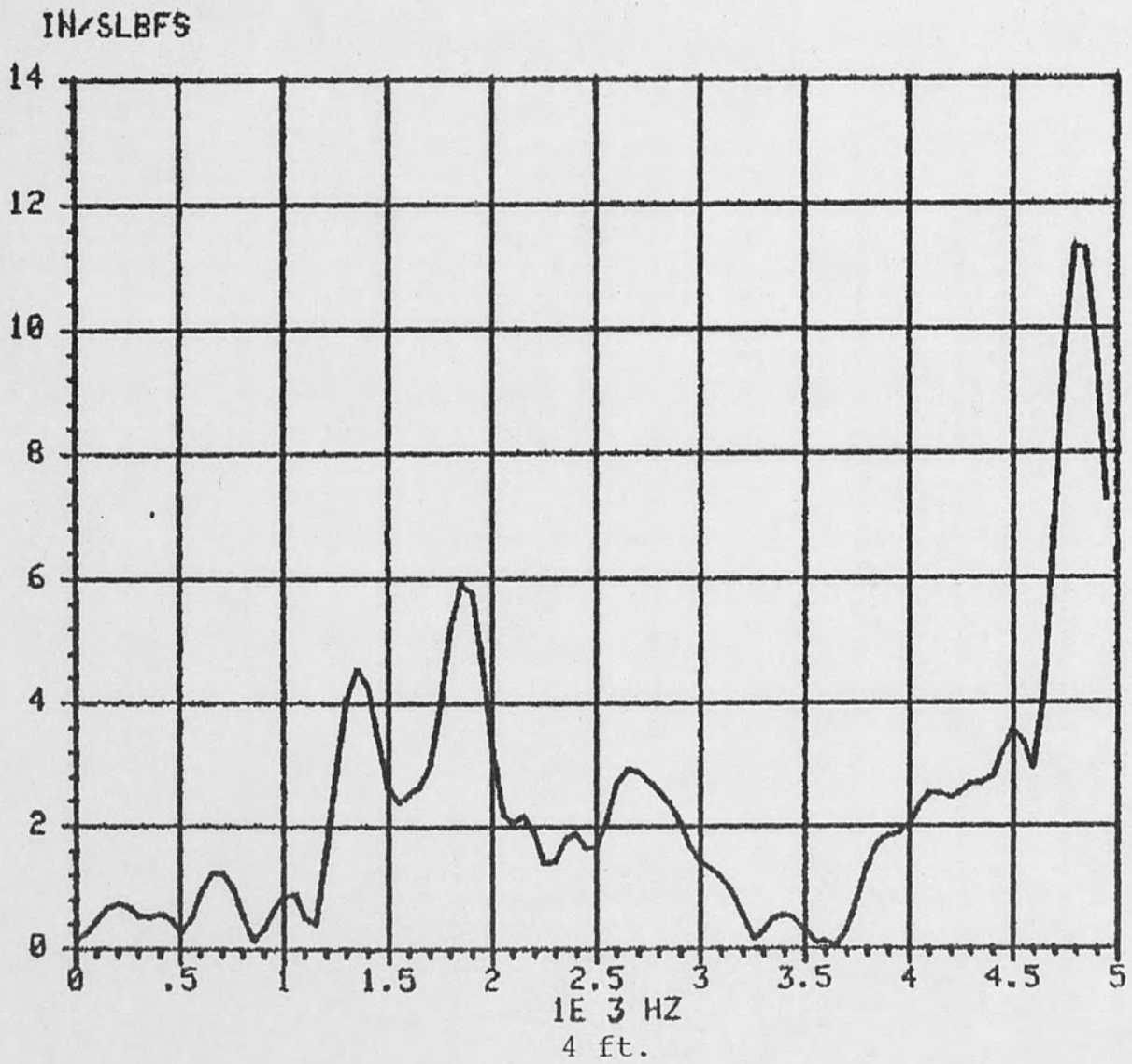

4 ft.

TRANSFER FUNCTION IMAGINARY PART

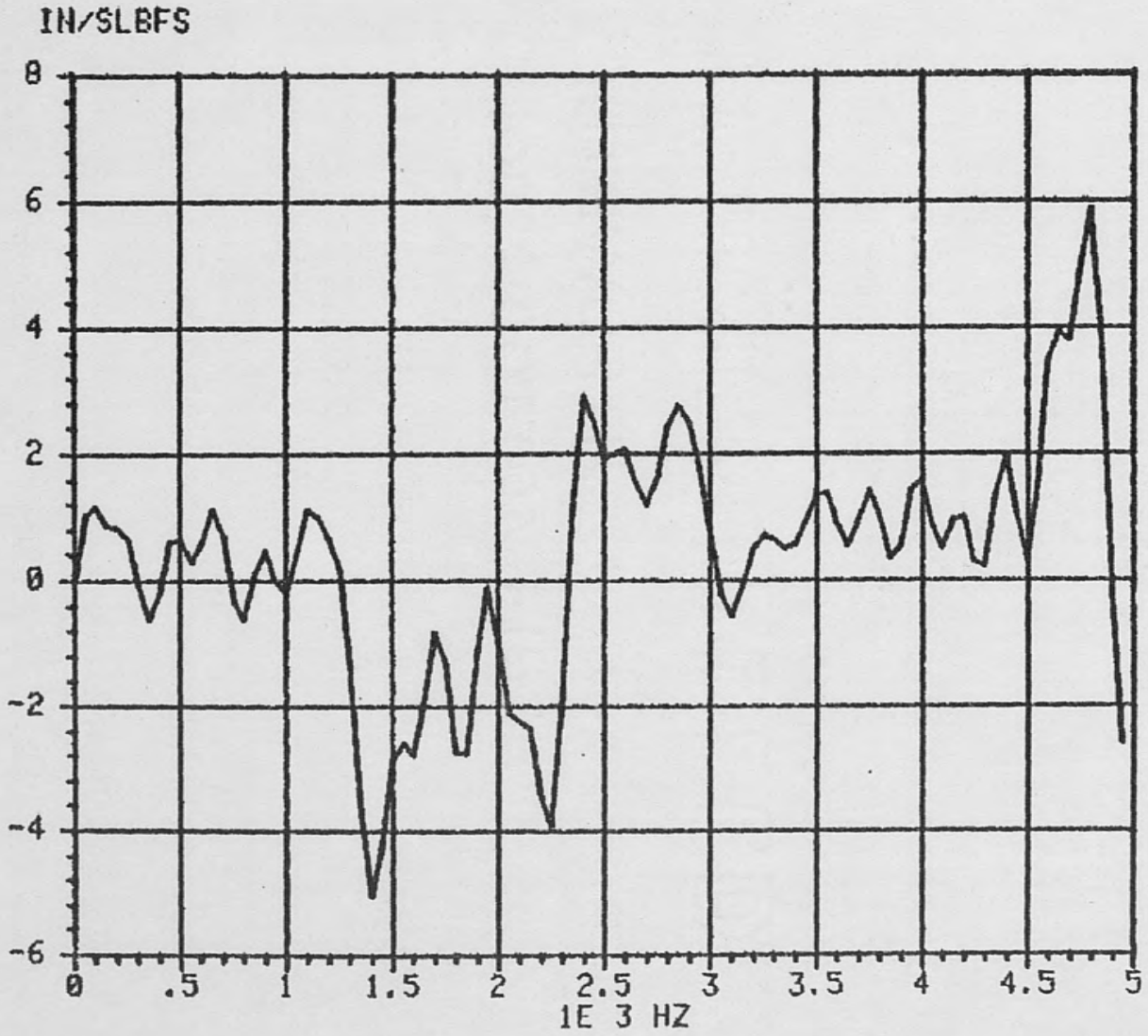

5 ft.

TRANSFER FUNCTION MAGNITUDE

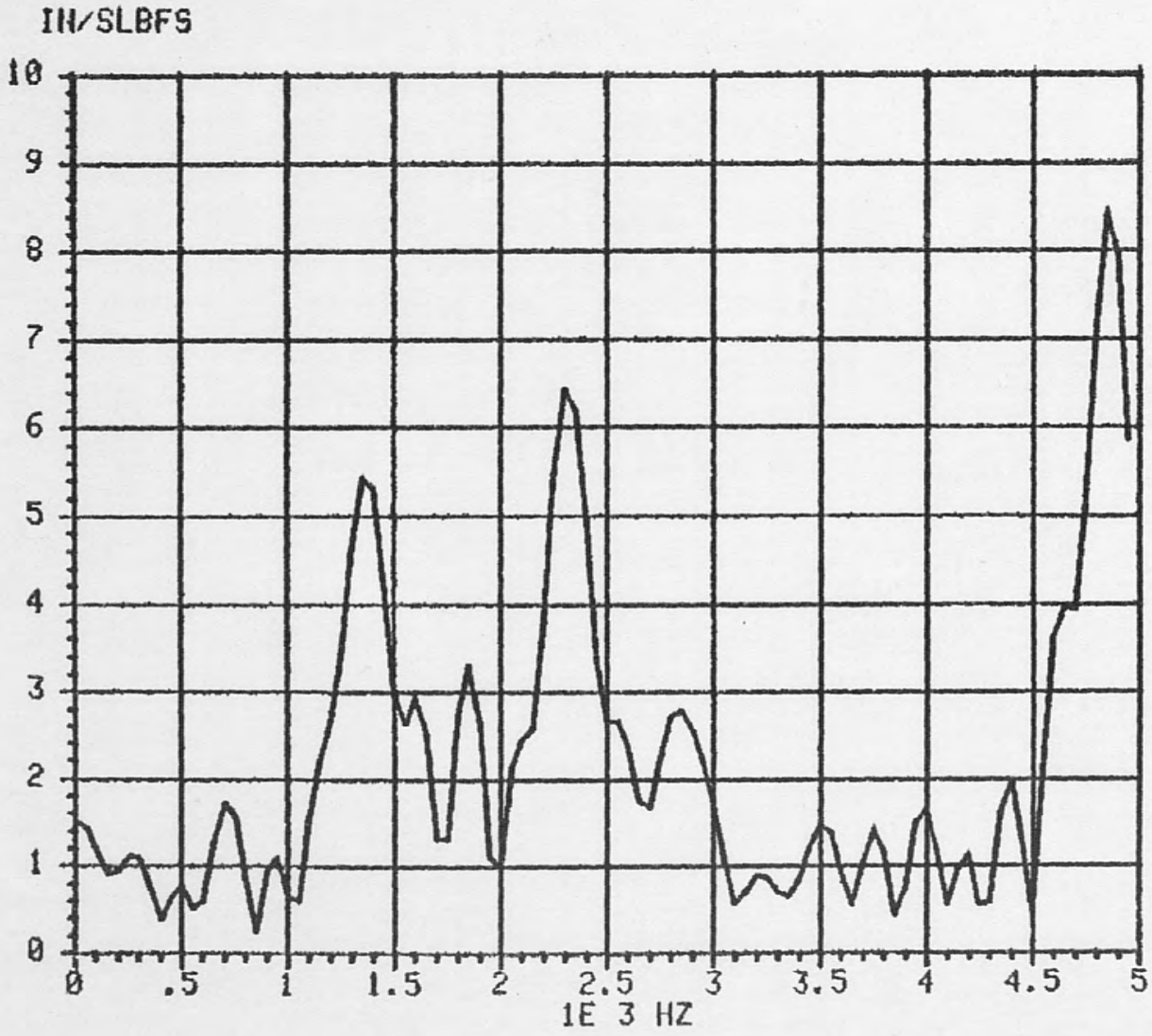

5 ft.

TRANSFER FUNCTION IMAGINARY PART

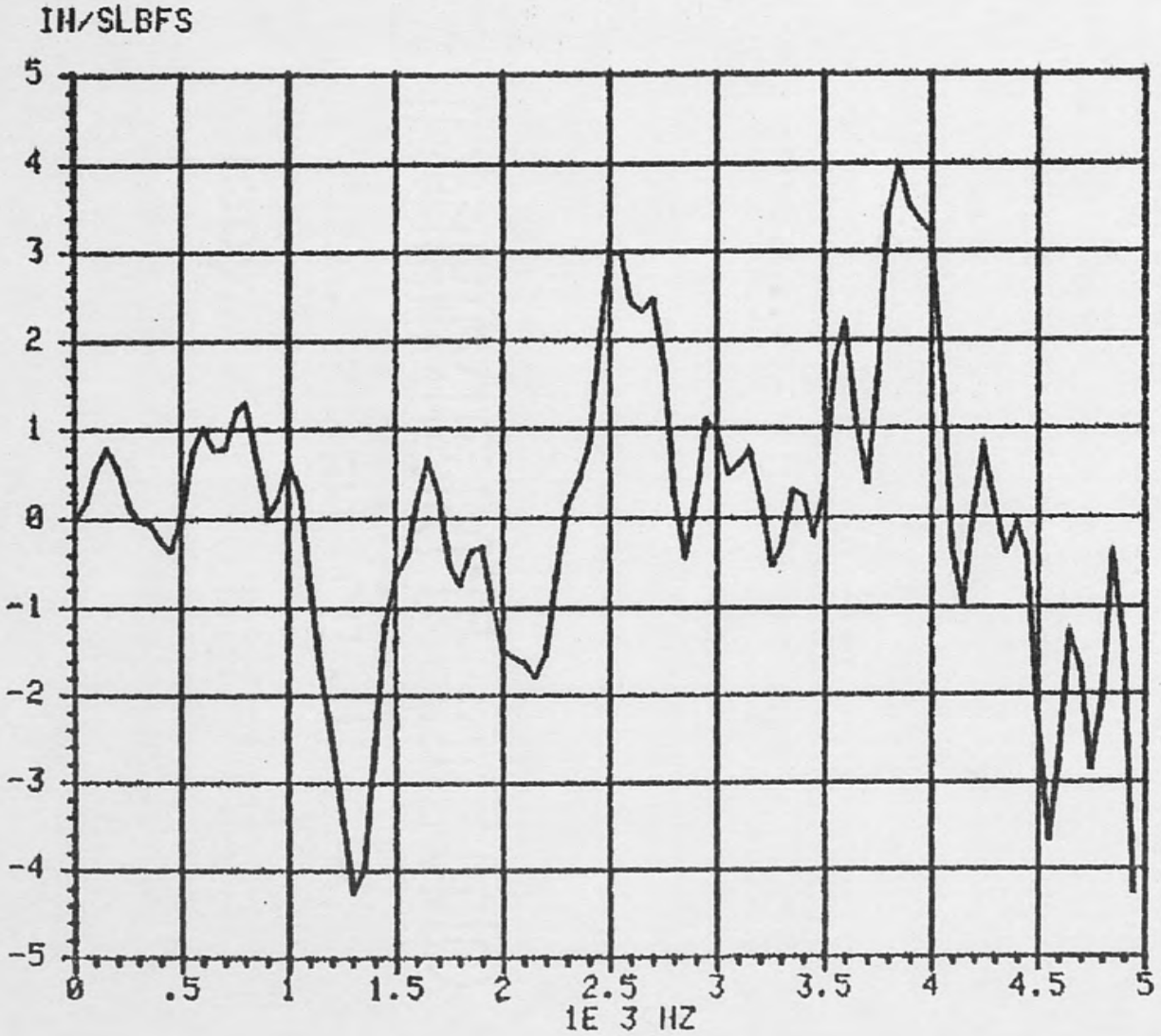

6 ft.

TRANSFER FUNCTION MAGNITUDE

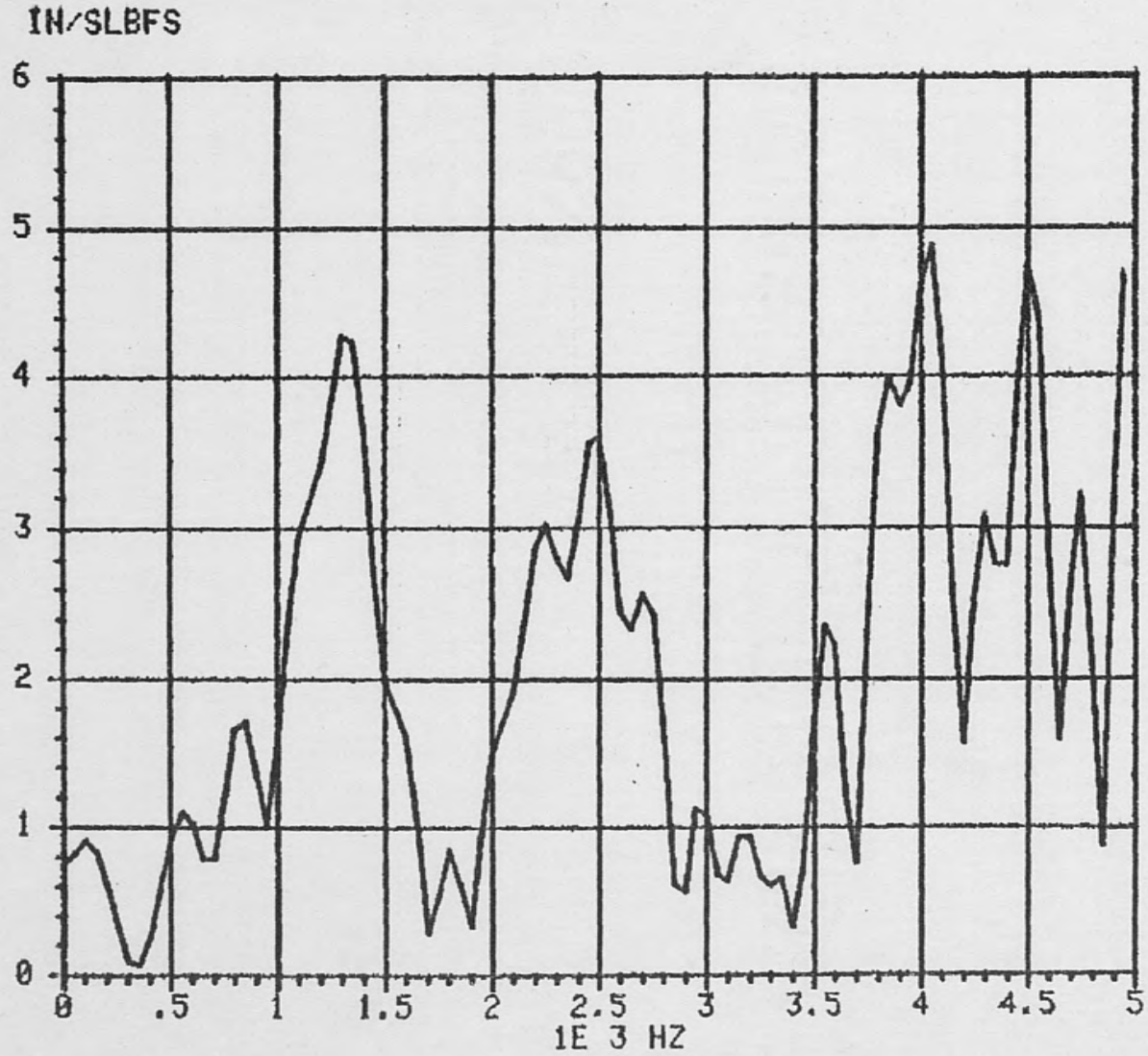

6 ft.

TRANSFER FUNCTION IMAGINARY PART

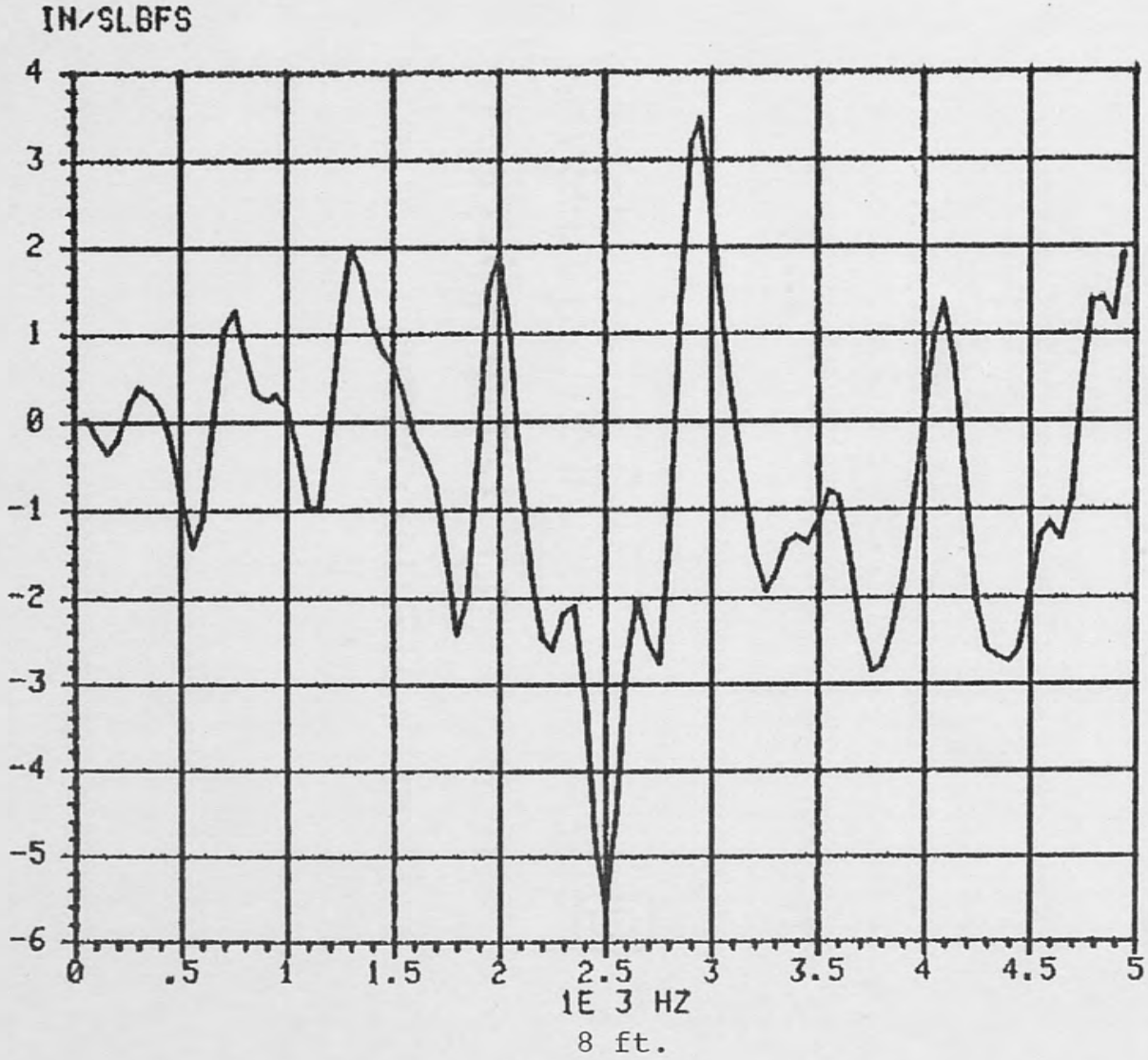

8 ft.

TRANSFER FUNCTION MAGNITUDE

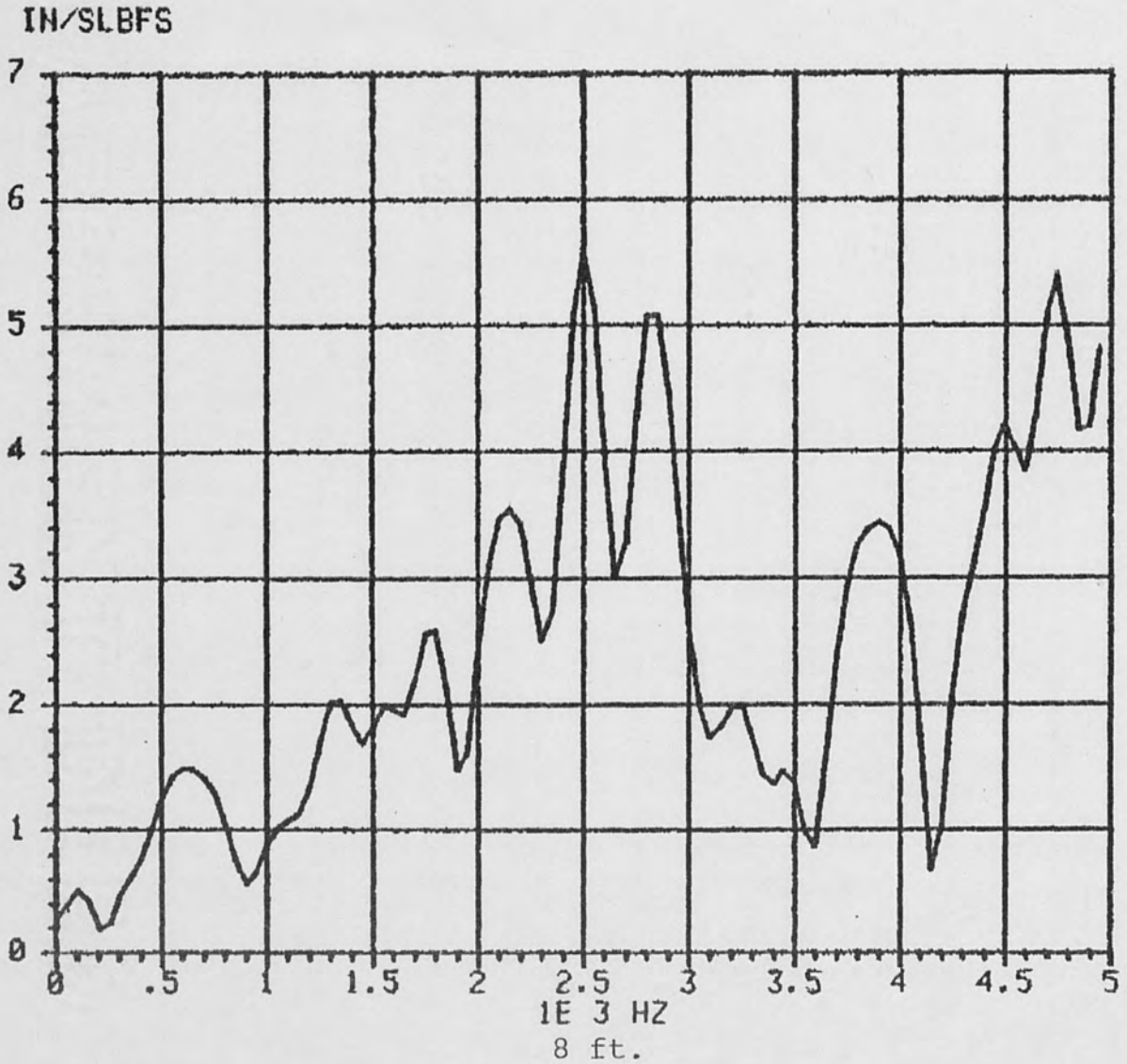

8 ft.

TRANSFER FUNCTION IMAGINARY PART

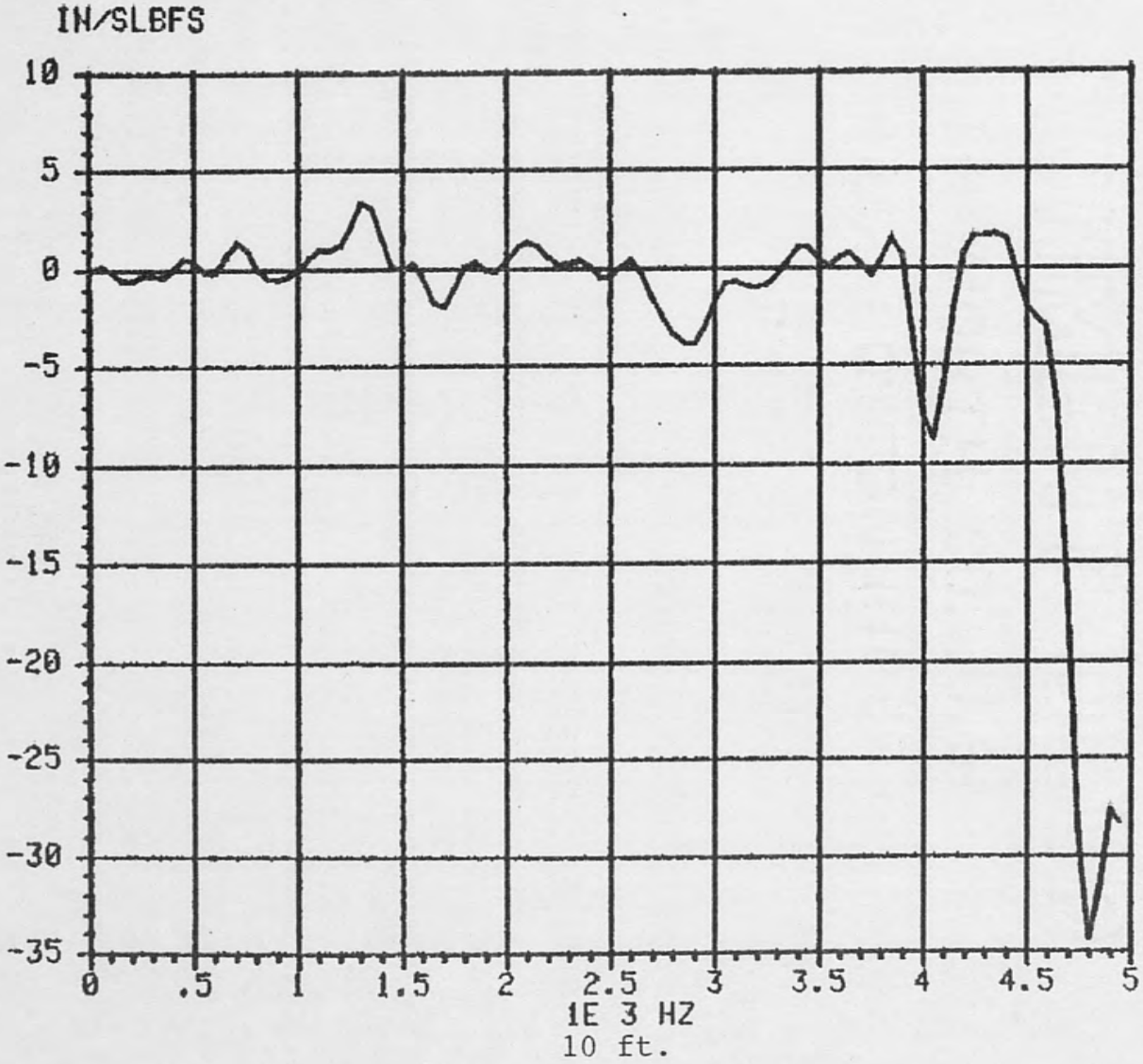

TRANSFER FUNCTION MAGNITUDE

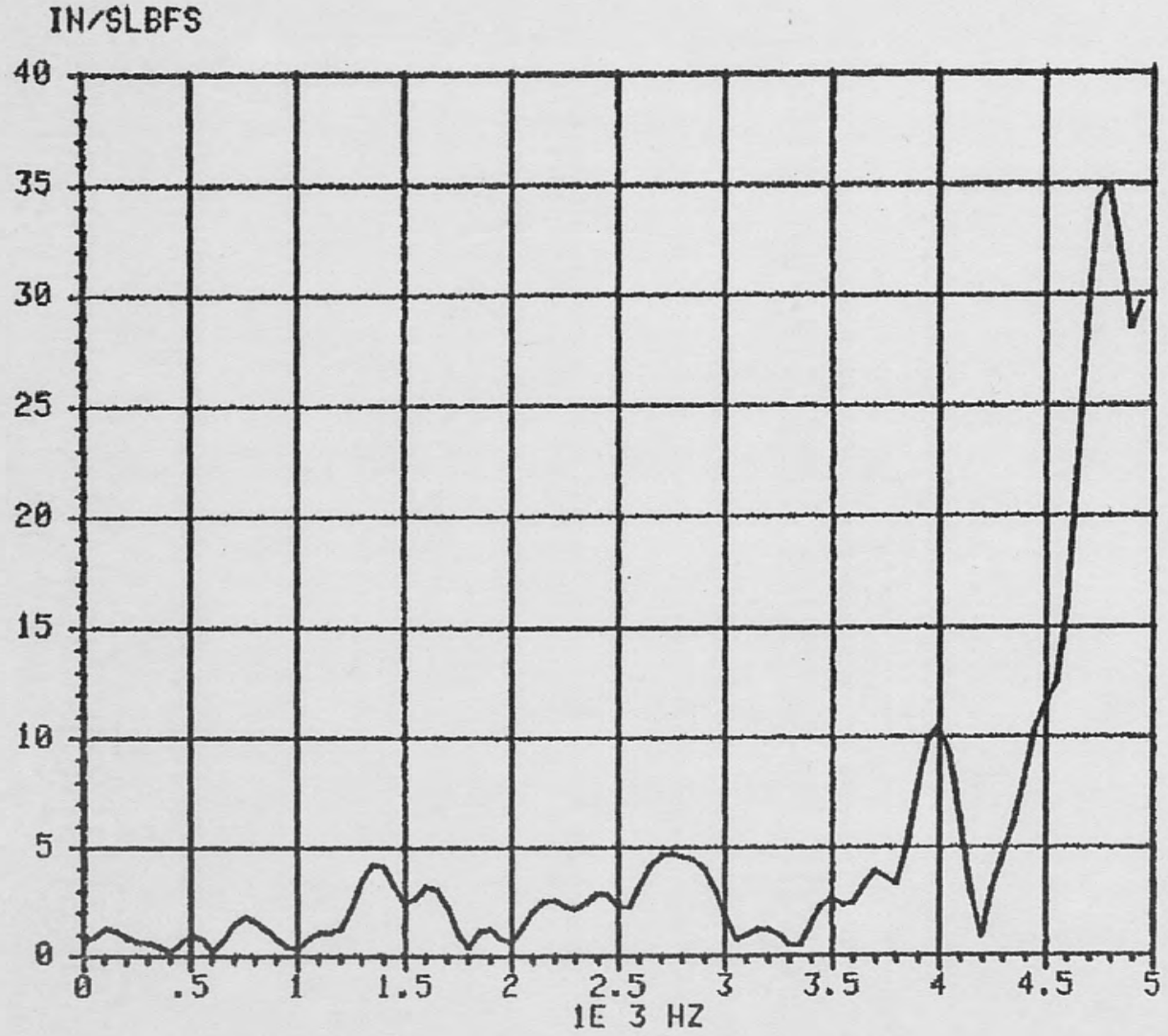

10 ft.

APPENDIX D

Finite Element Modal Analysis Results

This appendix contains the results of modal analysis of a finite element computer model. The first table contains a list of the predicted resonant frequencies of the model. The remaining six tables indicate the predicted mode shapes corresponding to the first six resonant frequencies (9).

```
00462      ***** EIGENVALUE (NATURAL FREQUENCY) SOLUTION *****
00463
00464    MODE    FREQUENCY (CYCLES/TIME)
00465
00466       1       0.0000000
00467       2        752.5326
00468       3        1423.030
00469       4        2173.381
00470       5        3158.212
00471       6        3836.665
00472       7        5189.620
00473       8        6027.580
00474       9        7310.425
00475      10        8712.773
00476      11        9144.648
00477      12        13197.08
00478      13        13477.48
00479      14        17792.62
00480      15        25935.75
00481      16        29209.94
00482 1                  ANSYS - ENGINEERING ANALYSIS SYSTEM   REVISION 3   UPDATE 67K  UCS-CRAY JUNE 1,1979
00483            SWANSON ANALYSIS SYSTEMS, INC.        HOUSTON, PENNSYLVANIA 15342   PHONE (412) 746-3304
```

```
00488              ***** EIGENVECTOR (MODE SHAPE) SOLUTION *****
00489
00490 0 REDUCED EIGENVECTOR FOR MODE    1      FREQUENCY =    0.000000     (CYCLES/TIME)
00491
00492      NODE       UX              UY              UZ              ROTX            ROTY            ROTZ
00493 0
00494         1    0.488301
00495         2    0.488301
00496         3    0.488301
00497         4    0.488301
00498         5    0.488301
00499         6    0.488301
00500         7    0.488301
00501         8    0.488301
00502         9    0.488301
00503        10    0.488301
00504        11    0.488301
00505        12    0.488301
00506        13    0.488301
00507        14    0.488301
00508        15    0.488301
00509        16    0.488301
00510 OMAXIMUM VALUE
00511  NODES          4               0               0               0               0               0
00512  DISPL     0.488301        0.000000        0.000000        0.000000        0.000000        0.000000
```

```
00513 0 REDUCED EIGENVECTOR FOR MODE    2      FREQUENCY =    752.533     (CYCLES/TIME)
00514
00515      NODE       UX              UY              UZ              ROTX            ROTY            ROTZ
00516 0
00517        1    -0.883881
00518        2    -0.875348
00519        3    -0.805262
00520        4    -0.642327
00521        5    -0.457064
00522        6    -0.259783
00523        7    -0.614279E-01
00524        8     0.127024
00525        9     0.156700
00526       10     0.180037
00527       11     0.258392
00528       12     0.394093
00529       13     0.495592
00530       14     0.557242
00531       15     0.563359
00532       16     0.565791
00533 0MAXIMUM VALUE
00534  NODES          1               0               0               0               0               0
00535  DISPL    -0.883881        0.000000        0.000000        0.000000        0.000000        0.000000
```

```
 0 REDUCED EIGENVECTUR FUR MUDE    3      FREQUENCY =    1423.03     (CYCLES/TIME)

     NODE       UX              UY              UZ             RUTX            RUTY            RUTZ
 0
        1   -0.701440
        2   -0.677425
        3   -0.482890
        4   -0.684052E-01
        5    0.303459
        6    0.557173
        7    0.646714
        8    0.564408
        9    0.535640
       10    0.502439
       11    0.340819
       12   -0.283354E-01
       13   -0.377836
       14   -0.620291
       15   -0.645456
       16   -0.655494
 0MAXIMUM VALUE
  NODES          1               0               0              0               0               0
  DISPL     -0.701440       0.000000        0.000000       0.000000        0.000000        0.000000
```

```
00559 O REDUCED EIGENVECTOR FOR MODE    4      FREQUENCY =    2173.38    (CYCLES/TIME)
00560
00561      NODE        UX              UY              UZ              ROTX            ROTY            ROTZ
00562 O
00563         1     0.655300
00564         2     0.603751
00565         3     0.196719
00566         4    -0.536581
00567         5    -0.873337
00568         6    -0.690278
00569         7    -0.138704
00570         8     0.450818
00571         9     0.527438
00572        10     0.566807
00573        11     0.589893
00574        12     0.377559
00575        13    -0.447117E-01
00576        14    -0.431517
00577        15    -0.475056
00578        16    -0.492530
00579 OMAXIMUM VALUE
00580  NODES          5               0               0               0               0               0
00581  DISPL.    -0.873337       0.000000        0.000000        0.000000        0.000000        0.000000
```

```
00582 0 REDUCED EIGENVECTOR FOR MODE    5      FREQUENCY =    3158.21    (CYCLES/TIME)
00583
00584      NODE       UX              UY              UZ              ROTX            ROTY            ROTZ
00585 0
00586        1     0.444555
00587        2     0.372802
00588        3    -0.166422
00589        4    -0.842395
00590        5    -0.549564
00591        6     0.287576
00592        7     0.742700
00593        8     0.367462
00594        9     0.246270
00595       10     0.127490
00596       11    -0.335246
00597       12    -0.831948
00598       13    -0.400972
00599       14     0.461546
00600       15     0.574465
00601       16     0.620336
00602 0MAXIMUM VALUE
00603  NODES          4              0               0               0               0               0
00604  DISPL     -0.842395       0.000000        0.000000        0.000000        0.000000        0.000000
```

```
00605 0 REDUCED EIGENVECTOR FOR MODE    6      FREQUENCY =    3836.66     (CYCLES/TIME)
00606
00607     NODE      UX              UY              UZ              ROTX            ROTY            ROTZ
00608 0
00609        1    0.424933
00610        2    0.326241
00611        3   -0.383230
00612        4   -0.979549
00613        5   -0.115139
00614        6    0.815081
00615        7    0.484904
00616        8   -0.527133
00617        9   -0.641163
00618       10   -0.648430
00619       11   -0.285199
00620       12    0.602744
00621       13    0.565857
00622       14   -0.314960
00623       15   -0.446363
00624       16   -0.500330
00625 OMAXIMUM VALUE
00626  NODES        4               0               0               0               0               0
00627  DISPL   -0.979549        0.000000        0.000000        0.000000        0.000000        0.000000
00628 1                    ANSYS - ENGINEERING ANALYSIS SYSTEM   REVISION 3   UPDATE 67K  UCS-CRAY JUNE 1,1979
00629            SWANSON ANALYSIS SYSTEMS, INC.        HOUSTON, PENNSYLVANIA 15342   PHONE (412) 746-3304
00630
00631  *                                                                          10.2242   6/22/81 CP=    0.478
00632
00633
00634
```

APPENDIX E

This appendix was included to show an example of impulse testing data obtained from the shock tube when empty. The following pages include three plots. The first plot shows the response waveform recorded from an accelerometer mounted axially at the center of the muzzle end plate. Impulsive excitation was applied to the center of the breach end plate. The second plot shows the same response waveform multiplied by an exponential window. In this case the window was devised to decay from an initial value of one to a value of about .01 at 5 m sec. The final plot shows the magnitude of the transfer function corresponding to this impulse/ response measurement.

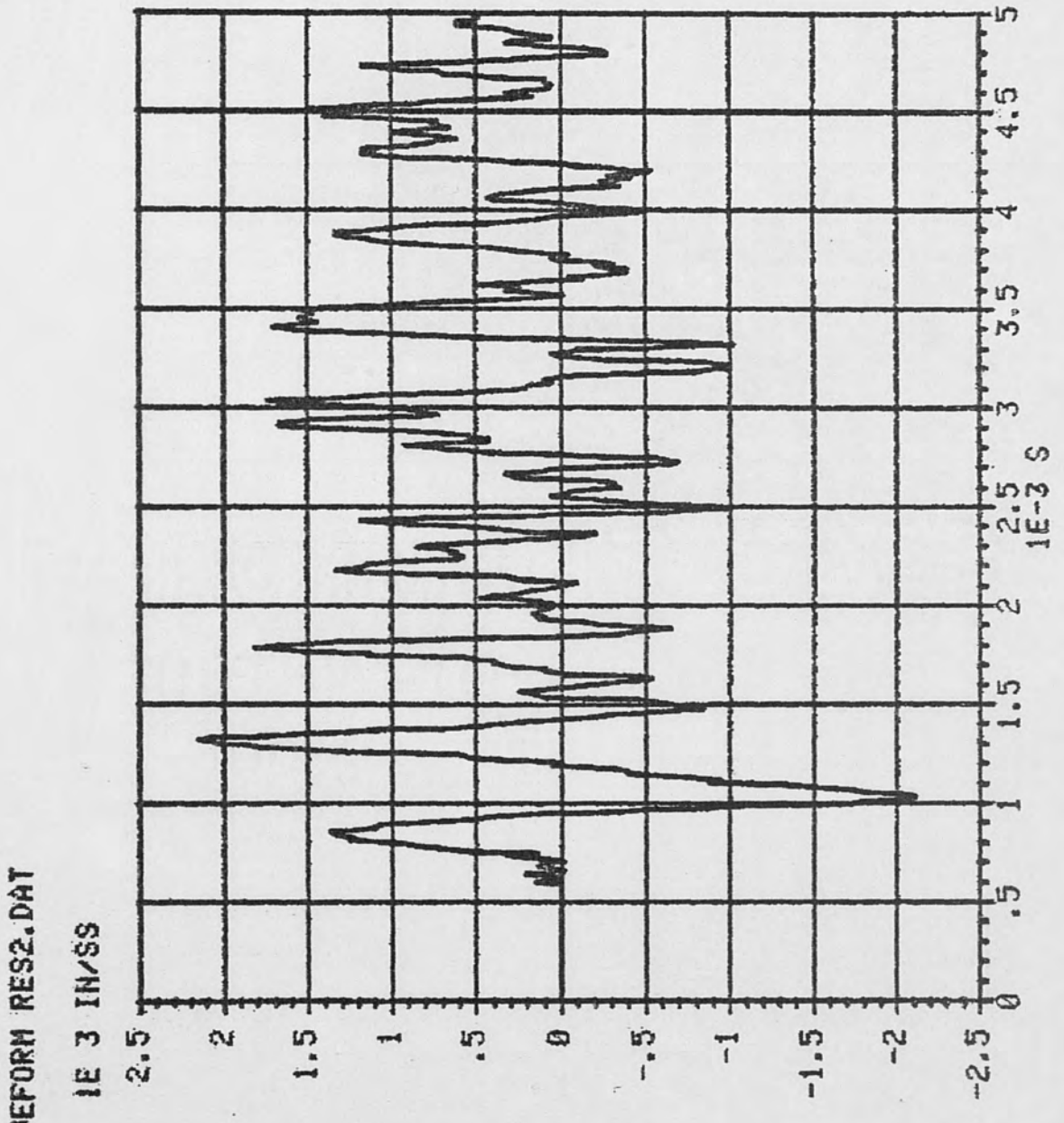
WAVEFORM RES2.DAT
1E 3 IN/SS
2.5
2
1.5
1
.5
0
-.5
-1
-1.5
-2
-2.5
0
.5
1
1.5
2
2.5
3
3.5
4
4.5
5
1E-3 S

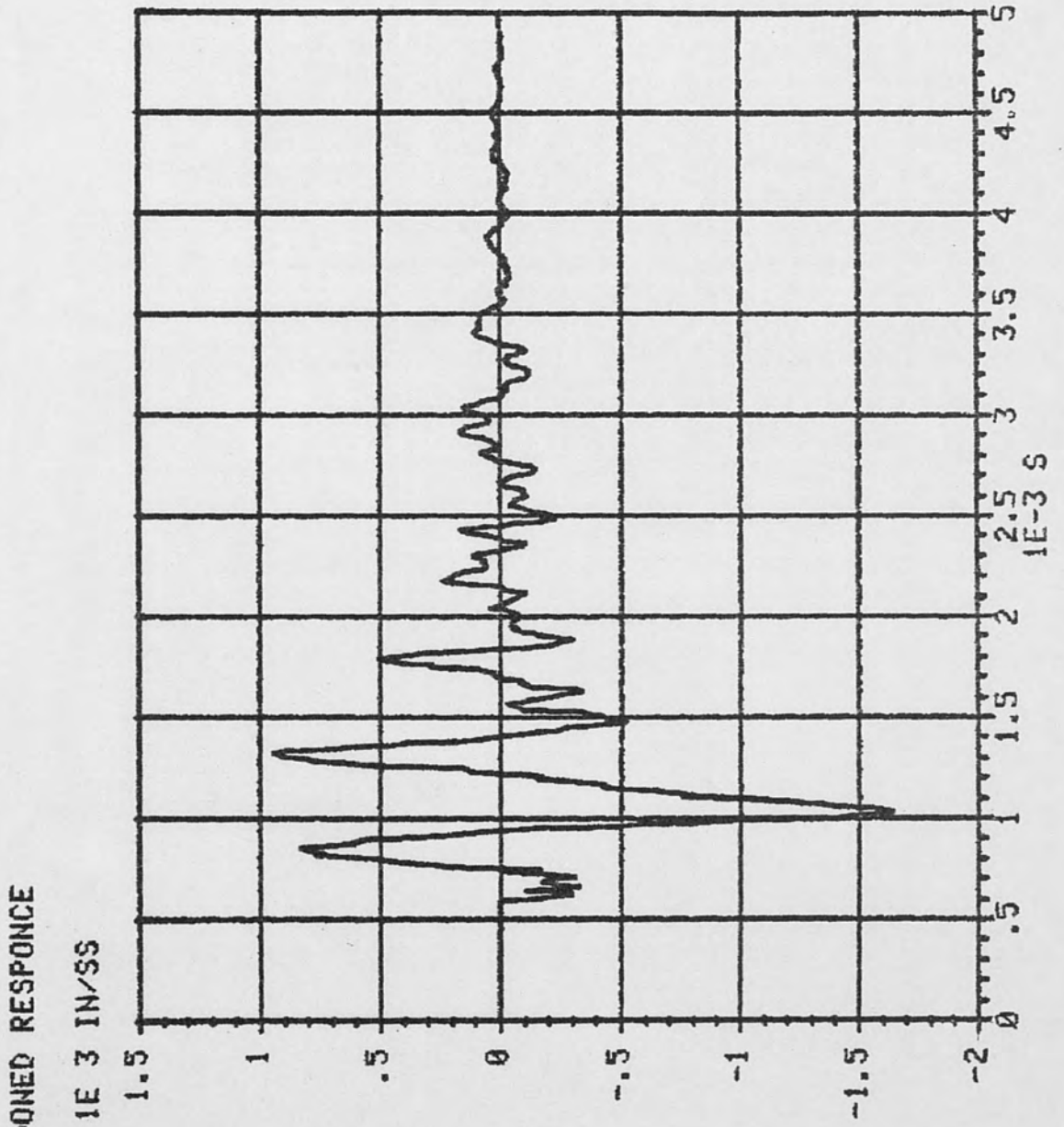
WINDOWED RESPONCE
1E 3 IN/SS
1.5
1
.5
0
-.5
-1
-1.5
-2
0
.5
1
1.5
2
2.5
3
3.5
4
4.5
5
1E-3 S

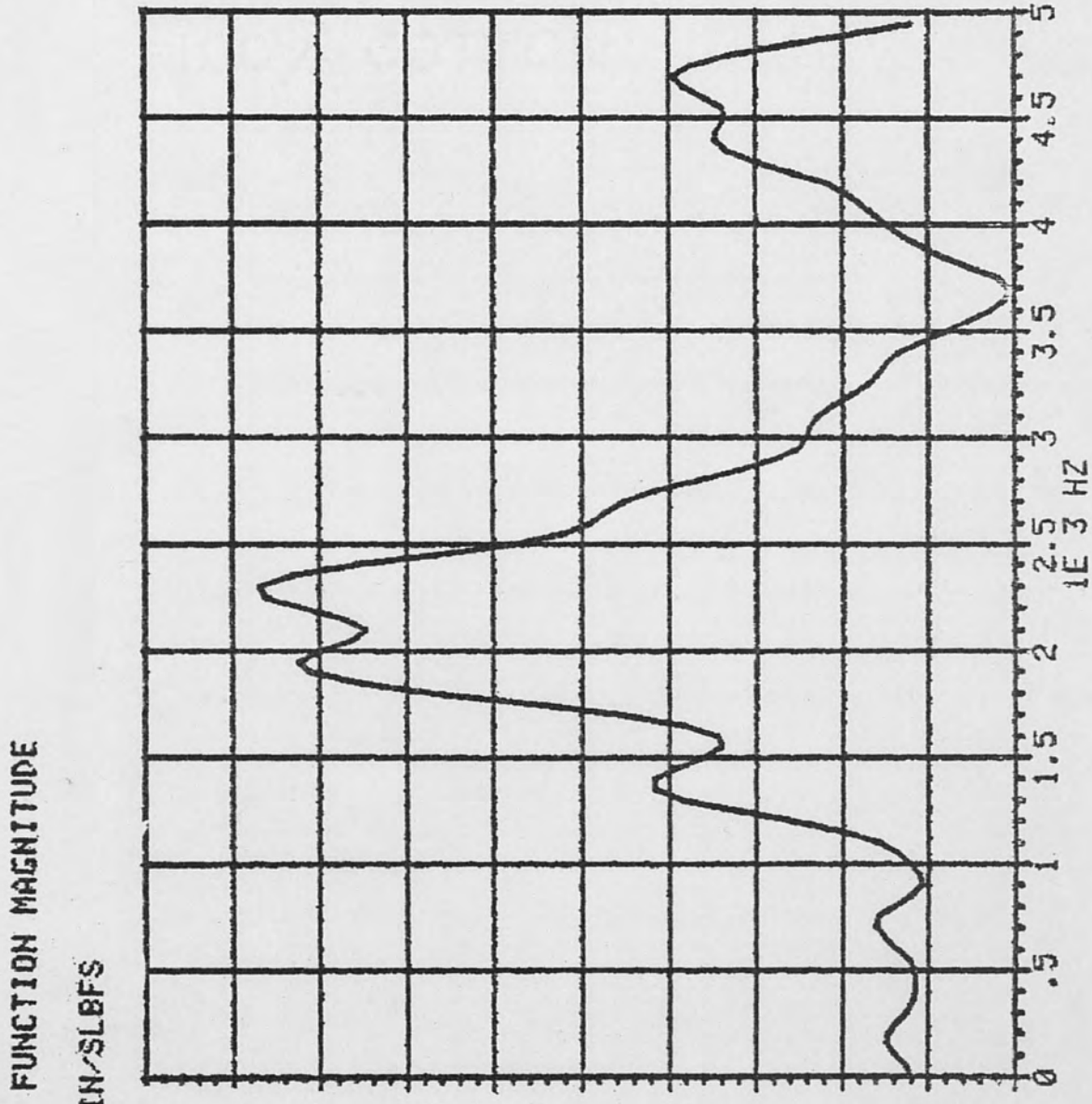
TRANSFER FUNCTION MAGNITUDE
IN/SLBFS
11
10
9
8
7
6
5
4
3
2
1
0
.5
1
1.5
2
2.5
3
3.5
4
4.5
5
1E 3 HZ

REFERENCES

1. Connell, L. W. "Design and Analysis of an Explosion Driven Hydrodynamic Conical Shock Tube." Masters research report, University of Central Florida, 1980.

2. Caruthers, J. W. Fundamentals of Marine Acoustics. New York: Elsevier Scientific Publishing Company, 1977, pp. 30-34.

3. Tektronix Incorporated. TEK SPS BASIC Software System VO1 CP85871, Instructional Manual. Beaverton, OR: SPS Information Group, 1976.

4. Freund, J. E., and Miller, I. Probability and Statistics for Engineers. Englewood Cliffs, NJ: Prentice Hall, 1975, pp. 255-256.

5. Smith, C. C.; Thronhill, R. J.; and Richardson, M. H. "Experimental Modal Analysis." Paper presented at the ASME Winter Annual Meeting, New York, NY, 6 December 1979.

6. Meirovitch, L. Analytical Methods In Vibrations. New York: Macmillan, 1967.

7. Brown, D. L., and Halvorsen, W. G. "Impulse Technique for Structural Frequency Response Testing." Sound and Vibration, November 1977, pp. 8-21.

8. Doebelin, E. Measurement System: Applications and Design. New York: McGraw Hill, 1966.

9. Swanson Analysis System Incorporated. ANSYS - Engineering Analysis System. Houston, PA: United Computing Systems, Inc., 1979.

10. Brigham, E. O. The Fast Fourier Transform. Englewood Cliffs, NJ: Prentice Hall, 1974.